Hochschule für Angewandte Wissenschaften Hamburg
Hamburg University of Applied Sciences

Master Thesis

Correlation of vanadium content to the occurrence of halogenated organic compounds in Rhodophyta species of the Baltic Sea

Master program: Pharmaceutical biotechnology
University of applied sciences Hamburg (HAW)

Summer semester 2025 (SS 25)

Laurie Ramadani
Matriculation number: [redacted]

19.09.2025

1. Supervisor: Prof. Dr. Serhat Sezei Çiçek (HAW Hamburg)
2. Supervisor: Prof. Dr. Christian Kaiser (HAW Hamburg)

Hamburg University of Applied Sciences
Faculty *Life Sciences*
Department *Biotechnology*

Declaration of Originality

I, Laurie Ramadani, hereby declare that I have written the present Master thesis on the topic "Correlation of vanadium content to the occurrence of halogenated organic compounds in Rhodophyta species of the Baltic Sea" independently and without external assistance, using only the sources and aids indicated.

Passages taken either verbatim or in substance from other works are identified as such with reference to the source.

Place, Date Name, Signature

Danksagung

Zuallererst möchte ich mich herzlich bei Prof. Dr. Çiçek bedanken, der das Thema dieser Arbeit *„Correlation of vanadium content to the occurrence of halogenated organic compounds in Rhodophyta species of the Baltic Sea“* zur Verfügung gestellt und mich während der Bearbeitung fachlich unterstützt hat.
Mein besonderer Dank gilt außerdem den Mitarbeitenden des IA-Labors, insbesondere Herrn Graß, für die kontinuierliche Betreuung, die hilfreichen Ratschläge sowie die geduldige Unterstützung bei der praktischen Durchführung der Experimente. Ohne Ihre Begleitung wäre die Umsetzung dieser Arbeit in dieser Form nicht möglich gewesen.

Ein großes Dankeschön geht auch an meine Freunde, meinen Geschwistern und vor allem an meine Eltern, die mir stets moralisch zur Seite standen und mir in herausfordernden Phasen Mut und Kraft gegeben haben.
In persönlicher Hinsicht markiert diese Arbeit das Ende meines Studiums. Sie stellt nicht nur den Abschluss einer intensiven akademischen Zeit dar, sondern auch einen wichtigen Meilenstein auf meinem weiteren beruflichen und persönlichen Weg.

Mein Dank gilt abschließend allen, die mich auf meinem bisherigen Weg unterstützt, ermutigt und an mich geglaubt haben.

I falënderoj nga zemra familjen dhe shoqërinë time për gjithçka. Suksesi nuk është vetëm arritja ime, por edhe fryti i mbështetjes tuaj.

„Rruga bëhet më e lehtë kur nuk ecën vetëm.“

Table of content

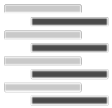

List of abbreviations

AIEXC	anion exchange chromatography
AS	Ammonium sulfate
BCA	Bicinchoninic acid
BSA	Bovine serum albumin
C. crispus	*Chondrus crispus*
CPO	Chloroperoxidase
CRM	Certified reference material
DF	Dilution factor
DW	Dry weight
DTT	Dithiothreitol
EDTA	Ethylenediaminetetraacetic acid
GFAAS	Graphite furnace atomic absorption spectroscopy
HCl	Hydrochloric acid
HOCs	Halogenated organic compounds
HPOs	Haloperoxidases
HI-HPOs	Heme-dependent HPOs
HR-CS-AAS	High-Resolution Continuum Source Atomic Absorption Spectrometry
IEXC	Ion exchange chromatography
KCl	Potassium chloride
LOD	Limit of detection
LOQ	Limit of quantification
MES	MES (2-(N-morpholino) ethanesulfonic acid)
MW	Molecular weight
P. palmata	*Palmaria palmata*
PSU	Practical salinity units
R	Correlation coefficient
RSD	Relative standard deviation
Rpm	Rounds per minute
SDS-PAGE	Sodium dodecyl sulfate–polyacrylamide gel electrophoresis
SEC	Size exclusion chromatography
Tris	Tris(hydroxymethyl)aminomethane

TXRF	Total reflection X-ray fluorescence spectroscopy
V	Vanadium
VBPOs	Vanadium bromoperoxidases
VCPOs	Vanadium chloroperoxidases
VIPOs	Vanadium iodoperoxidases
V-HPOs	Vanadium-dependent haloperoxidases
WC	Water content

List of figures

List of tables

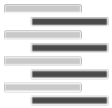

Abstract

Halogenated organic compounds (HOCs) occur naturally in marine environments, and red algae are known producers, often via vanadium-dependent haloperoxidases (V-HPOs). The aim of this study was to investigate whether the red algae *Palmaria palmata* and *Chondrus crispus* sampled from the Baltic Sea possess the biochemical prerequisites for HOC formation, additionally a correlation between the vanadium content and the abundance of HOCs in algae samples was to be studied. A HR-CS-GFAAS method was established and validated for vanadium determination, showing excellent sensitivity and accuracy. Using this method, *P. palmata* consistently exhibited high vanadium contents (up to ~38 µg/g dry weight), while *C. crispus* contained considerably lower levels (~9 µg/g dry weight), suggesting strong species dependence. Comparisons between fresh and dried samples, as well as different digestion and extraction approaches, demonstrated that sample preparation had a major impact on measured vanadium levels.

Further experiments focused on the enrichment of potential V-HPOs. Ammonium sulfate precipitation was not as effective in concentrating vanadium-associated proteins, whereas ion exchange chromatography of *P. palmata* extracts revealed vanadium enrichment in specific fractions, indicating moderate binding of vanadium-containing proteins. SDS-PAGE only provide clear protein band evidence for V-HPOs in *C. crispus*.

Overall, this study demonstrates that *P. palmata* and *C. crispus* could be promising candidates for vanadium-dependent halogenation in the Baltic Sea. The validated method and initial enrichment steps provide a foundation for future studies linking vanadium to enzyme activity and HOC production.

1 Introduction

In the diversity that the marine ecosystem offers, macroalgae have been a rich source of many natural chemical compounds, many of which have shown to have pharmacological significance. They have been utilized around the world since the ancient era as medicine as well as food source, since they are rich in protein, minerals and vitamins. Even now the diverse bioactive compounds found in macroalgae have been a big interest for pharmacological companies (Hasan 2017).

Among those are halogenated organic compounds (HOCs). While it was long believed that HOCs are produces through anthropogenic pollution, it is now known that in many marine organisms, especially in macroalgae species, these processes can also occur naturally through enzyme-mediated halogenation synthesize (Butler and Carter-Franklin 2004).

These HOCs often serve ecological purposes such as antimicrobial defense, antifouling, or allelopathy, and some display cytotoxic or bioactive properties with potential pharmaceutical applications (Butler and Sandy 2009).

HOCs are catalyzed by haloperoxidases (HPOs) which further catalyze the oxidation of halides (Cl^-, Br^-, I^-) in the presence of hydrogen peroxide, leading to the formation of hypohalous acids (HOCl, HOBr, HOI) which can halogenate organic subjects. HPOs are divided into different groups, vanadium-dependent haloperoxidases (V-HPOs) being one of them (Punitha et al. 2018).

V-HPOs play a prominent role in the halogenation process, it utilizes vanadium in this process as a catalytic cofactor for oxidation. They are most prominent in seaweeds, particularly bromperoxidases (BPOs) are widely distributed. Research has shown that in many marine algae including red algae (Rhodophyta) the occurrence of vanadium-depended bromperoxidases (V-BPOs) has been well documented. This strongly suggest that red algae, in general, possess the enzymatic mechanism to produce HOCs via vanadium-dependent haloperoxidation. Even though in the two Rhodophyta species *P. palmata* and *C. crispus* the existence of these V-HPOs and halogenated processes have yet to be fully proven and understood, taking the evolutionary and ecological similarities among Rhodophyta species into consideration, it is plausible that *P. palmata* and *C. crispus* express similar enzymes, particularly under environmental conditions favorable to haloperoxidase expression (Butler and Carter-Franklin 2004; Wever et al. 2018)

It is understood that the activity of V-HPOs in red algae may partially be influenced by the availability of vanadium in the algae tissue. Even though vanadium is just a trace element it has been found in measurable concentrations in different red algae. Especially *P. palmata* has shown to have high concentrations of vanadium, levels of 2.29 ppm have been measured in this species (Bergfeld et al., 2021)

Still the role of vanadium in the metabolic pathway in algae is not fully understood and is of need of further studies. Investigation of the correlation between vanadium and halogenated compound production could potentially provide a better understanding of the biochemical and ecological adaptation mechanisms of algae. Moreover, this knowledge could further help in the discovery of novel bioactive compounds, which may impact the pharmaceutical industry.

1.1 Aim of this study

The aim of this study was firstly to explore whether the red algae *Palmaria palmata* and *Chondrus crispus* from the Baltic Sea have the potential to produce halogenated organic compounds. Secondly if there is a correlation between vanadium enrichment within algae and the abundance of HOCs found within samples. The first step was to establish and validate a reliable method for determining vanadium content in algal samples. Using this method, the study set out to measure and compare vanadium levels between the two species, as well as between different sample states (fresh versus dried) and preparation techniques, in order to understand both biological and methodological influences on vanadium accumulation. The study also aimed to take first steps toward enriching vanadium-dependent enzymes, for this, different protein strategies such as ammonium sulfate precipitation and ion exchange chromatography were tested to evaluate whether vanadium-associated proteins could be concentrated and visualized. By combining accurate vanadium measurements with initial protein-level investigations, this study provides a basis for future investigations into the biochemical pathways of these algae.

1.2 Algae

Algae are among the most ancient photosynthetic organisms, with a fossil record stretching back over 3.5 billion years. They are a diverse group of aquatic organisms that vary in morphology, cellular structure, and size, ranging from a few micrometers to several meters in length, these large algae are called kelps. They are broadly divided into microalgae (microscopic, unicellular species) and macroalgae (multicellular, macroscopic species). Macroalgae, also referred to as seaweed, are large marine algae divided primarily by their color into three main groups, red algae (Rhodophyta), brown algae (Phaeophyta), and green algae (Chlorophyta), which are illustrated in Figure 1 (Park et al. 2024).

Figure 1: Macro algae species differentiated by color

The three main groups of macro algae are Phaeophyta (left), Chlorophyta (center) and Rhodophyta (right). The Figure shows representatives of the three subgroups from macro algae. For the brown algae *L. digitata*, for the green *N. opaca* and for the red algae *M. platyphlylla. (Created in https://BioRender.com)*

Macroalgae are of nutritional and ecological importance. They have been consumed as food and utilized for folk medicine for centuries, particularly in Asian countries. For example, many species have been used to treat diseases like diarrhea, dysentery, malnutrition and to help with deficiency such as iron and B12 deficiency. They are also known to have a high amount of antioxidants and to be low in cholesterol (Hasan 2017), that is why they are now also integrated into to the western cuisine as dietary habits seem to change. Furthermore, in addition to being eaten directly, some species are also being incorporated into food as an ingredient, like for example *Undaria pinnatifida* is added to pasta (Prabhasankar et al. 2009). In the economical view algae has been used as a raw material for products such as carrageenan, alginates and agar which is used in food products like tomato sauce, jelly, and ice cream (Hasan 2017)

In general, macroalgae are rich in protein, amino acids, minerals, vitamins, dietary fiber, and antioxidants which acts as a chemical defense against herbivores (Cardozo et al. 2007; Dawczynski et al. 2007). All these compositions have been related to have health benefits such as cardiovascular protection, anti-inflammatory effects, and cancer prevention. Seaweeds are also associated with lowering LDL cholesterol, improving glycemic response, and contributing to disease prevention (Jimenez-Escrig SC and Sanchez-Muniz Ph D Prf 2000; Hasan 2017). Some of the bio compounds and their applications are illustrated in Figure 2.

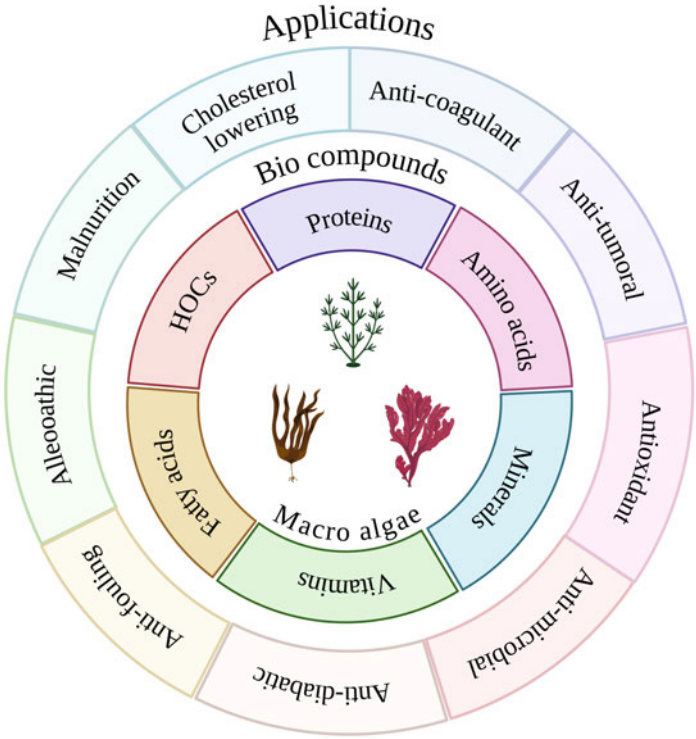

Figure 2: Schematic overview of bioactive compounds derived from macroalgae and their associated applications.

Macroalgae, including brown (*Phaeophyta*), green (*Chlorophyta*), and red (*Rhodophyta*) species, are sources of diverse bio compounds such as proteins, amino acids, minerals, vitamins, fatty acids, and halogenated organic compounds (HOCs). These compounds contribute to a wide range of biological activities and potential applications, including antioxidant, anti-tumoral, anti-coagulant, anti-microbial, anti-diabetic, anti-obesogenic, anti-aging, malnutrition prevention, and cholesterol-lowering effects. *(Created in https://BioRender.com)*

The chemical composition of seaweeds varies significantly depending on species, environmental conditions (light, temperature, nutrient levels), geographic location, and time of harvest. Even within the same species, nutrient and metabolite content can differ substantially. While some seaweed species may contain toxic compounds that limit their use in food or feed, the majority are considered valuable nutritional resources and potential sources of novel pharmaceuticals (Marinho-Soriano et al. 2006; Mišurcová 2011).

1.3 Heavy metal absorption in red and brown algae

Algae are widely recognized for their ability to bioaccumulate trace elements and heavy metals from the surrounding marine environment. This is linked to their cell wall composition, which is rich in polysaccharides with functional groups capable of binding metal ions. While this ability provides opportunities for applications in nutrient supplementation, it also raises concerns regarding food safety, as seaweeds may accumulate toxic elements depending on environmental conditions (Romera et al. 2007; Čmiková et al. 2024).

The efficiency and type of heavy metal accumulation differ significantly between brown algae (Phaeophyceae) and red algae (Rhodophyta). Brown algae are generally considered the most effective bio-accumulators of toxic metals such as lead (Pb), cadmium (Cd), copper (Cu), and zinc (Zn). As a result, they have been widely studied and applied as biosorbents in wastewater treatment and environmental clean-up (Domínguez-González et al. 2010).

By contrast, red algae accumulate heavy metals to a lesser extent overall, but they exhibit specific affinities for different elements. Their cell walls are composed mainly of carrageenans, agar, and other sulfated galactans, which provide binding sites for trace elements such as arsenic (As), vanadium (V), and manganese (Mn). Especially organic arsenicals can pose a safety concern when red algae are used in food products (Domínguez-González et al. 2010; Čmiková et al. 2024).

1.4 Red algae (Rhodophyta)

Rhodophyta are a diverse group of mostly marine macroalgae, there are around 8,000 known species, mostly inhabiting intertidal and subtidal zones that reach depths of 40 m, sometimes even up to 250 m. They are characterized by their red coloration, which is caused by the red and blue pigments phycoerythrin and phycocyanin, which are that optically strong, that they conceal the chlorophyll a, β-carotene, and unique xanthophylls, which are green or yellow pigments. Their cell walls are composed of cellulose, agars, and carrageenans. Numerous red algae are of significant economic value. Species such as *Palmaria palmata* (dulse) and *Chondrus crispus* (Irish moss) are edible, while *Kappaphycus*, *Gracilaria*, and *Gelidium* are important industrial sources of carrageenan and agar, generally used in the food, pharmaceutical, and biotechnology sectors (Sheath 2003; El Gamal 2010).

1.4.1 *Palmaria palmata* (Dulse)

Palmaria palmata (L.) Kuntze, commonly known as dulse, is a red alga (Rhodophyta) belonging to the family Palmariaceae. It is native to the cold and temperate waters of the North Atlantic, where it grows from Northern Portugal to the Barents Sea in Europe and from Long Island up to the Canadian Arctic in North America (Figure 3). It typically grows attached to rocks or larger seaweeds in the lower intertidal and upper subtidal zones. Its growth is influenced by temperature, light availability, and nutrient conditions, and it is particularly found in temperate and subarctic regions (Stévant et al. 2023).

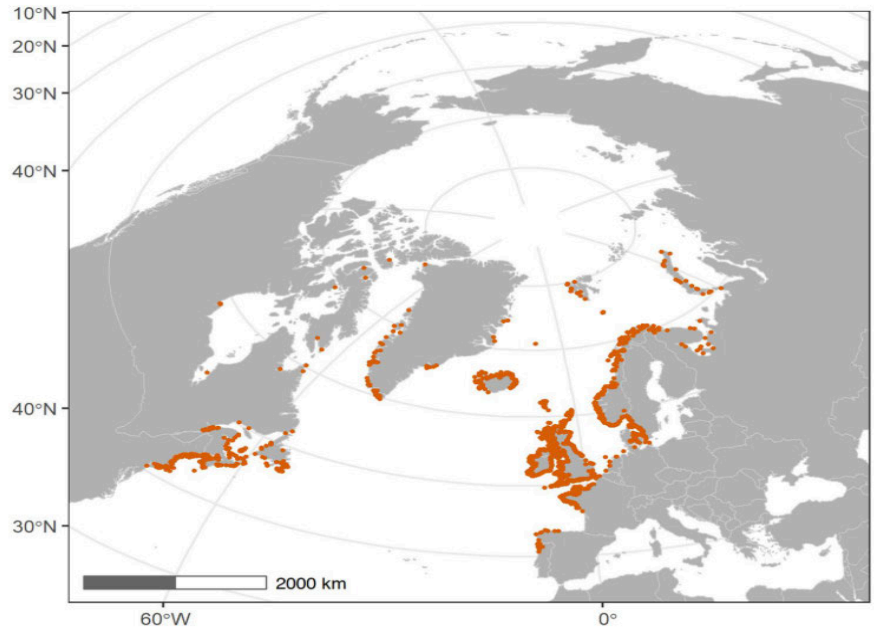

Figure 3: Geographic distribution of Palmaria palmata in the North Atlantic.

The species is found from Northern Portugal to the Barents Sea in Europe and from Long Island to the Canadian Arctic in North America, typically inhabiting the lower intertidal and upper subtidal zones (Source: Stévant et al. 2023)

The structure of *P. palmata* is characterized by flattened, oblong fronds that spread like the shape of a hand. The fronds usually measure 10-20 cm but can reach up to 50 cm in length under good conditions. Young fronds are bright red in color, while older darken to reddish-brown and may even turn greenish under strong sunlight (Figure 4). The texture changes as the algae mature, from tender in young plants to leathery in older ones. Reproduction is generally induced under low light and cold-water conditions, reflecting its adaptation to northern marine environments (Stévant et al. 2023).

Figure 4: Morphological appearance of Palmaria palmata (Dulse)

The red alga is characterized by flattened, oblong fronds resembling the shape of a hand, typically 10–20 cm in length (Source: Stévant et al. 2023).

Dulse has been part of human diets since at least the 5th century, especially in coastal regions of Ireland, Scotland, and Iceland, where it was eaten fresh, dried, or cooked in soups. It was valued as a famine food and also used as cattle feed. Today it remains a traditional food in parts of Canada and Northern Europe, while its global reputation as a nutritious and sustainable food source is growing (Xu et al. 2024).

Nutritionally, *P. palmata* is considered one of the most valuable edible seaweeds. It contains between 8-35% protein (dry weight), depending on season and location, making it one of the richest algal protein sources. Fresh fronds contain about 80-85% water. It is also a rich source of dietary fiber, dominated by xylans, which have prebiotic potential. Dulse provides essential vitamins, including A, C, E, and several B vitamins, notably vitamin B12, which is rare in plant-based foods. Its mineral composition includes high levels of iodine, iron, potassium, calcium, magnesium, and manganese. Lipid content is low but enriched in omega-3 fatty acids, its favorable omega-6/omega-3 ratio adds to its health benefits (Millan-Linares et al. 2019; Xu et al. 2024).

Like many seaweeds, *P. palmata* is capable of accumulating trace elements from seawater. It shows particularly high bioavailability for manganese and vanadium, a related species *Palmaria elongata* shows a vanadium concentration of 130.1 ± 11.51 µg/g. Vanadium, while not essential for humans, plays a role as an enzyme cofactor and can mimic insulin activity, but

careful monitoring is required since seaweeds can also concentrate heavy metals and environmental pollutants. Ensuring safe harvest locations and quality control is therefore important for its commercial use (Domínguez-González et al. 2010).

Today, dulse is consumed directly as a dried snack, incorporated into breads, soups, and plant-based products, or used as a seasoning and salt substitute. Beyond food, it has growing importance in aquaculture as a feed additive and in biorefinery approaches (Stévant et al. 2023). Overall, *P. palmata* is of remarkable cultural, nutritional, and scientific importance. Its high protein and mineral content, rare vitamins, beneficial fatty acids, and diverse bioactive compounds make it nutritional rich and a promising resource for sustainable food production, health-promoting products, cosmetics, and biotechnology.

1.4.2 *Chondrus crispus* (Irish Moss)

Chondrus crispus Stackhouse, commonly known as Irish moss or carrageen moss, is a red macroalga (Rhodophyta) belonging to the family of Gigartinaceae which is widely distributed along the North Atlantic coasts of Europe and North America, particularly abundant in Ireland and parts of Northern Europe. It typically inhabits the lower intertidal to subtidal zones, growing on rocky substrates in relatively sheltered areas. Like other Rhodophyta, it possesses the red pigments phycoerythrin and phycocyanin, which mask chlorophyll-a and enable efficient light harvesting in deeper or shaded waters (Collén et al. 2014; Čmiková et al. 2024; Park et al. 2024).

Structurally, *C. crispus* is one of the more diverse algae, showing more variability in size and morphology that other algae species (Chopin et al. 1996). *C. crispus* is generally characterized by a fan-like thallus and a triphasic reproductive cycle typical of red algae. The fronds are typically up to 15 cm long, flat, cartilaginous, and dichotomously branched (Figure 5), with coloration ranging from greenish-yellow to reddish-brown or purple depending on environmental conditions such as light intensity and water depth (Fredericqi et al. 1992; Collén et al. 2014; Park et al. 2024).

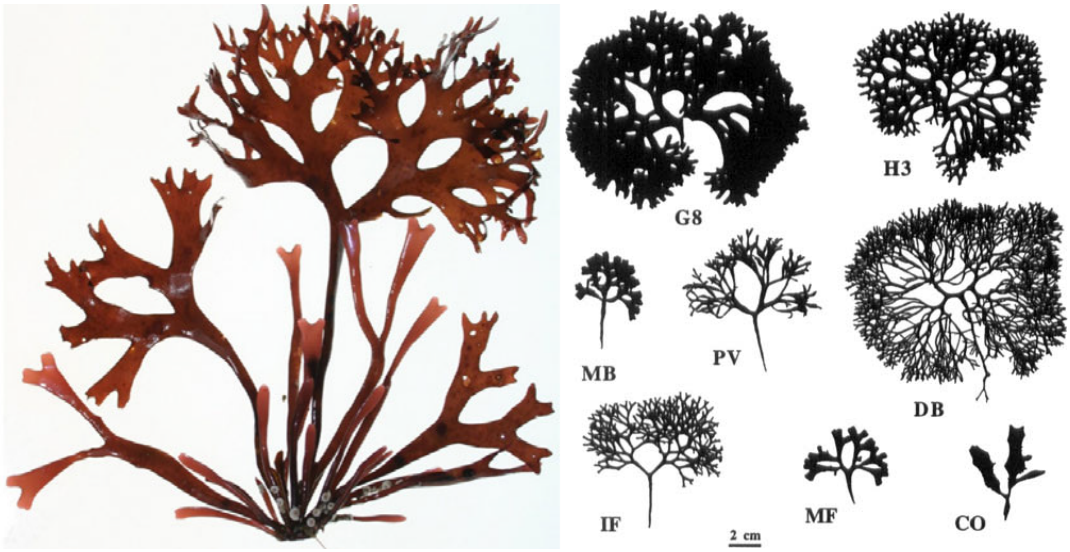

Figure 5: Morphological appearance of Chondrus crispus (Irish moss)

The red alga is characterized by dichotomously branched, fan-like fronds, varying in color from greenish-yellow to reddish-brown or purple depending on environmental conditions and also varying in size and morphology (Source: left: Chopin et al. 1996; right: Collén et al. 2014).

Irish moss has a long history of human use, particularly in Ireland, where it was traditionally harvested as food, medicine, and a thickening agent. During famines, it provided a vital source of nourishment, while in daily use it was boiled into puddings, soups, and tonics. Its common name “carrageen moss” derives from the district of Carrageen in Ireland, which became well known for collecting and processing this seaweed for carrageenan extraction (Collén et al. 2014; Hasan 2017; Park et al. 2024).

C. crispus is a rich source of proteins, dietary fibers, minerals, and bioactive compounds. Protein content ranges from 10–27% of dry weight, with amino acid that are rich in alanine, glutamic acid, glycine and arginine(Čmiková et al. 2024; Park et al. 2024). Mineral content is particularly high, with substantial levels of calcium, magnesium, potassium, sodium, iron, zinc, and iodine, making it a valuable source of micronutrients (Hasan 2017; Čmiková et al. 2024). The nutritional composition, however, is highly variable and influenced by environmental factors such as season, geography, salinity, and nutrient availability (Marinho-Soriano et al. 2006).

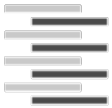

The most important bioactive compounds of *C. crispus* are carrageenans, which have widespread industrial application as gelling, thickening, and stabilizing agents in the food, pharmaceutical, and cosmetic industries. Beyond their functional properties, carrageenans and other sulfated polysaccharides exhibit antioxidant, antimicrobial, antiviral, anticoagulant, immunomodulatory, and anticancer activities. Recent studies confirm that extracts of *C. crispus* possess significant antioxidant and cytotoxic activity (Collén et al. 2014; Park et al. 2024)

1.5 Vanadium

Vanadium (V) is a natural occurring transition metal that is found in the earth-crust, seawater and in living organisms. In seawater the typical concentration of V ranges from 30-50 nM, making it one of the more common trace metals in the ocean (Crans et al., 2004; Winter and Moore, 2009). While vanadium is not universally essential for all organisms, it plays indispensable roles in certain algae, fungi, bacteria, and marine invertebrates, where it participates in nitrogen fixation, halogenation, and metal storage (Crans et al. 2004).
In marine environment vanadium is mostly found in its pentavalent form as vanadate ($H_2VO_4^-$), which is structurally and chemically similar to phosphate and is stabilized within the enzymes active site by a conserved histidine residue, this cofactor is important for catalytic activity. Because of this similarity, vanadate can fit into phosphate-binding sites in proteins and enzymes and therefor can act as a substitute or interfere with phosphate in biological processes (Butler and Carter-Franklin 2004; Crans et al. 2004; Rehder 2012).

Marine macroalgae, particularly kelp, can accumulate high quantities of vanadium. The tissue concentrations can reach several hundred milligrams per kilogram of dry weight, and in some brown algae up to 1% of their dry weight (Leblanc et al. 2015; Wever et al. 2018). This accumulation is assumed to be linked to the existence of vanadium-dependent haloperoxidases in these organisms, since the activity of V-HPOs is partially linked to the amount of vanadium that is available to the macroalgae. The amount of vanadium present in algal tissues, however, is not constant, it changes depending on the species, season, and local environment (Crans et al. 2004; Punitha et al. 2018).

Modern methods such as graphite furnace atomic absorption spectroscopy (GFAAS) make it possible to measure vanadium concentrations in algae very precisely (Punitha, 2018). This allows researchers to study how trace metal availability affects algal metabolism.

1.6 Baltic Sea and vanadium concentration

The Baltic Sea is a semi-enclosed, brackish body of water bordered by nine countries and home to about 85 million people in its catchment area (Figure 6) (Korpinen et al. 2010). Unlike the open ocean, which has a relatively stable salinity of about 35 practical salinity units (PSU), the Baltic Sea receives vast amounts of freshwater from rivers and has only a narrow connection to the North Sea. This restricted exchange results in much lower salinity levels and distinct gradients. In the northernmost areas, such as the Bothnian Bay, surface waters can be almost fresh, with salinity below 3 PSU. In the central Baltic Sea, surface salinity averages around 6–7 PSU, while deeper layers reach approximately 10 PSU (Bauer et al. 2017). A permanent halocline, typically between 50- and 70-meters depth, separates the fresher surface water from the more saline deep water. Because vertical mixing is limited, deep basins often develop oxygen-depleted (sulfidic) conditions, interrupted only occasionally by inflows of oxygen-rich North Sea water (Korpinen et al. 2010; Bauer et al. 2017).

Figure 6: Map of the Baltic Sea and surrounding countries

The Baltic Sea is a semi-enclosed brackish water body bordered by nine countries. Its restricted connection to the North Sea results in strong salinity gradients, limited water exchange, and long residence times, making it highly sensitive to environmental stress and pollutant accumulation (Source: Korpinen et al. 2010).

Its natural features make it especially sensitive to pollution with water residence times of around 30 years, depths are relatively shallow, and the connection to the North Sea is narrow. These factors limit water exchange and cause pollutants to accumulate rather than disappear. The sea is also biologically fragile, as relatively few species are adapted to its brackish environment, leaving ecosystems more vulnerable to stress from human activities and contaminants (Korpinen et al. 2010; Bauer et al. 2017).

Pollution from heavy metals like cadmium, mercury and lead occur at concentrations up to 20 times higher than in North Atlantic seawater. Which are caused by pollution through industrial sources, agriculture, wastewater, shipping ports, and consumer products, also atmospheric transport brings in pollutants from far beyond the Baltic region (Figure 7) (Korpinen et al. 2010). Surprisingly, the concentration of vanadium remains low. In the open ocean, dissolved vanadium maintains stable concentrations of around 39 nmol/L. In contrast, the Baltic Sea is significantly poor in vanadium, with typical surface concentrations near 3 nmol/L, which is roughly 60% lower than North Atlantic seawater values (Bauer et al. 2017).

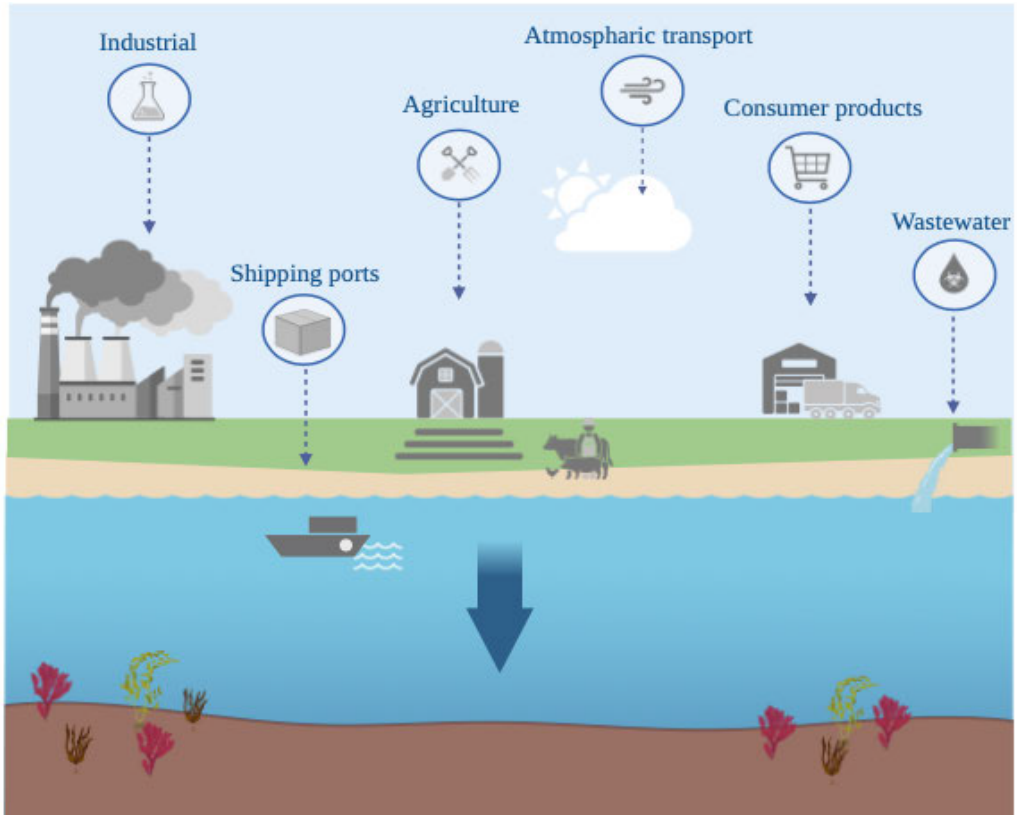

Figure 7: Sources of heavy metal pollution to the Baltic Sea

Main anthropogenetic inputs include industry, agriculture, wastewater, shipping ports, consumer products, and atmospheric transport. These contribute to the accumulation of heavy metals and other contaminants in the ecologically vulnerable brackish ecosystem. *(Created in https://BioRender.com)*

Reasons for the low vanadium content in the Baltic Sea could be explained through different factors. Firstly, when river water mixes with seawater, much of the vanadium is scavenged onto iron-rich particles or bound to organic matter, preventing it from entering the open waters. Within the Baltic Sea itself, manganese redox cycling in laminated zones further reduces dissolved vanadium, as it is adsorbed onto manganese oxides. Lastly, the river water inputs are also relatively low in vanadium compared to other coastal systems, reinforcing the overall deficit (Bauer et al. 2017).

1.7 Halogenated organic compounds (HOCs) & Haloperoxidases (HPOs)

Halogenated organic compounds are naturally produced chemicals that are very common in marine environments, especially in seaweeds. They represent a diverse class of natural products like volatile halocarbons such as bromoform, chloroform, dibromoethane and also larger metabolites like halogenated terpenes, phenols, peptides and polyketides (Butler and Carter-Franklin 2004; Butler and Sandy 2009; Wever and Van Der Horst 2013)

For macroalgae, these compounds serve many ecological purposes. They can act as chemical defenses against herbivores and microbial infections, they can also prevent a formation of biofilm on their surfaces (antifouling) and help reduce the growth of competing species (allelopathy)(Butler and Sandy 2009; Wever et al. 2018) (Butler & Sandy, 2009; Wever et al., 2018). Some halogenated compounds also help algae control reactive oxygen species inside their cells, thereby reducing oxidative stress (Punitha et al. 2018). Figure 8 shows some examples of halogenated organic compounds found in macro algae and other marine products.

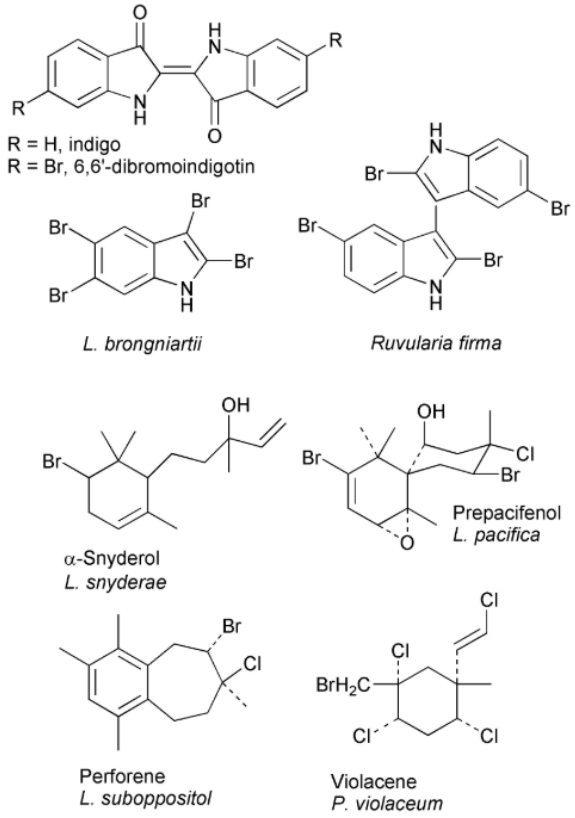

Figure 8: Example of halogenated marine products

Chemical structures of selected halogenated metabolites isolated from different marine algae, including indigo derivatives, brominated indoles, terpenes, and phenolic compounds. These halogenated organic compounds (HOCs) play key ecological roles (Source: Butler and Carter-Franklin 2004).

The first halogenating enzyme identified was a haem-dependent chloroperoxidase (CPO) from the fungus *Caldariomyces fumago*, discovered in the 1960s. Following that discovery other enzyme classes have been identified. The formation of HOCs is catalyzed by a group of enzymes known as haloperoxidases. These enzymes use hydrogen peroxide to oxidize halides (Cl^-, Br^-, I^-), forming hypohalous acids (HOCl, HOBr, HOI), which then halogenate organic substrates (Butler and Sandy 2009). HPOs are widespread in nature and can be found in bacteria, fungi, algae, lichens, and marine invertebrates. In macroalgae, they play particularly important roles in ecological interactions and in coping with environmental stress. Depending on their cofactor requirements, HPOs are divided into three main groups: cofactor-free HPOs, heme-dependent HPOs (HI-HPOs), and vanadium-dependent HPOs (V-HPOs) (Punitha et al. 2018). While they perform similar chemically, they can be differentiated by their cofactors, substrate ranges, and ecological roles. Among these, V-HPOs are particularly relevant in marine macroalgae (Leblanc et al. 2015).

1.8 Vanadium-dependent haloperoxidases (V-HPOs)

Vanadium-dependent haloperoxidases (V-HPOs) were first discovered in the brown alga *Ascophyllum nodosum* in the 1980s, marking it the first identification of an enzyme containing vanadium as a prosthetic group. Since then, V-HPOs have been found across diverse organisms, including fungi, bacteria, and especially marine macroalgae. (Leblanc et al. 2015)

Among haloperoxidases, vanadium-dependent haloperoxidases (V-HPOs) stand out because they use vanadate as a cofactor to catalyze halogenation (Butler and Carter-Franklin 2004). They are classified by halide specificity into vanadium chloroperoxidases (VCPOs), which oxidize Cl^-, Br^-, and I^- with vanadium bromoperoxidases (VBPOs), which act on Br^- and I^- and vanadium iodoperoxidases (VIPOs), which are specific for I^- (Crans et al. 2004; Leblanc et al. 2015). Rhodophyta like *Palmaria decipiens, Delisa pulchra* are particularly rich in VBPO, although *P. palmata* is not listed, its Antarctic relative *P. decipiens* demonstrates similar enzymatic activity, supporting the likelihood of VBPO presence in *P. palmata* as well (Wever et al. 2018). In Figure 9 the reaction scheme of VBPOs can be observed.

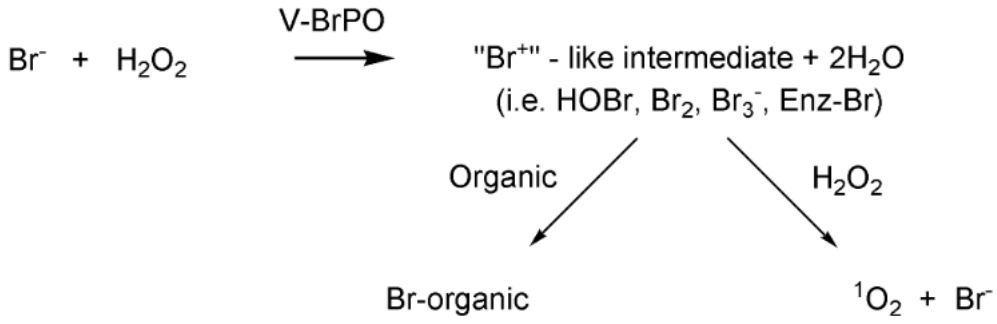

Figure 9: Reaction scheme of vanadium bromoperoxidase (VBPO)

VBPO catalyzes the oxidation of bromide ions (Br^-) by hydrogen peroxide (H_2O_2), forming reactive brominating intermediates (e.g., HOBr, Br_2, Br_3^-, enzyme-bound Br). These intermediates can either halogenate organic substrates, leading to the formation of brominated organic compounds, or react with excess H_2O_2 to produce singlet oxygen ($^1O_2$) and regenerate Br^- (Source: Butler and Carter-Franklin 2004).

Structurally, V-HPOs are relatively conserved, with molecular masses around 67 kDa, and they share a similar coordination of vanadium in the active site (Punitha et al. 2018). V-HPOs share a conserved α-helical protein fold with a funnel-shaped active site that houses a vanadate ion in trigonal bipyramidal geometry. This vanadate is tightly coordinated to a conserved histidine residue and stabilized by surrounding hydrogen bonds (Leblanc et al. 2015). The catalytic cycle begins with the binding of hydrogen peroxide to the vanadium center, leading to the formation

of a peroxovanadate. This activated complex oxidizes halide ions to generate hypohalous acids (e.g., HOBr), which can halogenate substrates within the active site, such as terpenes, phenols, or indoles, with significant regio- and stereoselectivity or escape into the medium if no suitable substrate is present (Butler and Sandy 2009). The vanadium cofactor is very stable, and V-HPOs shows high tolerance to heat and organic solvents (Wever et al. 2018). The three-dimensional structure of an VBPO analyzed from the macro algae *A. nododmus* is visualized in Figure 10, it shows the dimeric structure of the enzyme and the vanadate ions that bind to its active sides (Leblanc et al. 2015).

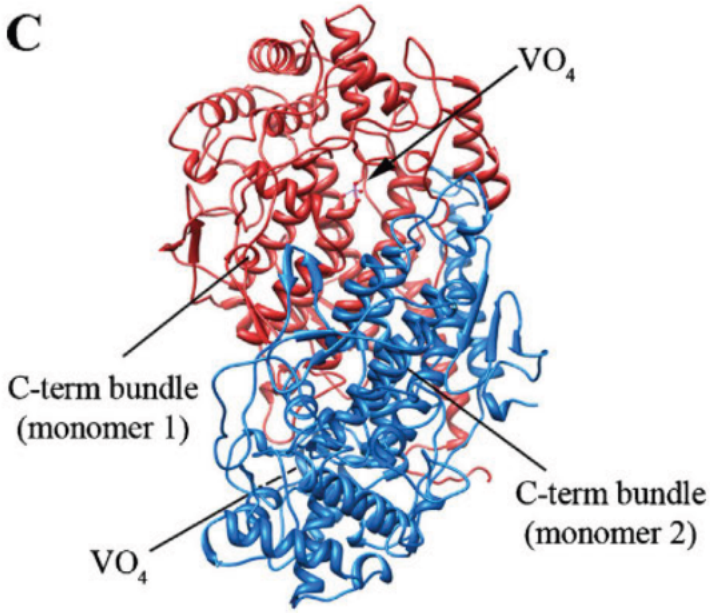

Figure 10: Three-dimensional structure of a vanadium-dependent bromoperoxidase (VBPO) from A. nodosums

Crystal structure of VBPO from the algae *A. nodosmus* shown as a dimer with monomer 1 (red) and monomer 2 (blue). Each monomer contains a conserved α-helical fold with a C-terminal bundle and an active site coordinated with vanadate (VO_4), essential for catalytic halogenation reactions (Source: Leblanc et al. 2015).

In terms of localization, V-HPO activity is often concentrated near the outer surfaces of algal thalli. This localization supports their defensive role, placing halogenating activity at the border between algal tissue and the surrounding seawater where microbial colonization and pathogen attacks occur (Punitha et al. 2018). In Rhodophyta specifically V-BPOs are often stored in specialized gland cells, which suggests a tightly regulated halogenation system (Wever et al. 2018). Moreover, expression of V-HPOs is strongly influenced by environmental stress. Pathogen infection, heavy metal exposure, or oxidative stress can upregulate their production.

A further important ecological role of V-HPOs is their contribution to the production of volatile halogenated organic compounds (halocarbons). Under stress conditions, such as exposure to light or elevated H_2O_2 levels, VBPOs can release HOBr into the surrounding seawater, where it reacts with dissolved organic matter to that leads to the formation of volatile halocarbons like bromoform ($CHBr_3$) and dibromomethane (CH_2Br_2). These volatile compounds enter the atmosphere, contributing to halogen cycling and ozone depletion (Wever et al. 2018). Beyond their ecological importance, the stability, selectivity, and versatility of V-HPOs highlights their potential in biotechnology (Butler and Sandy 2009; Wever et al. 2018).

2 Material

2.1 Investigated algae species

Table 1: Name and sample condition of investigated algae species

Species Name	Sample condition
Palmaria palmata	Dried and milled
Chondrus crispus (A1)	Dried and milled
Chondrus crispus (A2)	Dried and milled
Himanthalia elongata	Dried and milled
Ascophyllum nodosum	Dried and milled
Lithothamnium	Dried and milled
Palmaria palmata	Fresh
Chondrus crispus	Fresh

2.2 Solutions and chemicals

Table 2: Solutions and chemicals

Description	Manufacturer
Bovine serum albumin (BSA)	Sigma-Aldrich
Ethylenediaminetetraacetic acid (EDTA)	ROTH
Tris(hydroxymethyl)aminomethane (Tris)	ROTH
MES (2-(*N*-morpholino) ethanesulfonic acid) (MES)	ROTH
Vanadium standard solution	Supelco (Sigma-Aldrich)
Sulfuric acid	ROTH
Hydrogen peroxide	ROTH
Nitric acid	ROTH
Certified reference material (CRM) Trace Metals 1 – WP	Supelco (Sigma-Aldrich)

Phenylmethanesulfonyl fluoride	Sigma-Aldrich
NaOH	ROTH
β-mercaptoethanol	ROTH
Hydrochloric acid (HCl)	ROTH
ROTI® Quant universal kit	ROTH
Ammonium sulfate (AS)	ROTH
Potassium chloride (KCl)	ROTH
TGX FastCast acrylamide kits	Bio-Rad
Dithiothreitol (DTT)	Sigma-Aldrich
ROTI® Blue quick	ROTH
peqGOLD Marker unstained	VWR Life Science

2.3 Laboratory equipment

Table 3: Laboratory Equipment

Description	Manufacturer
HACH Digesdahl® digestion apparatus	HACH Company
Muffle furnace	Nabertherm
contraAA800 (HR-CS-AAS)	AnalytikJena
Brandson Ultarsonics Sonifier SFX250	Fisher Scientific GmbH
Ultra-Turrax® T25	IKA
ÄKTApurifier	GE Healthcare
Orbital shaker	neoLab Migge GmbH
UV spectrometer	Shimadzu
Laboratory scale	ACCULAB
Electrophoreses chamber	Bio-Rad
Magnetic stirrer	2mag AG
Biofuge® stratos	Heraeus Instrument
pH Meter	Knick International
Drying oven	Memmert
Arium® Pro Ultrapure water system	Sartorius

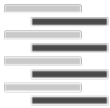

2.4 Consumables

Table 4: Consumables

Description
Centrifuge tubes 50 ml
Reaction tube 1.5 ml
Micro UV cuvettes
Plastic lab spoon
Pasteur pipette

2.5 Glassware and porcelain

Table 5: Glassware and porcelain

Description
Porcelain mortar
Porcelain disk
Digestion flask
Volumetric flask
Ceramic knife
Beaker
Stirrer magnet
Laboratory bottle with screw cap

2.6 Chromatogram columns

Table 6: Chromatogram columns

Description	Manufacturer
5 ml HiTrap Desalting column	GE Healthcare
1 ml HiTrap DEAE FF column	GE Healthcare

3 Methods

In all steps of the present Master thesis, either pre-dried and milled algae (dry material) or fresh and frozen algae (fresh material) were used, all of which were kindly provided by Dr. Thomas Stegemann from the Pharmaceutical institution at the University of Kiel. The fresh and dried materials consisted of *Palmaria palmata* and *Chondrus crispus*. In addition, other pre-dried and milled algae species were used as references, namely *Himanthalia elongata*, *Ascophyllum nodosum*, *Lithothamnium*, and another *Chondrus crispus* variant (A1). All experimental work was carried out at the University of applied sciences Hamburg (HAW) under the supervision of Prof. Çiçek.

3.1 Vanadium extraction

To determine which preparation method is better suited to measure the vanadium content in a sample, three different methods were tested, the digestion apparatus, dry ashing and wet digestion. For all three methods, a pre dried and milled sample of *P. palmata* was used to determine wish method is best suited for further experiments.

3.1.1 HACH digestion

The HACH Digesdahl® digestion apparatus is designed for the rapid wet-chemical decomposition of a wide range of sample types, including food products, feedstuffs, plant tissues, fertilizers, oils, sludges, and wastewaters. Its main purpose is to break down organic and inorganic matrices in preparation to determination of total amount of trace metals, minerals, and nutrients by subsequent analytical methods such as colorimetry, titrimetry, or turbidimetry (HACH Company, 2000).

The apparatus consists of a compact heating unit with adjustable digital temperature control (100-480 °C), a specially shaped 100 mL digestion flask, and a fractionating head system. The fractionating system includes a vertical column, a capillary funnel for reagent addition, and a fume collection hood that is connected to a water jet pump. Protective components such as a heat shield, flask weight, and safety screen ensure stable operation and user safety (HACH Company, 2000).

The digestion process itself is carried out in two main stages; the schematic process is illustrated in Figure 12. In the first stage, a sample amount of approximately 0.1-3.0 g is mixed with 5 ml concentrated sulfuric acid in the digestion flask and heated to around 350 °C. The acid dehydrates and carbonizes the sample, producing a reducing environment that helps convert organically bound nitrogen into ammonium, this is visible by white fumes forming in the flask. In the second stage, 5 ml of hydrogen peroxide is introduced dropwise through the capillary funnel. Under the hot acidic conditions, it reacts to form peroxymonosulfuric acid, a very powerful oxidizing agent that quickly and efficiently destroys remaining organic matter. When the solution becomes clear, the digestion is complete. Excess peroxide is boiled off, and the digest is cooled and diluted with 100 ml of ultrapure water, for further analysis of the vanadium content with the GFAAS (HACH Company, 2000).

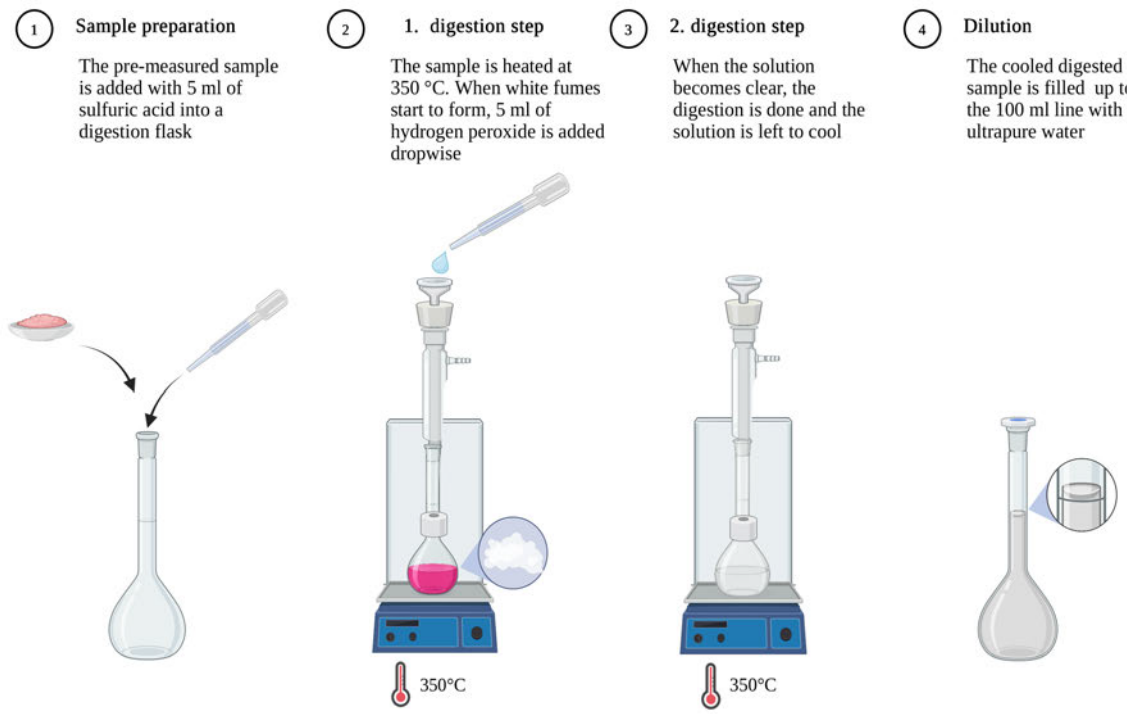

Figure 11: Digestion process using the HACH Digesdahl® apparatus

Schematic overview of the chemical digestion procedure. (1) A pre-weighed sample is mixed with 5 mL concentrated sulfuric acid. (2) The sample is heated at 350 °C, and 5 mL hydrogen peroxide is added dropwise until white fumes appear. (3) Digestion continues until the solution becomes clear, after which it is cooled. (4) The digest is diluted to 100 mL with ultrapure water for subsequent analysis *(Created in https://BioRender.com)*.

3.1.2 Dry ashing

Dry ashing is a classical sample preparation technique that aims to remove all organic matter from a material by thermal decomposition, leaving only the inorganic residue (ash). The method is commonly applied in food and feed analysis to determine the overall mineral content, in environmental studies to quantify the inorganic portion of sludges, soils, and wastes, and as a preparatory step for instrumental techniques such as atomic absorption spectroscopy (AAS) (Marshall 2010)

Despite its broad use, ashing has certain limitations. Volatile elements such as chlorine, phosphorus, sulfur, and some metals (e.g., mercury, lead) can be lost at high temperature, which can result in an underestimation of total mineral content (Tack et al. 1997; Marshall 2010). Furthermore, ashing is relatively slow compared to modern wet digestion techniques (e.g., HACH digestion), which achieve faster results (Marshall 2010) .

The principle is based on incineration of the sample in a muffle furnace. In this case 50 mg of the sample was measured on to a porcelain disk and then put into the preheated muffle furnace at a set temperature of 600 °C for 5 h until the sample turns into white ash. It was then left overnight to cool down, furthermore 2 ml of nitric acid was added to the sample before it was transferred into a 100 ml volumetric flask, which was then filled with 100 ml of ultrapure water to further analyze with GFAAS. An overview of the procedure is shown in Figure 12.

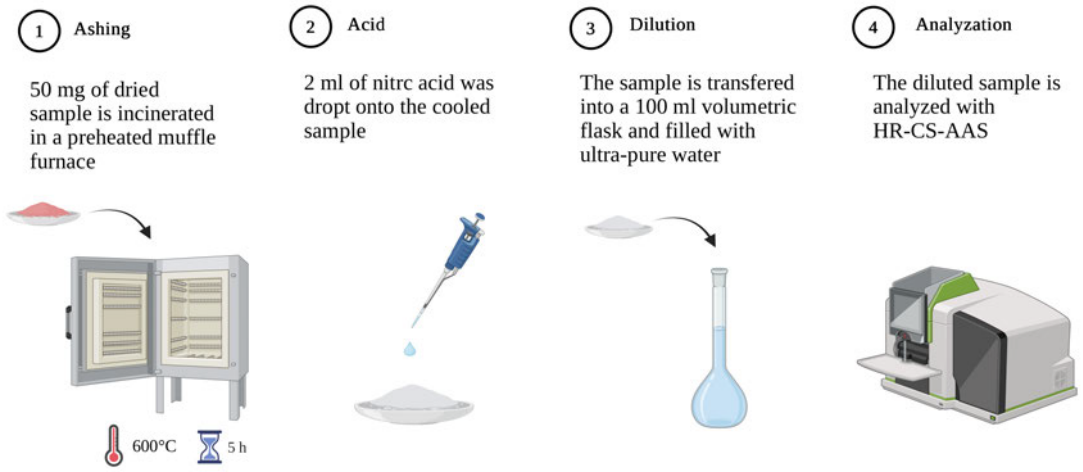

Figure 12: Dry ashing procedure for sample preparation

Stepwise overview of the dry ashing method. (1) 50 mg of dried sample is incinerated in a preheated muffle furnace at 600 °C for 5 h. (2) After cooling, 2 mL of nitric acid is added to the ash. (3) The residue is transferred into a 100 mL volumetric flask and diluted with ultrapure water. (4) The diluted sample is analyzed by high-resolution continuum source atomic absorption spectroscopy (HR-CS-AAS) *(Created in https://BioRender.com)*.

3.1.3 Wet digestion

In addition to the HACH digestion method and dry ashing, a further approach was the wet digestion. This technique doesn't follow a specific method. It was used mostly as a reference to see if extended exposure with water and nitric acid would be sufficient for the extraction of trace metals from an organic sample.

For this procedure, weighed portions of the samples were transferred into volumetric flasks. One sample was ground beforehand in a porcelain mortar to ensure homogeneity and improve the efficiency of the digestion. Each flask was then filled with 50 mL of ultrapure water and 2 mL of concentrated nitric acid. The flasks were subsequently shaken at room temperature for 18 h at 450 rpm, with the shaking direction reversed after every 50 rotations to ensure thorough suspension and contact of the acid with the sample matrix. After digestion, the solutions were diluted to 100 mL with ultrapure water. The final solutions were measured using HC-CS GFAAS.

Grinding of the sample prior to digestion increases the available surface area, thus enhancing the rate of acid attack (Holthuizen and Çopuroğlu 2024). Extended shaking at controlled speed provides consistent exposure of the sample to the acid, promoting reproducibility and preventing incomplete dissolution. A schematic representation of the procedure is provided in Figure 13.

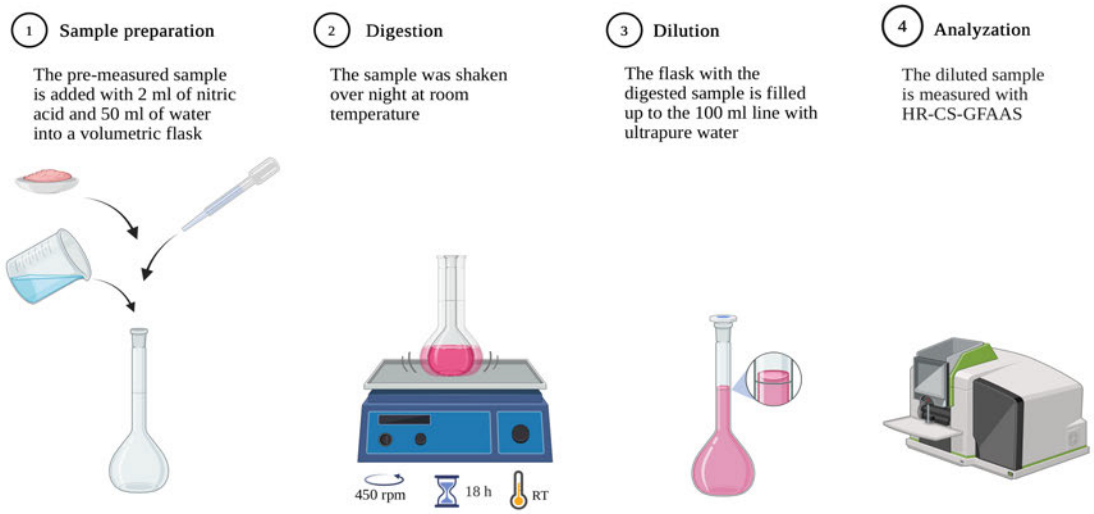

Figure 13: Wet digestion procedure for sample preparation

Stepwise overview of the wet digestion method. (1) A pre-weighed sample is mixed with 2 mL of nitric acid and 50 mL of ultrapure water in a volumetric flask. (2) The sample is shaken overnight at room temperature (450 rpm, 18 h). (3) After digestion, the solution is diluted to 100 mL with ultrapure water. (4) The diluted sample is analyzed by high-resolution continuum source graphite furnace atomic absorption spectroscopy (HR-CS-GFAAS) *(Created in https://BioRender.com)*.

3.2 High-Resolution Continuum Source Atomic Absorption Spectrometry (HR-CS-AAS)

High-Resolution Continuum Source Atomic Absorption Spectrometry (HR-CS AAS) is a modern and highly sensitive technique for the determination of trace elements in complex matrices. The instrument consists of four main components: a light source, an atomization unit, a monochromator, and a detector (Figure 14) (Welz 2005).

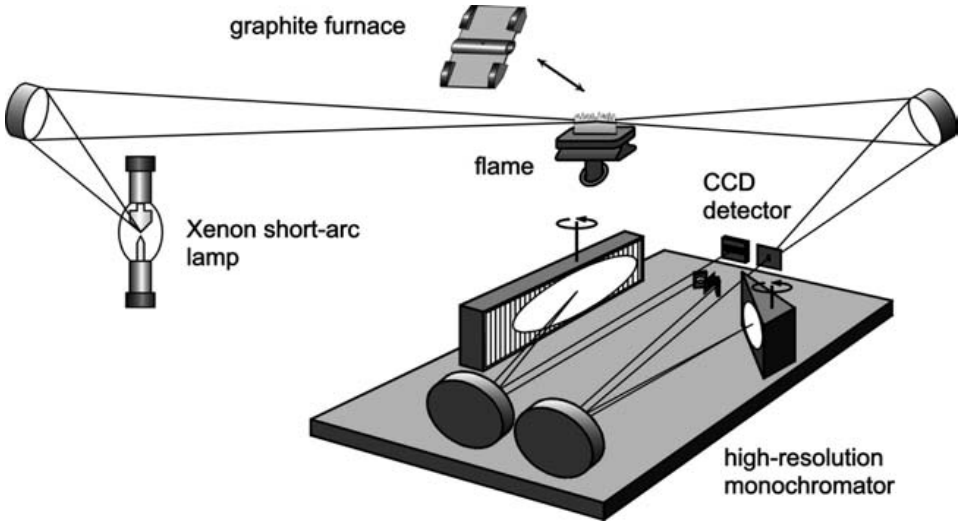

Figure 14: Schematic overview of the High-Resolution Continuum Source Atomic Absorption Spectrometer (HR-CS AAS)

The instrument consists of a xenon short-arc lamp as a continuum light source, an atomization unit (graphite furnace or flame), a high-resolution echelle double monochromator for wavelength selection, and a CCD array detector for simultaneous multi-pixel measurement. This setup allows sensitive and selective detection of trace elements across the UV–visible range (Source: Welz 2005)

Unlike conventional atomic absorption spectrometry, which relies on element-specific hollow cathode lamps, HR-CS AAS uses a powerful xenon short-arc lamp as a continuum emitter. Due to the special shape of its electrode, a so-called hot spot is formed, which produces an extremely high radiation density covering the entire ultraviolet and visible range, from 190 nm to 900 nm. This allows all elements whose absorption lines lie within this spectral range to be analyzed without the need to change lamps (Welz 2005; Zvěřina et al. 2023).

The HR-CS-AAS is a dual atomizer, with the choice to use the flame atomization or the graphite furnace atomization unit. The decision lays both in the analyte and the concentration expected in the sample. For the flame atomization, samples with a higher concentration and a less complex matrix are preferred. For the use of the graphite furnace unit as an electrothermal atomizer, samples with small sample volumes and low concentration of the analyte are better suited (Welz 2005). That is why for this study the graphite furnace is used.

The samples are all introduced in liquid form. The graphite tube is purged with argon, an inert gas, throughout the process. Detection limits for graphite furnace AAS typically reach the ppb–ppt range (µg/L to ng/L). Heating of the graphite tube is achieved by applying an electrical voltage, taking advantage of the excellent conductivity of graphite, which acts as a resistance heater. The furnace is operated in the programmed stages, drying, pyrolysis, atomization, and clean-out, that ensures controlled volatilization of the analyte while removing matrix components (Welz 2005; Zvěřina et al. 2023). The program can be adjusted allowing to tailor the temperature program to the analyte and the sample matrix. The program used in this study is seen in Table 7.

Table 7: Temperature program of HR-CS-AAS for vanadium detection

Step	Name	Temp [°C]	Time [s]
1	Drying 1	80	20
2	Drying 2	90	20
3	Drying 3	110	10
4	Pyrolysis 1	350	20
5	Pyrolysis 2	1200	10
6	Gas adjustment	1200	5
7	Atomization	2550	8
8	Clean-out	2700	4

The wavelength for vanadium is at 318.3982 nm. This specific wavelength was chosen through a “cookbook” which is integrated into the program of the HR-CS AAS, for each heavy metal a pre-determined wavelength and temperature program can be chosen.

A high-resolution echelle double monochromator is used to disperse the broadband radiation of the xenon lamp and isolate the relevant absorption lines. This optical system provides wavelength stability and prevents spectral drift. The dispersed light is recorded by a CCD array detector, where each pixel functions as an independent measurement channel. Typically, the analyte absorption line is monitored across three pixels, while additional pixels may be assigned for background correction, independent of the wavelength chosen (Welz 2005; Zvěřina et al. 2023).

Before the measurement of the samples, the AAS needed to be calibrated, therefore four vanadium standard solutions ranging from concentration 1 µg/L to 10 µg/L (1 µg/L, 2.5 µg/L, 5 µg/L, 10 µg/L) and a blank were prepared and measured. The measuring method can be adjusted depending on the chosen concentration range and further allows the calculation of the calibration curve automatically. This allowed to have an immediate knowledge of the concentration of vanadium in the sample.

3.3 Validation of the AAS Method

Before cell disruption experiments and further measurements could be performed, the analytical method of HR-CS GFAAS was validated to ensure accuracy, precision, and reliability of vanadium quantification. Method validation is an essential condition in trace metal analysis, as it demonstrates that the method is suitable for its intended purpose and can provide reproducible and accurate results under defined conditions (EURACHEM, 2014). Several validation steps were carried out as described below.

3.3.1 Calibration curve and determination of LOD/LOQ:

A 10-point calibration curve was prepared using vanadium standards in the concentration range of 1-10 µg/L, plus a blank (ultrapure water). The calibration was used to establish the linearity of the method and to calculate the limit of detection (LOD) and limit of quantification (LOQ) according to standard procedures (Kruse et al. 2024).

3.3.2 Spike recovery experiments:

To assess potential analyte losses during the sample preparation process, particularly the digestion step, three digested algal samples were spiked with vanadium standards at concentrations within the calibration range (2.2 µg/L, 5.6 µg/L, and 9.5 µg/L). Recovery rates were calculated to verify that vanadium was not destroyed or lost during digestion, ensuring the reliability of the sample preparation procedure.

3.3.3 Reference standard solution:

A certified standard material (CRM, Trace Metals 1 – WP, Supelco, Merck) containing known amounts of vanadium, among other trace elements, was analyzed to confirm the accuracy of the AAS measurements. According to the certificate of analysis, the CRM contained 1500 ± 11 µg/L vanadium in 5 % HNO_3. The material is manufactured under ISO 17034 and ISO 17025 accreditation and is fully traceable to NIST standards.

A working standard solution with a target concentration of 6 µg/L vanadium was prepared by dilution of the CRM with ultrapure water. The dilution factor (DF) was set as 250, 1 ml of the CRM was diluted to a final volume of 250 ml, to achieve the desired concentration. The solution was prepared fresh on the day of analysis and measurement immediately.

Agreement between the measured and certified values provided an additional quality control for the method.

3.3.4 Comparison with an external reference method:

To further validate the method, one digested *P. palmata* sample that was previously analyzed by AAS was submitted for independent analysis using total reflection X-ray fluorescence spectroscopy (TXRF). TXRF is a multi-element technique that is well established for trace metal determination in biological samples (Zhang et al. 2024). Comparing results between HR-CS GFAAS and TXRF helped to confirm the reliability of vanadium quantification.

3.3.5 Precision and repeatability:

Method precision was evaluated in terms of intra-day and inter-day variability. Intra-day precision was assessed by preparing and analyzing six replicate samples within a single day, while inter-day precision was determined by preparing and measuring another six replicates one day later and comparing them with the initial set. Repeatability was further tested by measuring the same sample six consecutive times. These procedures follow established guidelines for analytical method validation in trace element analysis (EURACHEM, 2014).

Together, these validation steps can establish if the HR-CS GFAAS method provides accurate, precise, and reproducible measurements of vanadium in algal extracts and digested samples, ensuring the reliability of further measurements.

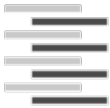

3.4 Determination of dry matter content

The dry matter content of fresh algal samples (*P. palmata* and *C. crispus*) was determined in order to express vanadium concentrations on a dry weight (DW) basis. Approximately 5 g of fresh algal material were weighed into pre-dried and pre-weighed containers. The samples were dried in a drying oven at 105 °C for up to 5 h, with intermediate weighing after 4 h to monitor weight stability. Drying was continued until a constant weight was reached (weight difference <0.5% between measurements).

The dry matter fraction (DM%) and water content (WC%) were calculated according to the following formulas:

$$DM\% = \frac{m_{dry}}{m_{fresh}} \cdot 100$$

$$WC\% = 100 - DM\%$$

where m_{fresh} is the fresh mass and m_{dry} the mass after drying. The dry matter content was then used to convert measured concentrations in fresh samples to dry weight equivalents (µg/g DW) for comparison with pre-dried, milled samples.

3.5 Cell disruption

Cell disruption serves to break the cell wall in order to release specific intracellular components. The choice of an appropriate disruption method depends on both the sample quantity and the size and morphology of the cells to be processed (Wada et al. 2024). A distinction is made between non-mechanical and mechanical disruption methods (Kakko et al. 2017). Three different methods were tested to find the most effective and gentle one for crude enzyme extraction.

As a preparative step before cell disruption the dried and fresh materials needed to be handled according to their physical state. For pre-milled and dried algal samples, the required amount of biomass was weighed, then suspended in extraction buffer and lastly stirred for 10 minutes to ensure complete resuspension. The sample-to-buffer ratio was standardized at 0.05 g algae per 1 mL buffer.

For fresh and frozen material, additional preparation was necessary. Frozen algae stored at –20 °C were thawed and carefully washed with ultrapure water to remove any residual impurities such as sand, sea salt, or vanadium originating from seawater, which could otherwise interfere with or falsify subsequent analyses. Excess water was drained, and the algae were left to air-dry for 10 minutes before being gently blotted with paper towels. Fresh algal material was finely chopped using a ceramic knife to increase the surface area for the following cell disruption. For fresh and frozen material, the sample-to-buffer ratio was standardized at 0.1 g algae per 0.5 mL buffer (Kamenarska et al. 2007). Following these preparative steps, one of the selected cell disruption methods was applied to extract the target enzymes.

Manly two different buffers were used according to two different publications (Kamenarska et al. 2007; Harnedy and FitzGerald 2013). Both buffers are listed in Table 8.

Table 8: Buffer compositions

Buffer nr.	Buffer composition	pH	publication
1	10 mM MES	7	(Kamenarska et al. 2007)
2	50 mM Tris-HCl +1 mM phenylmethanesulfonyl fluoride and 0.5 mM EDTA	7.4	(Harnedy and FitzGerald 2013)

3.5.1 Ultrasonic cell disruption

Ultrasonic cell disruption was one of the methods used to release V-HPOs from algal biomass. In ultrasonic disruption, a high-frequency generator produces mechanical vibrations that are transmitted to a sonotrode, which directs the acoustic energy into the sample. Pressure fluctuations in the liquid generate cavitation bubbles, which collapse violently and create extremely high local velocities and microjets at the liquid–solid interfaces. The resulting shear forces rupture surrounding cell walls and membranes, thereby releasing intracellular contents (Gomes et al. 2020).

The geometry of the vessel also plays an important role in ensuring effective lysis. A rosette cooling vessel was used in this study, which allows for more uniform sonication and continuous circulation of the suspension (Yasumitsu et al. 2013). Because algal cell walls are particularly stable due to their rigid polysaccharide and protein structures, longer treatment times of 10–20 minutes are often required to achieve complete disruption (D'Hondt et al. 2017).

One limitation of ultrasonic disruption is the generation of heat during cavitation, which can cause protein denaturation if uncontrolled. To prevent this, the algal suspension was placed in a rosette vessel submerged in an ice-water bath, maintaining the sample at approximately 20°C-25°C throughout the process (Yasumitsu et al. 2013; Gomes et al. 2020).

The algal–buffer mixture was transferred into the rosette vessel and subjected to ultrasonic treatment for 15 minutes at maximum amplitude and 100% duty cycle, ensuring complete disruption. The resulting suspension was centrifuged at 10,000 × g for 30 minutes at 4 °C to separate insoluble cell debris (pellet) from the soluble protein fraction (supernatant). The supernatant was retained for further purification steps, while the pellet was discarded. A stepwise representation of the procedure can be seen in Figure 15.

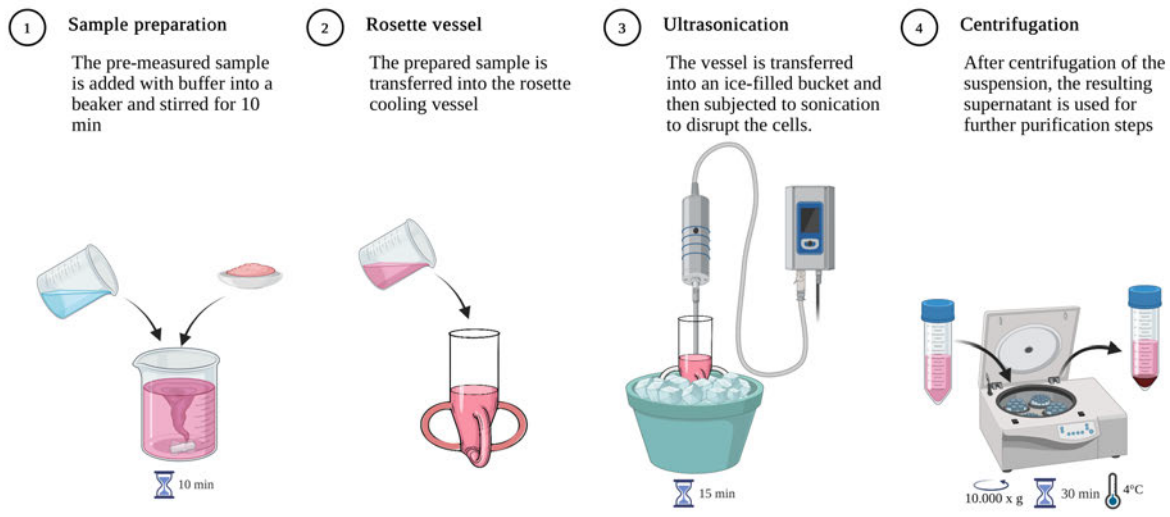

Figure 15: Ultrasonic cell disruption procedure

Stepwise overview of ultrasonic disruption used for protein extraction. (1) A pre-weighed algal sample is suspended in buffer and stirred for 10 min. (2) The suspension is transferred into a rosette cooling vessel. (3) The vessel is placed in an ice bath and subjected to 15 min of ultrasonication to rupture cell walls. (4) The disrupted suspension is centrifuged at 10.000 × g for 30 min at 4 °C, and the supernatant is collected for further purification *(Created in https://BioRender.com)*.

3.5.2 Homogenizer (Ultra-Turrax®)

The Ultra-Turrax® device is a high-shear homogenizer, it belongs to the mechanical methods of cell disruption, where the biomass is exposed to intense shear forces and turbulences that are generated by the rotor stator system. The device works by rapidly rotating a rotor inside a stationary stator, which creates localized shear gradients, cavitation and turbulences. This effectively breaks down cell walls and membranes, releasing intracellular proteins into the surrounding medium and homogenizes the suspension. Depending on the shaft size, volumes from a few milliliters up to several liters can be processed, making this technique highly versatile. Homogenization with an Ultra-Turrax® is suitable for plant and algal cells, which often possess rigid cell walls that are not easily permeabilized (Maa and Hsu 1996; Tonkur et al. 2022).

A potential limitation of this homogenization is the generation of heat during operation, which may lead to protein denaturation. Another problem is that shear-sensitive proteins, particularly enzymes and membrane proteins, may lose activity due to the mechanical stress. Furthermore, through the incorporation of air foam can form, which could potentially destabilize proteins (Maa and Hsu 1997; D'Hondt et al. 2017).

In this thesis, algal samples were prepared as described in the preparative section and then homogenized using an Ultra-Turrax®, the method is further described in Figure 16. Homogenization was carried out at gradual increasement of speed from 10.000 rpm to 24.000 rpm for a maximal duration of 5 min to avoid heat generation and potential protein denaturation. After the homogenization, the suspension was centrifuged at 10.000 × g for 30 min at 4 °C to separate the cell debris (pellet P1) from the protein-containing supernatant (S1). The supernatant was retained for further purification steps. An overview of the procedure is shown in Figure 16.

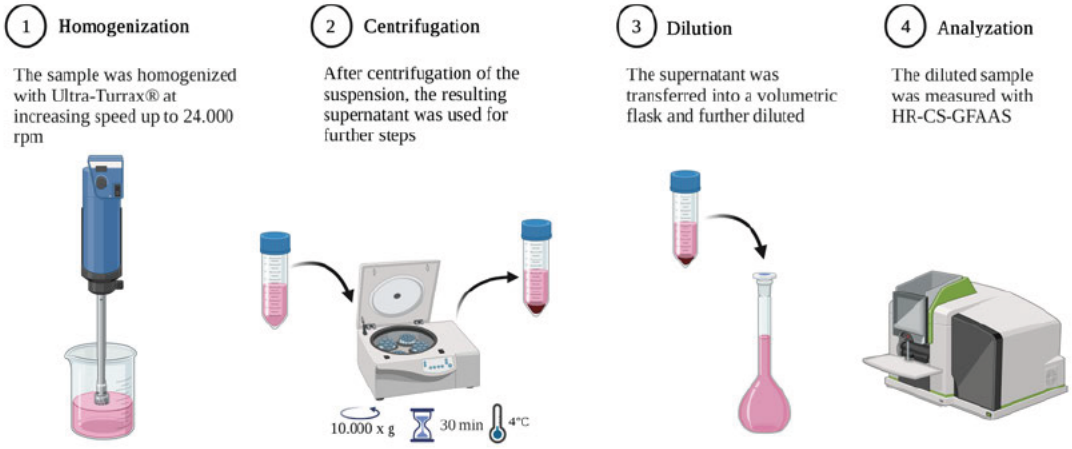

Figure 16: Homogenization procedure using Ultra-Turrax®

Stepwise overview of mechanical cell disruption. (1) The algal sample is homogenized with an Ultra-Turrax® at gradually increasing speeds up to 24,000 rpm. (2) The homogenized suspension is centrifuged at 10.000 × g for 30 min at 4 °C. (3) The resulting supernatant is transferred into a volumetric flask and diluted. (4) The diluted sample is analyzed by high-resolution continuum source graphite furnace atomic absorption spectrometry (HR-CS-GFAAS) *(Created in https://BioRender.com).*

3.5.3 Osmotic shock

Osmotic shock is a non-mechanical method for the disruption of algae cells. The principle relies on suspending cells in a hypotonic environment, such as deionized water, which causes water influx, swelling, and eventual rupture of the plasma membrane. This allows the release of native, water-soluble proteins under mild conditions, minimizing shear stress and preserving enzyme activity (Show et al. 2015; Magpusao et al. 2021). Since osmotic shock mainly releases soluble proteins, it is often complemented by alkaline extraction, which help release proteins that are more tightly bound to the membrane, cell walls, or insoluble complexes. The use of both methods either combined or as following each other enables the recovery of water soluble alkaline soluble proteins (Harnedy and FitzGerald 2013; Magpusao et al. 2021).

In this study, two approaches were applied. In the combined method, algal biomass was first subjected to osmotic shock by incubation in deionised water at room temperature for 3 h. The suspension was then centrifuged at 10.000 × g for 30 min at 4 °C to separate the supernatant containing water-soluble proteins from the cell pellet. The pellet was than resuspended in an alkaline extraction medium consisting of 0.12 mol/L NaOH and 10 mM β-mercaptoethanol and incubated for 1 h at room temperature. A second centrifugation under the same conditions generated the alkali-solubilized protein fraction.

In the alkaline extraction, the osmotic shock and intermediate centrifugation steps were skiped. Instead, the algal biomass was directly extracted in the same alkaline medium (0.12 mol/L NaOH with 10 mM β-mercaptoethanol) for 1 h at room temperature. After incubation, the suspension was centrifuged at 10.000 × g for 30 min at 4 °C, and the resulting supernatant was collected as a combined extract. Both procedures are illustrated in Figure 17.

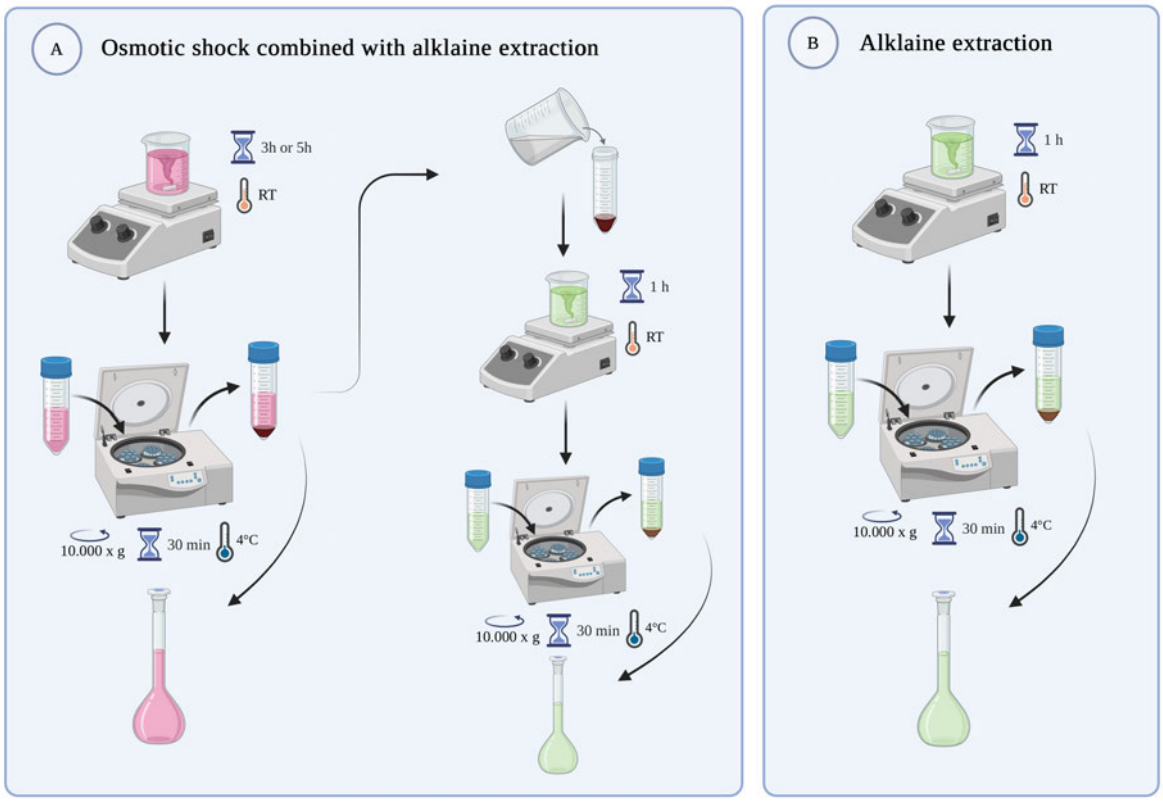

Figure 17: Osmotic shock and alkaline extraction procedures

(A) Combined method: Algal biomass is incubated in deionized water for 3–5 h at room temperature to induce osmotic shock. After centrifugation at 10.000 × g for 30 min at 4 °C, the pellet is resuspended in 0.12 mol/L NaOH with 10 mM β-mercaptoethanol and incubated for 1 h at room temperature, followed by a second centrifugation to recover alkali-solubilized proteins.
(B) Alkaline extraction: Biomass is directly extracted in the alkaline medium for 1 h at room temperature and centrifuged at 10.000 × g for 30 min at 4 °C, yielding the alkaline protein fraction *(Created in https://BioRender.com)*.

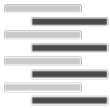

3.6 Protein quantification

The protein content of algal extracts was determined using the ROTI® Quant universal kit (Carl Roth, Karlsruhe, Germany), a colorimetric protein assay based on the bicinchoninic acid (BCA)-like principle. The method relies on the biuret reaction, in which peptide bonds reduce Cu^{2+} to Cu^{+} under alkaline conditions. The resulting copper ions form a purple chelate complex with the proprietary enhancer reagent, and the color intensity is directly proportional to the protein concentration. The assay shows high tolerance toward detergents, salts, and buffer components that frequently interfere with other protein assays such as Bradford (ROTI® Quant universal, 2021).

For quantification, a bovine serum albumin (BSA) standard curve (5–2000 µg/mL) (Table 9) was prepared in parallel to the samples like described in the manufacturer's protocol. The assay was carried out in the macro format. 100 µL of sample or standard were mixed with the appropriate volume of working solution (15:1 mixture of Reagent 1 and Reagent 2) at a ratio of 1:10 and 1:50. After mixing, the tubes were incubated for 2 h at room temperature. Absorbance was measured at 492 nm using a spectrophotometer against a reagent blank (ROTI® Quant universal, 2021).

Table 9: BSA-standards dilution schema

Solution	C_{BSA} [µg/ml]	V_{Buffer} [µl]	V_{BSA} [µl]
A	2000	0	400 from stock solution (2.0 mg/ml)
B	1500	125	375 from stock solution (2.0 mg/ml)
C	1000	325	325 from stock solution (2.0 mg/ml)
D	750	325	325 from B
E	500	325	325 from C
F	250	325	325 from E
G	125	325	325 from F
H	50	450	300 from G
I	25	400	100 from G
K	5	400	100 from I
Blank	0	400	0

All measurements were performed in duplicates. The protein concentrations of the samples were calculated by interpolation from the standard curve after blank correction. The linear quantification range of the assay extended from 5 µg/mL to 2000 µg/mL, ensuring reliable determination across different extract concentrations (ROTI® Quant universal, 2021).

3.7 Protein precipitation with ammonium sulfate

The purpose of protein precipitation is to reduce the solubility of proteins to the point where they separate from the solution. Protein solubility is determined primarily by the chemical nature of its surface. Hydrophilic amino acid residues favor solubility in aqueous environments, while hydrophobic regions tend to aggregate when exposed. By adding high concentrations of salt, the surface tension of water increases, and competition for solvent molecules intensifies. This forces proteins out of solution, as hydrophobic regions interact more strongly with each other, leading to precipitation (Wingfield 1998; Duong-Ly and Gabelli 2014).

Ammonium sulfate is the most used salt for protein precipitation due to its high solubility in water, stabilizing effect on proteins, and low cost. At low salt concentrations, proteins may initially become more soluble (salting in) due to charge shielding. However, at high salt concentrations, water molecules preferentially hydrate the salt ions, leaving fewer solvent molecules available to solvate the protein surface. This reduced hydration lowers protein solubility and drives aggregation and precipitation (salting out) (Wingfield 1998; Duong-Ly and Gabelli 2014).

In this study, a fractionated ammonium sulfate precipitation was performed to separate the target protein from contaminating proteins. A stepwise approach was chosen, as gradual addition of salt prevents local oversaturation and uncontrolled precipitation, which could otherwise trap or denature the target protein (Wingfield 1998).

In the first precipitation step, the goal was to selectively precipitate unwanted proteins. Ammonium sulfate was added previously prepared enzyme extract to a final concentration corresponding to 30 % saturation (164 g/L), while the solution was gently stirred to ensure even distribution. The mixture was left to equilibrate for 30 minutes, after which it was centrifuged at 10.000 × g for 30 minutes at 4 °C**.** The resulting pellet contained predominantly contaminant proteins, while the **s**upernatant (S2) contained the target protein and was retained for the next step.

In the second precipitation step, the target protein itself was precipitated. Ammonium sulfate was added to the supernatant to reach 60 % saturation (181 g/L), again by gradual addition under stirring. The solution was incubated for 30 minutes and then centrifuged under the same conditions. The Figure 18 visualizes the protein precipitation after 60 % AS saturation. This time, the pellet (P3) contained the target protein, while the supernatant (S3) was discarded. The pellet was then carefully resuspended for further downstream purification.

Precipitation with 60 % ammonium sulfate of *P. palmata*

Precipitation with 60 % ammonium sulfate of *C. crispus*

Figure 18: Protein precipitation with 60 % ammonium sulfate in Palmaria palmata (left) and Chondrus crispus (right)

The images show the differences in pellet and supernatant formation after stepwise ammonium sulfate precipitation. In both species, proteins were salted out by reducing their solubility, with the pellet containing the precipitated proteins for further downstream purification (Source: own image, Laurie Ramadani 2025).

3.8 Desalting with size exclusion chromatography (SEC)

For desalting, a size exclusion chromatography (SEC) system with a desalting column was used. This column is packed with a gel filtration medium and serves both for desalting and for buffer exchange of the sample. In this case, buffer exchange was necessary to transfer the sample into the buffer required for the following ion exchange chromatography (Andrews 1965; Hall 2018)

A desalting column in SEC can be applied whenever low-molecular-weight components need to be removed. Separation occurs by group separation**,** in which the components of a sample are divided into two groups, in high-molecular-weight substances (proteins), which are excluded from the pores of the medium and therefore elute first, and low-molecular-weight substances (salt), which can enter the pores and elute later (Hall 2018).

The elution process is typically monitored by UV absorbance and conductivity. Protein elution is detected via UV absorbance at 280 nm, whereas the presence of salts is tracked by conductivity measurements. Since proteins are considerably larger than salt ions, they elute earlier and can be effectively separated from salts using SEC desalting columns (Figure 19) (Barth et al. 1994; Hall 2018).

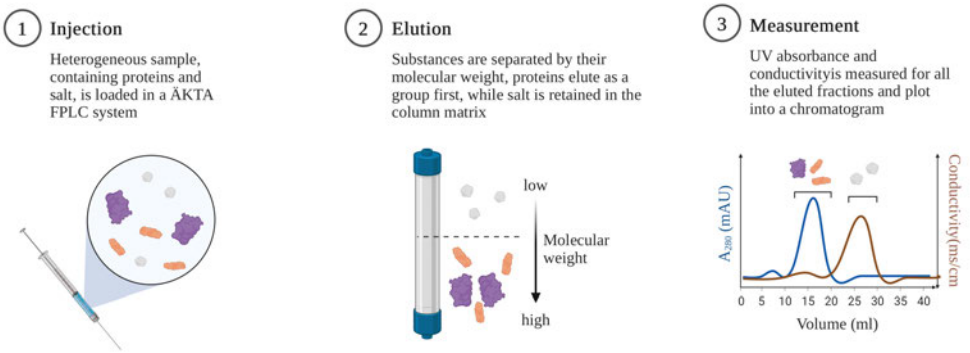

Figure 19: Desalting by size exclusion chromatography (SEC)

Stepwise overview of the desalting process using a gel filtration column. (1) The protein sample containing salts is injected into the SEC system. (2) Components are separated by size: proteins, as high-molecular-weight compounds, elute first, while salts enter the pores of the matrix and elute later. (3) Elution is monitored by UV absorbance at 280 nm for proteins and conductivity for salts, resulting in a chromatogram that distinguishes protein and salt fractions *(Created in https://BioRender.com).*

Desalting is an essential prerequisite for downstream analytical. High salt concentrations interfere with many biochemical methods, including ion exchange chromatography (IEXC). In IEXC, salt competes with proteins for charged groups on the stationary phase, reducing binding efficiency and resolution. Therefore, desalting ensures that the protein sample is in a low-salt environment compatible with the chosen purification method (Walch and Jungbauer 2017).

In this study, SEC with a 5 mL HiTrap Desalting column (GE Healthcare) was used for desalting and buffer exchange. The protein pellet (P3) obtained from 60% ammonium sulfate precipitation was resuspended in the equilibration buffer required for ion exchange chromatography. Since only up to 30% of the column volume can be loaded per run, the desalting step was repeated several times. Aliquots of 1 mL were applied to the column, using a linear gradient with a flow rate of 1 mL/min. Fractions of 0.5 mL were collected throughout the run.

3.9 Ion exchange chromatography (IEXC)

Ion exchange chromatography (IEXC) is an interactive chromatographic technique that separates proteins according to their net surface charge. The stationary phase consists of a polymeric resin functionalized with covalently bound charged groups, either positively charged (anion exchanger) or negatively charged (cation exchanger). Proteins bind to the exchanger when their net charge is opposite to that of the stationary phase. Binding strength is governed by the pH of the buffer relative to the protein's isoelectric point (pI). At pH values above their pI, proteins carry a net negative charge and bind to anion exchangers, while at pH values below their pI they bind to cation exchangers. Elution is typically achieved by introducing salts that compete with protein binding, and the strength of interaction determines the elution order. Separation is monitored by UV absorbance at 280 nm and by conductivity measurements, which reflect the ionic strength of the mobile phase (Figure 20) (Jungbauer and Hahn 2009; Martin 2013).

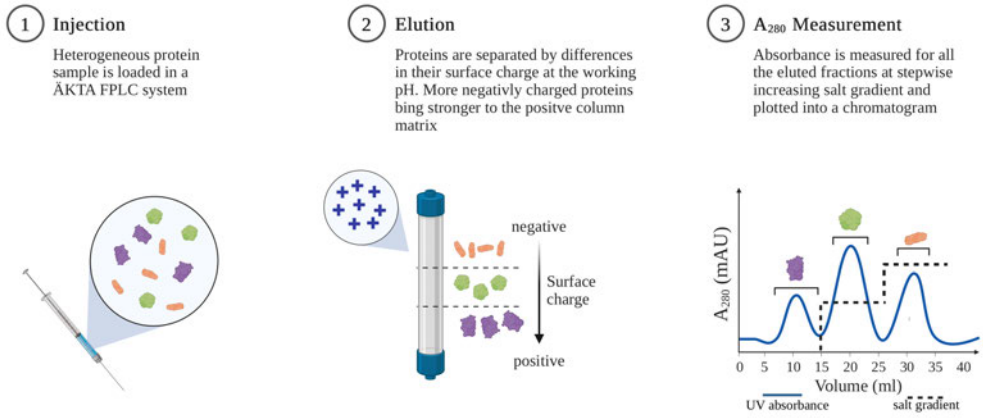

Figure 20: Ion exchange chromatography (IEXC) procedure

Stepwise overview of protein separation by ion exchange chromatography. (1) Protein samples are injected into an ÄKTA FPLC system. (2) Proteins are separated based on their net surface charge: negatively charged proteins bind to the positively charged column matrix and are eluted stepwise with increasing salt concentrations. (3) Elution is monitored by UV absorbance at 280 nm and conductivity, producing a chromatogram with distinct protein peaks *(Created in https://BioRender.com)*.

In this study, an anion exchange chromatography (AIEXC) was chosen for the purification of vanadium-dependent haloperoxidases (V-HPOs) from algal extracts, following established protocols (Ohshiro 2002). Protein samples obtained after desalting were applied to a HiTrap DEAE Fast Flow column (1 mL, GE Healthcare) equilibrated with 50 mM Tris-HCl buffer, pH 7.4 at a flow rate of 1 mL/min**.** After washing the column with equilibration buffer to remove

unbound proteins, elution was carried out using two elution buffers with different concentrations of potassium chloride (KCl)**.**

The first elution step, with 0.2 M KCl in 50 mM Tris-HCl (pH 7.4), was used to release proteins that were weakly bound to the resin, thereby reducing impurities. In the second elution step, 0.3 M KCl in 50 mM Tris-HCl (pH 7.4) was applied to release the more strongly bound proteins, including the target haloperoxidase enzyme. The use of a stepwise salt concentration rather than a continuous gradient enables a selective fractionation of proteins based on binding affinity, ensuring that weakly associated contaminants are removed before eluting the target enzyme fraction (Ohshiro 2002).

Fractions of 0.5 mL were collected throughout the run, and distinct protein peaks were monitored by absorbance at 280 nm. Conductivity was measured simultaneously to verify the ionic strength of each elution step. Collected fractions were pooled according to their elution profile and further analyzed.

3.10 SDS-PAGE

To assess the purity of the protein samples, sodium dodecyl sulfate–polyacrylamide gel electrophoresis (SDS-PAGE) was performed. SDS-PAGE is a widely used analytical method that separates proteins primarily according to their molecular weight (Hofmann and Clokie 2018; Kielkopf et al. 2021).

The samples were mixed with Laemmli buffer, which contains sodium dodecyl sulfate (SDS) and dithiothreitol (DTT). SDS denatures the proteins by disrupting non-covalent interactions and binding to their hydrophobic regions. As a result, the intrinsic charge of the proteins is changed by the negatively charged sulfate groups, resulting that the net charge is now proportional to molecular mass. DTT reduces disulfide bonds, thereby eliminating covalent bonds that stabilize protein structure. The denaturation step was carried out by incubating the samples at 95 °C for 5 minutes in a heating block (Hofmann and Clokie 2018; Kielkopf et al. 2021).

The SDS-PAGE consisting of a stacking gel and a separating gel. The stacking gel has a lower acrylamide concentration and a lower buffer pH resulting in a more porous matrix. It concentrates the proteins into a tight band before they enter the separating gel, thereby improving resolution. The separating gel, with a higher acrylamide concentration and buffer pH, provides a sieving matrix that separates proteins according to their molecular weight. Smaller proteins migrate more quickly through the gel matrix than larger ones, allowing size-dependent separation (Hofmann and Clokie 2018; Kielkopf et al. 2021).

In the electrophoresis chamber the gels were clamped vertically and the chamber was then filled with SDS running buffer. A molecular weight marker (10 µL) was loaded into one well, while 20 µL of each protein sample was loaded into the remaining wells. An electric field of 200 V was applied for approximately 30 minutes, during which the negatively charged protein–SDS complexes migrated from the sample wells through the stacking gel and into the separating gel.

The electrophoresis was stopped once the tracking dye (bromophenol blue) approached the lower edge of the gel. The gels were then stained with Coomassie Brilliant Blue (ROTI® quick blue) to visualize the protein bands. The apparent molecular masses of the proteins were determined by comparison with the protein molecular weight marker.

The target protein should have a molecular mass around 67 kDa (Punitha et al. 2018). Subsequently the marker consists of the following proteins in

Table 10 and is visualized in Figure 21.

Table 10: Composition of the marker

Protein	Molecular weight (kDa)
β-galaktosidase	116.0
Bovine serum albumin	66.2
Ovalbumin	45.0
Lactate dehydrogenase	35.0
REase Bsp98I	25.0
β-Lactoglobulin	18.4
Lysozyme	14.4

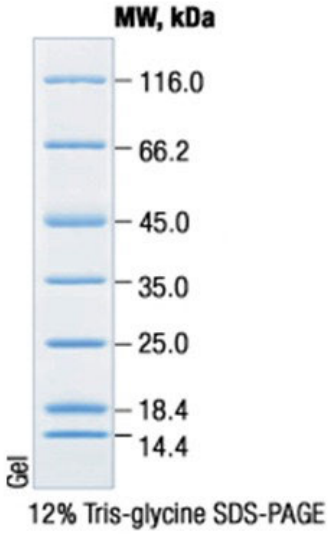

Figure 21: Representation of the MW of the marker proteins

The marker contains β-galactosidase (116 kDa), bovine serum albumin (66.2 kDa), ovalbumin (45 kDa), lactate dehydrogenase (35 kDa), REase Bsp98I (25 kDa), β-lactoglobulin (18.4 kDa), and lysozyme (14.4 kDa) (Source: VWR International GmbH, 2018).

3.11 Experimental design

Figure 22 shows a schematic overview of the protein extraction and purification workflow applied in this thesis. Fresh or dried algal biomass was subjected to different cell disruption methods to release intracellular proteins. The resulting crude extracts were clarified by centrifugation yielding supernatant fraction S1 and pellet fraction P1.

Proteins in S1 were fractionated by stepwise ammonium sulfate precipitation. The first precipitation at 30 % AS, yielded pellet P2 and supernatant S2. Subsequently, proteins remaining in S2 were further precipitated at 60 % AS, generating pellet P3 and supernatant S3. Pellet P3 was desalted by SEC using a HiTrap Desalting column, resulting in desalted protein fractions F_{SEC}. These fractions were subjected to AIEX chromatography using a HiTrap DEAE FF column to further separate proteins based on charge.

The purified protein fractions (S1, S2, S3, and F_{SEC}) were subsequently analyzed by SDS-PAGE and quantified with a protein assay.

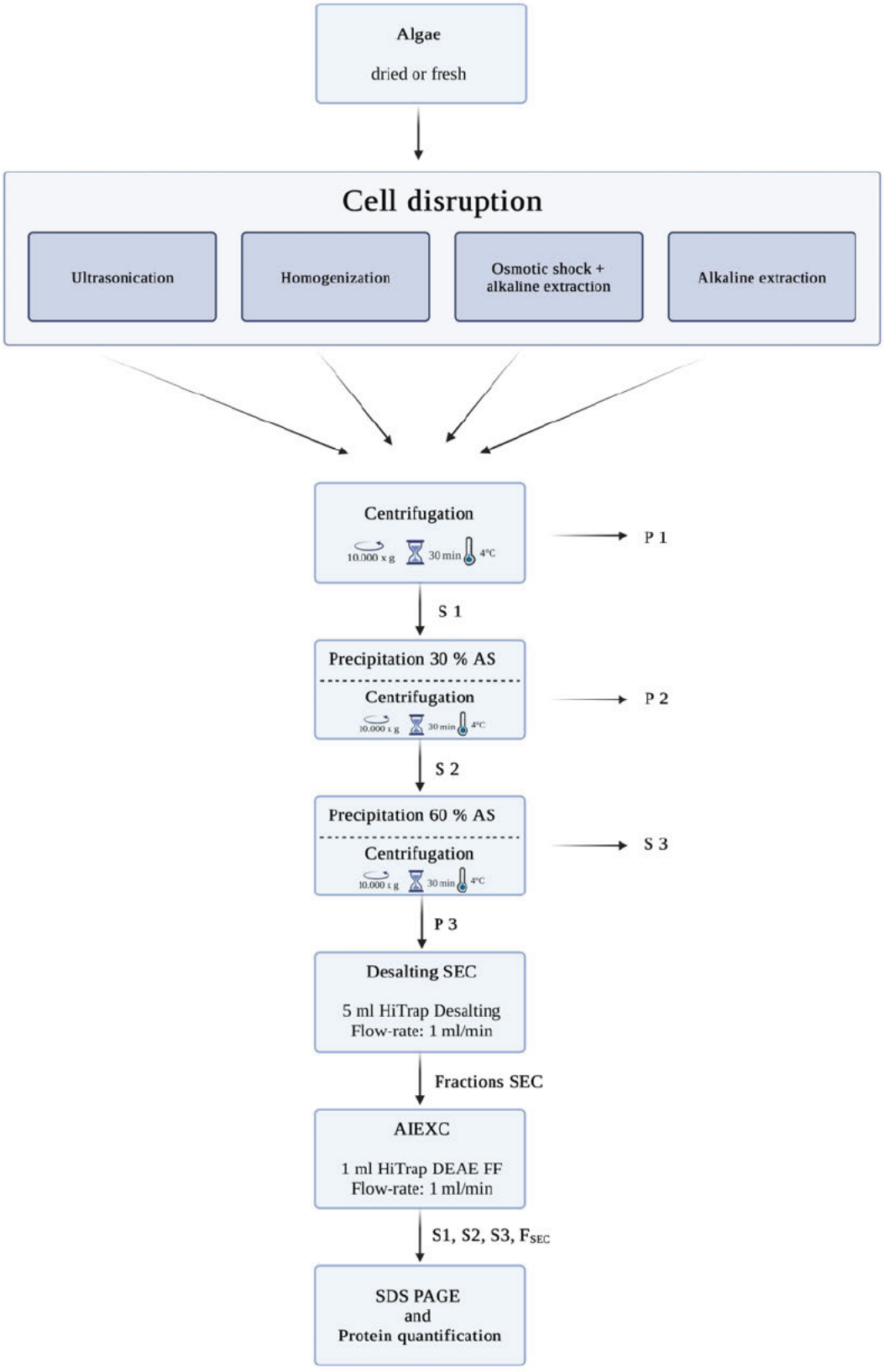

Figure 22: Schematic overview of the experimental design

(Created in https://BioRender.com)

4 Results and discussion

The HR-CS GFAAS provides vanadium concentrations in µg/L of solution. However, since part of the aim of this study was to compare different extraction and disruption methods on a biomass basis, the raw values had to be converted into µg vanadium per g dry weight of algae (µg/g DW). This normalization takes into account the dilution factor, the total sample volume, and the initial sample mass, which are not considered in the instrument output.

Vanadium concentration in sample:

$$C_{sample} = \frac{C_{AAS} \cdot DF \cdot V_{tot}}{m_{sample}}$$

Where:

- C_{AAS} = concentration measured by AAS [µg/L]
- DF = dilution factor applied before analysis
- V_{tot} = total volume of the digest or extract [L]
- m_{sample} = sample mass [g DW]
- C_{sample}= calculated concentration of vanadium in sample [µg/g DW]

This calculation converts the solution-based concentration into a biomass-normalized value, enabling direct comparison between samples and experimental conditions.

4.1 Results: Vanadium extraction

The vanadium concentrations were obtained from pre-dried and milled *P. palmata* samples after different digestion methods. They are summarized in Table 11. All values were normalized to µg vanadium per g dry weight (µg/g DW) according to the calculation described above.

Table 11: Results of different vanadium extraction methods

Methods	**C_{AAS}**	**m_{sample}**	**DF**	**V_{tot}**	**C_{sample}**
	[µg/L]	**[mg]**		**[ml]**	**[µg/g DW]**
HACH digestion	2.055	57.9	10	100	35.49
Dry ashing	1.406	50.1	10	100	28.06
Wet digestion (ground)	1.122	50.5	10	100	22.22
Wet digestion (not ground)	1.082	50.7	10	100	21.34

The measured vanadium concentrations varied depending on the digestion method applied. The highest concentration was observed in the HACH digestion (35.49 µg/g DW), followed by dry ashing (28.06 µg/g DW). Both wet digestion approaches resulted in lower vanadium concentrations, with similar values for ground (22.22 µg/g DW) and non-ground (21.34 µg/g DW) samples.

4.1.1 Discussion: Vanadium extraction

Looking at the results of the different methods, it is firstly clear that all were able to achieve a quantification of vanadium, however the HACH digestion apparatus provided the highest concentration in relation to the sample dry weight. This suggests that the HACH digestion system provides a more complete digestion of algae matrix without the loss of vanadium during the process. In addition to having the highest concentration, the HACH digestion system, compared to dry ashing and wet digestion is less time consuming and has an easier handling. Moreover, the closed digestion environment reduces the likelihood of contamination from external sources, which is important when working at trace concentration levels.

Taking all of this into account, the results indicate that the HACH digestion system is the most suitable method for vanadium determination. For these reasons, it was selected as the standard method for further experiments in this study.

4.2 Results: Validation

For all parts of the validation method pre dried and milled *P. palmata* was used and all values were normalized to µg vanadium per g dry weight (µg/g DW) according to the calculation described above.

4.2.1 Results: Calibration curve and determination of LOD/LOQ

For this experiment, no samples were used only the vanadium standard solution, which was diluted to the desired concentrations ranging from 1 µg/L to 10 µg/L. The results are visualized in the Figure 23.

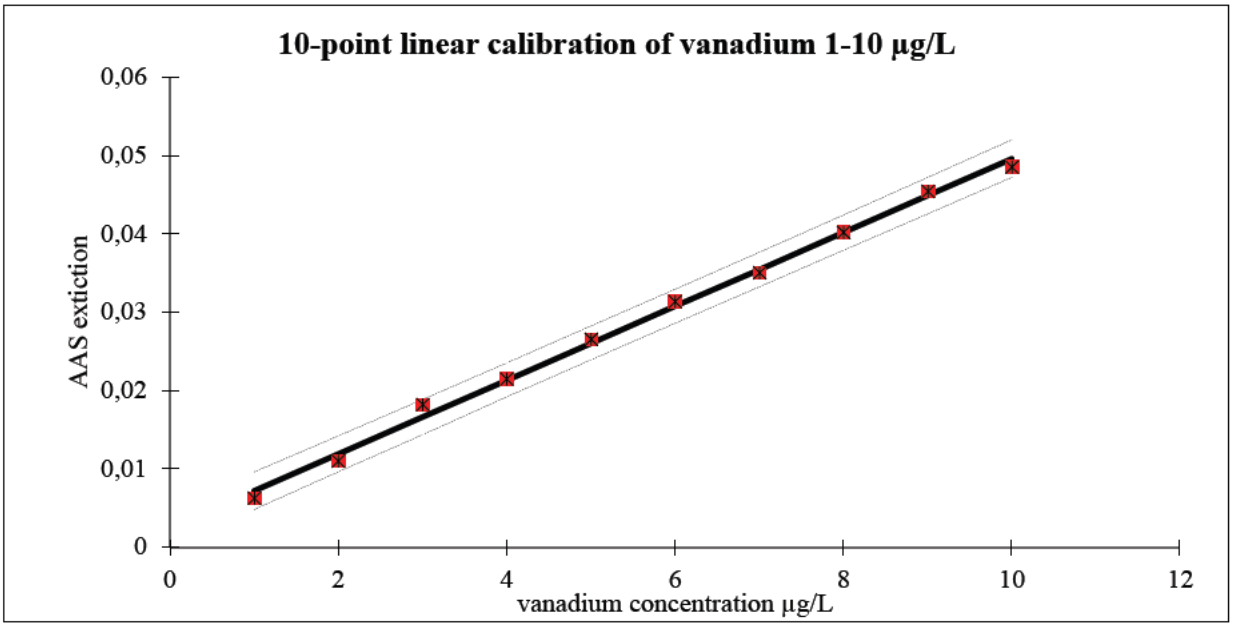

Figure 23: 10-point calibration curve of vanadium standards 1-10 µg/L

The calibration curve for vanadium was established in the concentration range 1–10 µg/L using 10 standard solutions. The resulting plot shows a linear relationship between absorbance and concentration, with all calibration points lying close to the regression line.

Visually, the calibration curve shows a steady increase in signal intensity with increasing vanadium concentration, without curvature or outliers, indicating that the chosen concentration range falls well within the instrument's linear working range.

The regression equation was determined as:

$y=0.00446\,x+0.00443$

The correlation coefficient is at r = 0.9987 and the coefficient of variation at 3.0 %, also the calibration was classified as statistically significant. The critical value was determined as 0.00698, this represents the smallest absorbance signal distinguishable from the blank. The LOD corresponds to the concentration at which analyte presence can be confirmed with statistical certainty, while the LOQ indicates the lowest concentration that can be determined with acceptable accuracy and precision. LOD was determined as 0.57 µg/L, and LOQ as 1.85 µg/L. These results are summarized in Table 12 and in the addendum.

Table 12: Results of vanadium calibration (1–10 µg/L) with HR-CS GFAAS

Parameter	Value
Regression function	y = 0.00446·x + 0.00443
Correlation coefficient (r)	0.9987
Coefficient of variation	3.0 %
Critical value (signal)	0.00698
Limit of detection (LOD)	0.57 µg/L
Limit of quantification (LOQ)	1.85 µg/L

4.2.2 Discussion: Calibration curve and determination of LOD/LOQ

The calibration results demonstrate that the HR-CS GFAAS method provides a highly linear response for vanadium in the range of 1–10 µg/L, as indicated by the correlation coefficient of r = 0.9987. The low coefficient of variation (3.0 %) confirms the reproducibility of the calibration. The calculated detection (0.57 µg/L) and quantification limits (1.85 µg/L) indicate that the method is sufficiently sensitive for trace vanadium determination in algal extracts. Since the measured sample concentrations corresponded to solution concentrations well above the LOQ, all values obtained in following experiments fall within the validated working range of the instrument. These results confirm both the sensitivity and the reliability of the method for the intended application.

4.2.3 Results: Spike recovery experiments

To verify whether vanadium is lost during sample digestion, spike recovery experiments were performed at three concentration levels within the calibration range (2.2 µg/L, 5.6 µg/L, and 9.5 µg/L). The measured values for each spike level are summarized in Table 13. All three concentration levels were measured three times, the mean value was used for the calculations.

Table 13: Results of spike recovery experiment with spike levels low, mid and high

Spike level	Expected [µg/L]	Mean conc. [µg/L]	SD	RSD [%]	Recovery [%]
Low	2.2	2.313	0.048	2.05	105.1
Mid	5.6	5.021	0.076	1.51	89.7
High	9.5	8.675	0.070	0.81	91.3

The recoveries ranged between around 90–105 %**,** with relative standard deviations (RSDs) below 3 %. The concentration of vanadium in the spiked samples, ranged from 44.6 µg/g (low spike) to 66.8 µg/g **(**high spike) (Table 14).

Table 14: Vanadium concentrations of the spike recovery experiment

Spike level	C_{sample} [µg/g DW]
Low	44.64
Mid	49.27
High	66.78

4.2.4 Discussion: Spike recovery experiments

The spike recovery results demonstrate that vanadium doesn't get lost during the digestion and sample preparation procedure. Recovery values close to 100 % are considered acceptable in trace element analysis, with 80–120 % generally regarded as the acceptable range (EURACHEM, 2014). The observed recoveries of 105 % at low spike, 89.7 % at mid spike, and 91.3 % at high spike therefore confirm that the method is both accurate and reliable.

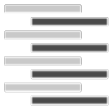

The slightly higher recovery at the low concentration (105 %) could be explained by analytical variability at concentrations close to the detection limit, while the slightly lower recoveries at mid and high levels may reflect minor matrix effects or pipetting imprecision during spiking. However, the deviations remain small and do not indicate drastic losses of vanadium during digestion.

Furthermore, the low relative standard deviations (<2.1 %) confirm that the spiking experiments were highly reproducible. This confirms that the HACH digestion and the HR-CS GFAAS provide accurate measurements of vanadium.

4.2.5 Results: Reference standard solution

To confirm the accuracy of the method, a certified reference material (CRM, Trace Metals 1 – WP, Supelco, Merck) containing vanadium was used. According to the certificate of analysis, the CRM contains vanadium at a concentration of 1500 ± 11 µg/L, dissolved in 5% nitric acid. A working solution was prepared by dilution, to achieve a final concentration of 6 µg/L vanadium. The diluted solution was measured three times with the HR-CS GFAAS. The results can be seen in Table 15.

Table 15: Results of the reference material with replicates

Replicate	**C_{AAS} [µg/L]**
1	5.17
2	5.10
3	5.25
Mean	5.17
SD	0.075
RSD [%]	1.45
Expected [µg/L]	6
Recovery [%]	86.2

The three replicate gave concentrations of 5.17, 5.10, and 5.25 µg/L, corresponding to a mean of 5.17 µg/L. The standard deviation was 0.075 µg/L, and the RSD was 1.45 %. Compared to the expected concentration, the recovery was 86.2 %.

4.2.6 Discussion: Reference standard solution

The analysis of the reference standard demonstrated good precision, as indicated by the low RSD (1.45 %). However, the mean measured value 5.17 µg/L was approximately 14 % lower than the expected concentration of 6.0 µg/L, with a recovery of only of 86.2 %.

This could be caused by a small instrumental sensitivity drift, or potential inaccuracies during the dilution of the concentrated CRM solution. Still, the recovery falls within the generally accepted range of 80–120 % for trace element analysis (EURACHEM, 2014), supporting the reliability of the results.

Given that the spike recovery experiments in digested samples showed recoveries close to 100%, it is likely that the lower recovery observed here reflects a minor preparation or calibration mistake, rather than analytical inaccuracy.

4.2.7 Results: Comparison with external reference method (TXRF)

To further validate the accuracy of vanadium determination by HR-CS GFAAS, one digested *P. palmata* sample previously analyzed by AAS was submitted for independent measurement using total reflection X-ray fluorescence spectroscopy (TXRF). The results can be seen in Table 16.

Table 16: Comparison of results from TXRF and AAS

Method	Replicate 1 [µg/L]	Replicate 2 [µg/L]	Mean [µg/L]
TXRF	222	196	209
AAS	184	181	182.5

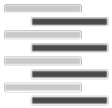

TXRF analysis was performed in duplicate, yielding concentrations of 222 µg/L and 196 µg/L, corresponding to a mean of 209 µg/L.

For comparison, the same sample had been analyzed by HR-CS GFAAS in duplicate. After applying the dilution factor (DF = 100), the measured concentrations were 184 µg/L and 181 µg/L, with a mean of 182.5 µg/L.

4.2.8 Discussion: Comparison with external reference method (TXRF)

The comparison between HR-CS GFAAS and TXRF showed that both techniques delivered results of the same order of magnitude for vanadium in digested *P. palmata*. The mean concentration determined by TXRF (209 µg/L) was approximately 14% higher than that measured by AAS (182.5 µg/L).

This difference may reflect the difference between the two analytical techniques. TXRF is a multi-element, non-destructive method that analyzes a small aliquot of the sample deposited on a carrier, whereas AAS relies on atomization of a sample. Matrix effects, sample inhomogeneity, or slight calibration differences between the instruments may therefore contribute to the observed difference (Zhang et al. 2024). While TXRF yielded slightly higher concentrations, the overlap confirms that no major analyte losses occurred during digestion or AAS measurement.

4.2.9 Results: Precision and repeatability

Precision of the HR-CS GFAAS method was evaluated in terms of repeatability, intra-day, and inter-day variability. Six replicate measurements were performed for each test. The results are summarized in Table 17.

Table 17: Results of the repeatability, intra-day and inter-day experiment

N	Repeatability [µg/g]	Intra-day 1 [µg/g]	Intra-day 2 [µg/g]	Inter-day [µg/g]
1	34.991	36.694	35.376	
2	39.304	35.610	35.844	
3	37.570	35.642	36.261	
4	37.334	35.998	35.077	
5	36.954	36.409	35.689	
6	36.694	36.421	36.208	
mean	37.14	36.13	35.74	35.94
SD	1.397	0.449	0.464	0.480
RSD %	3.761	1.242	1.298	1.335

The repeatability tests yielded a mean vanadium concentration of 37.14 µg/g, with a standard deviation of 1.40 µg/g and an RSD of 3.76 %. Intra-day precision measurements performed on two different days showed mean values of 36.13 µg/g with an RSD of 1.24 % and 35.74 µg/g with an RSD of 1.30 %. The inter-day precision resulted in a mean value of 35.94 µg/g with an RSD of 1.34 %.

4.2.10 Discussion: Precision and repeatability

The results demonstrate that the HR-CS GFAAS method provides precise and reproducible measurements of vanadium in digested algal samples. The repeatability RSD of 3.76% indicates acceptable variation when the same sample is measured repeatedly. The low RSD values obtained in both intra-day (1.24–1.30 %) and inter-day (1.34 %) analyses reflect good short-term and long-term precision. These values fall well below the generally accepted threshold of 5% RSD for method validation in trace element analysis (EURACHEM, 2014).

The close agreement between intra-day and inter-day means (35.7–36.1 µg/g) also confirms that day-to-day variability is minimal, indicating robust method performance over time. The slightly higher variation observed in the repeatability test likely reflects instrumental noise and matrix effects when measuring the same solution multiple times without re-preparation.

4.2.11 Discussion: Validation

The reliability of the HR-CS GFAAS method for the determination of vanadium was evaluated through a series of validation experiments addressing linearity, sensitivity, accuracy, recovery, and precision.

Taking all results into account they confirm that HR-CS GFAAS provides sensitive, accurate, and precise measurements of vanadium in algal samples. Small deviations observed in the CRM recovery and TXRF comparison are within acceptable limits and likely attributable to inter-method differences or preparation uncertainties rather than methodological shortcomings. Importantly, both recovery experiments and precision testing demonstrated that digestion and measurement do not introduce significant analyte losses or variability.

4.3 Results: Vanadium concentrations in different algal species

Vanadium concentrations were determined in six pre-dried and milled algal samples from different species using HR-CS GFAAS. The concentrations were normalized to dry weight and are summarized in Table 18.

Table 18: Comparison of vanadium content in different algae species

Species	**Group**	**C_{AAS} [µg/L]**	**DF**	**m_{sample} [g]**	**C_{sample} [µg/g DW]**
Ascophyllum nodosum	Brown alga	6.58	2	1.0031	1.31
Chondrus crispus A1	Red alga	0.056	1	0.5018	0.01
Chondrus crispus A2	Red alga	9.29	5	0.5024	9.25
Lithothamnium sp.	Calcified red alga	4.29	5	0.5029	4.27
Himanthalia elongata	Brown alga	3.85	2	0.5675	1.36
Palmaria palmata	Red alga	9.20	20	0.5053	36.40

The results revealed large differences in vanadium content between the species. The highest concentration was found in *P. palmata* (36.40 µg/g DW), followed by *C. crispus* A2 (9.25 µg/g DW) and *Lithothamnium* sp. (4.27 µg/g DW). Much lower values were obtained for *A. nodosum* (1.31 µg/g DW) and *H. elongata* (1.36 µg/g DW), while *C. crispus* A1 showed only trace amounts (0.01 µg/g DW).

4.3.1 Discussion: Vanadium concentrations in different algal species

The results demonstrate that vanadium accumulation varies strongly between algal species. Among the tested samples, *P. palmata* shows by far the highest concentration (36.4 µg/g DW), which is consistent with previous reports identifying red algae as effective accumulators of trace metals (Michalak & Chojnacka, 2015). The elevated levels in *P. palmata* suggest that this species may play a more significant role in biogeochemical cycling of vanadium compared to brown (*A. nodosum*, *H. elongata*) and calcified (*Lithothamnium*) algae.

Interestingly, the two *C. crispus* samples showed highly different results, with one replicate (A2) containing a concentration of 9.25 µg/g DW, while the other (A1) contained only negligible amounts (0.01 µg/g DW). This difference may be explained by sample heterogeneity, differences in collection site or environmental exposure (e.g., seawater vanadium concentration, anthropogenic inputs), or by preparation effects. Such variability highlights the importance of replication and careful sample handling when comparing species.

The relatively low concentrations in *A. nodosum* (1.31 µg/g DW) and *H. elongata* (1.36 µg/g DW) are in line with previous findings that many brown algae generally accumulate less vanadium than red species. Calcified algae such as *Lithothamnium* contained intermediate levels (4.27 µg/g DW), possibly reflecting differences in cell wall composition and ion binding affinity.

Overall, the comparison confirms that vanadium accumulation is species-dependent, with *P. palmata* being the most efficient accumulator among the analyzed samples. These differences may relate to species-specific physiology, environmental conditions, or chemical interactions with seawater, and should be further investigated in future studies with larger sample sets.

4.4 Results: Comparison of fresh and pre-dried algal samples

The dry matter content of fresh *P. palmata* and *C. crispus* was determined in order to express vanadium concentrations on a dry weight (DW) basis and allow comparison with pre-dried, milled samples. The dry matter and water content are calculated like described in the method section. Figure 24 shows the fresh material before drying. Results are seen in Table 19.

Table 19: Determination of dry matter content for P. palmata and C. crispus

Species	Dry matter [%]	Water content [%]	C_{fresh} [µg/g DW]	$C_{pre\text{-}dried}$ [µg/g DW]
P. palmata	15.2	84.8	22.6	38.4
C. crispus	18.8	81.3	7.60	9.16

After drying, *P. palmata* contained a dry matter fraction of 15.2%, while *C. crispus* contained 18.8%, corresponding to water contents of 84.8% and 81.3%, respectively.

Vanadium concentrations determined in fresh material were 22.6 µg/g DW for *P. palmata* and 7.60 µg/g DW for *C. crispus*. In comparison, pre-dried and milled samples yielded higher concentrations with 38.4 µg/g DW for *P. palmata* and 9.16 µg/g DW for *C. crispus.*

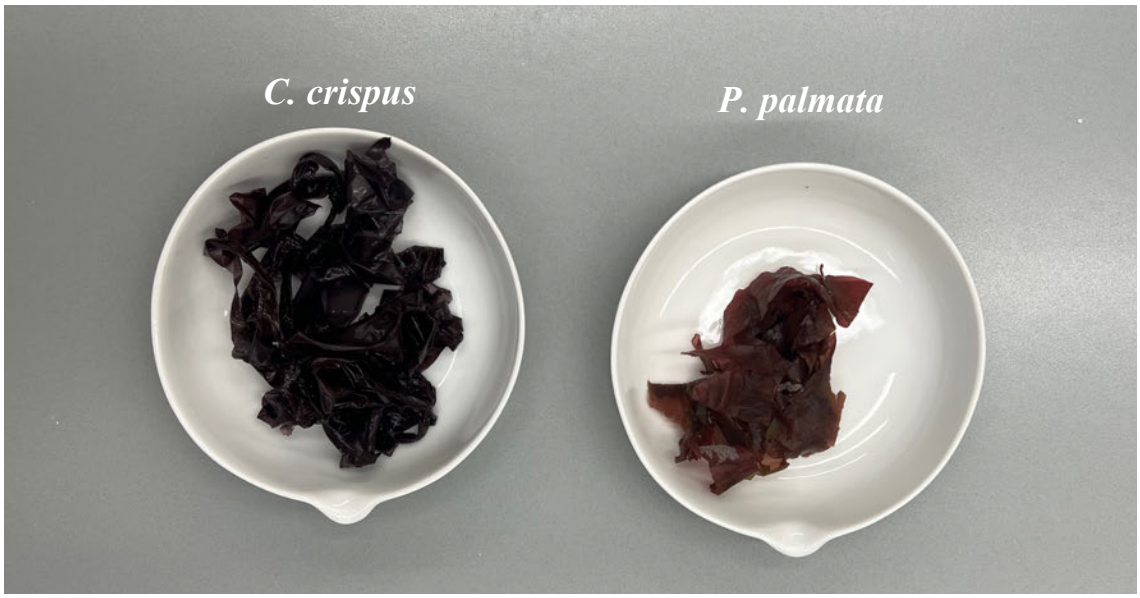

Figure 24: Fresh material of C. cripus and P. palmata before drying

The figure illustrates both fresh materials used in in this experiment with C. crispus in the left and P. palmata to the right. The difference in color and structure can also be observed (Source: own image; Laurie Ramadani 2025)

4.4.1 Discussion: Comparison of fresh and pre-dried algal samples

The determination of dry matter content confirmed that both species contained a high proportion of water (>80%), which is typical for marine macroalgae. Normalizing results to dry weight is therefore essential to ensure comparability between fresh and dried samples and across studies.

For both *P. palmata* and *C. crispus*, vanadium concentrations expressed on a dry weight basis were higher in pre-dried and milled samples compared to fresh material. In *P. palmata*, the difference was particularly notable, with values of 38.4 µg/g DW in pre-dried samples compared to 22.6 µg/g DW in fresh samples. For *C. crispus*, the difference was smaller but still notable from 9.16 µg/g DW and in pre-dried and 7.60 µg/g DW in fresh samples.

Several factors may explain these differences. First, sample preparation (grinding and homogenization of pre-dried material) likely improved extraction efficiency and measurement reproducibility, leading to higher concentrations. Second, loss of soluble components during drying or washing may alter the relative proportion of trace metals in the matrix. Finally, small variations between individual samples may also contribute, given the known heterogeneity of algal tissues and environmental exposure to trace metals.

Despite these variations, the results consistently show that *P. palmata* contains markedly higher vanadium concentrations than *C. crispus*, independent of whether fresh or dried samples were analyzed. This confirms species-specific differences in vanadium accumulation.

4.5 Results: Cell disruption

To determine which cell disruption method is simultaneously the most effective and most gentle toward the extraction of vanadium and proteins, three different methods were tested alone and in combination with each other. Additionally, two buffer systems were tests regarding their efficiency in enzyme extraction.

4.5.1 Results: Crude enzyme extraction with two buffer systems

Two buffer systems reported in the literature for haloperoxidase extraction were tested for their ability to solubilize vanadium-containing enzymes from *P. palmata*. Pre-dried and milled algal powder was suspended at a concentration of 5 mg/mL in either Buffer 1 or Buffer 2, both buffers are described in the method section. The supernatant (crude extract) was analyzed by HR-CS GFAAS after 1:100 dilution. The pellet was subjected to HACH digestion, diluted 1:10, and likewise measured for vanadium content. The results are seen in Table 20.

Table 20: Results of enzyme extraction with two different buffer systems

Fraction	Buffer 1 [µg/g DW]	% of V	Buffer 2 [µg/g DW]	% of V
Supernatant	26.23	75.07	26.66	73.71
Pellet	8.71	24.93	9.51	26.29
Total	34.94	100	36.17	100

In the supernatant, vanadium concentrations of 26.23 µg/g DW for Buffer 1 and 26.66 µg/g DW for Buffer 2 were detected, both make about 75 % of the total vanadium content in the samples. The corresponding pellets contained lower amounts of vanadium, with 8.71 µg/g DW for Buffer 1 and 9.51 µg/g DW for Buffer 2, which correspond to around 25 % of the total vanadium content. Taking both values together we can estimate the total vanadium content from both buffer extracts. Buffer 1 yielded 34.94 µg/g DW while buffer 2 got 36.17 µg/g DW. For comparison, digestion of pre-dried and milled *P. palmata* yielded a total vanadium concentration of approximately 36-38 µg/g DW.

4.5.2 Discussion: Crude enzyme extraction with two buffer systems

Both buffer systems successfully extracted a substantial proportion of the vanadium from *P. palmata* into the crude enzyme extract, with concentrations of around 26 µg/g DW measured in the supernatant. This corresponds to approximately 75 % of the total vanadium content in the sample, suggesting that a large fraction of vanadium is solubilized under the tested extraction conditions. The remaining 9 µg/g DW were detected in the pellet after digestion, indicating that not all vanadium was released into the extract.

The similar results obtained with the MES buffer and the Tris-HCl buffer suggest that buffer composition had little influence on the overall vanadium recovery under the tested conditions. Both appear suitable for solubilization of vanadium-containing enzymes. The presence of vanadium in the supernatant supports the working hypothesis that vanadium is largely associated with soluble V-HPOs, rather than being bound exclusively to insoluble cell wall material.

However, since the supernatant yield did not reach the total vanadium concentration, it is possible that either a portion of vanadium-containing enzymes remained insoluble, that vanadium may also be bound in other cell-associated fractions or remains unbound. Additional optimization of extraction conditions, like coupling buffer extraction with mechanical cell disruption techniques, may therefore be necessary to achieve complete recovery.

For all following experiments Tis-HCl buffer was used unless mentioned otherwise.

4.5.3 Results: Ultrasonic cell disruption of *P. palmata*

The sample of pre-dried *P. palmata* was prepared like described in the method section. The sample, solubilized in Tris-HCL, was transferred in a rosette vessel and placed in an ice bath to counter the heat building during the ultrasonic cell disruption. After cell disruption the sample was centrifuged, and the supernatant was diluted for further measurement with HR-CS GFAAS.

Since some steel tools use chromium-vanadium as an alloy, which has the properties to heighten the wear residence and its hardness, it is possible that the steel probe could be made of such material (Liu et al. 2024). To determine if the ultrasound probe itself may act as a disturbance a blank of just buffer was also measured. The results of both measurements are shown in Table 21.

Table 21: Vanadium content after ultrasonic cell disruption of a sample and a blank

Method	C_{AAS} [µg/L]	DF	m_{sample} [g]	C_{sample} [µg/g DW]
Ultrasonic (sample)	5.662	100	1.5054	28.21
Ultrasonic (blank)	8.103	100	–	60.77

For dried *P. palmata*, ultrasonic cell disruption was tested as a potential method to release vanadium-containing enzymes. After sonication, the vanadium concentration in the extract was determined to be 28.21 µg/g DW.

To control for possible contamination, the ultrasonic probe was measured as a blank. The blank solution showed a vanadium concentration of 60.77 µg/g, which was substantially higher than the value obtained from the algal sample itself.

4.5.4 Discussion: Ultrasonic cell disruption of *P. palmata*

Although the vanadium concentration obtained from the ultrasonic extract with 28.21 µg/g DW initially appeared reasonable and comparable to values obtained with buffer-based crude extraction, the blank measurement revealed significant contamination. The ultrasonic probe itself contributed vanadium to the solution, most likely because the probe tip was made of chromium-vanadium steel, which released vanadium ions during sonication.

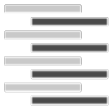

As a result, the measured vanadium concentration in the algal extract cannot be clearly attributed to the biological sample. The similarity between the extracted concentration and previously determined values is therefore considered coincidental.

Due to this high and uncontrollable blank value, ultrasonic disruption was deemed unsuitable for further experiments. The method was excluded from subsequent analyses, as it could not reliably distinguish between vanadium originating from the algae and vanadium released from the probe material.

4.5.5 Results: Ultra-Turrax® cell disruption of *P. palmata*

For dried *P. palmata*, cell disruption was performed using an Ultra-Turrax® homogenizer. The algal biomass was suspended in 50 mM Tris-HCl buffer (pH 7.4) at 5 mg/mL, which had previously been tested as a crude extraction buffer. The suspension was homogenized, and the resulting supernatant was analyzed by HR-CS GFAAS. Similarly, to the previous method, a blank with just buffer was measured to determine possible contamination from the probe. The results are seen in Table 22.

Table 22: Vanadium content after homogenization with Ultra-Turrax® of a sample and a blank

Method	**C_{AAS} [µg/L]**	**DF**	**m_{sample} [g]**	**C_{sample} [µg/g DW]**
Ultra-Turrax® (sample)	5.648	100	0.5012	28.17
Ultra-Turrax® (blank)	2.104	1	–	0.105

The vanadium concentration in the supernatant was determined to be 28.17 µg/g DW. The blank measurement of the Ultra-Turrax® homogenizer in Tris-HCl buffer yielded only 0.105 µg/g, which is just above the detection limit and therefore negligible compared to the sample concentration.

4.5.6 Discussion: Ultra-Turrax® cell disruption of *P. palmata*

When applied in Tris-HCl buffer, the Ultra-Turrax® homogenizer released vanadium concentrations of 28.17 µg/g DW into the supernatant. This result is very similar to the concentrations obtained with buffer-only crude extractions (26–27 µg/g DW), suggesting that both approaches solubilize comparable amounts of vanadium-containing proteins.

Unlike ultrasonic disruption, the Ultra-Turrax® did not introduce significant contamination. The blank was very low (0.105 µg/g), just above the detection limit, and therefore not relevant to

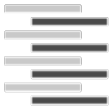

the interpretation of vanadium concentrations. This indicates that the Ultra-Turrax® is a reliable mechanical disruption method in combination with Tris-HCl buffer.

However, the concentration recovered in the supernatant was still lower than the total vanadium content measured after complete digestion (36-38 µg/g DW). This shows that not all vanadium-containing enzymes were released into the soluble fraction, and some remained in insoluble cellular material.

4.5.7 Results: Osmotic shock extraction of *P. palmata*

Osmotic shock was tested as a non-mechanical method for releasing vanadium-containing enzymes from *P. palmata*. Two different time points were tested 3h and 5h, for the 3h extraction an additional extraction of 1h with an alkaline extraction buffer was performed. The results are demonstrated as aqueous phase for the extraction with de-ionized water and alkaline phase for the extraction with alkaline buffer (0.12 M NaOH + 10 mM β-mercaptoethanol). The results of aqueous phase 3h and alkaline phase 1h were combined as a total extraction amount of vanadium. All results are seen in Table 23.

Table 23: Vanadium content after osmotic shock and alkaline extraction

Phase	Time	C_{AAS} [µg/L]	DF	m_{sample} [g]	C_{sample} [µg/g DW]	% of V
Aqueous	3 h	7.085	200	2.5	28.34	73
Alkaline	1 h	1.297	200	2.5	10.38	27
Total	–	–	–	–	**38.72**	100
Aqueous	5 h	6.604	200	2.5	26.42	–

The resulting aqueous phase for the 3h extraction contained 28.34 µg/g DW vanadium, while the extraction of the pellet with an alkaline buffer released an additional 10.38 µg/g DW. Together, the two phases had a total of 38.72 µg/g DW, which is in line with the concentration measured after complete digestion (36-38 µg/g DW).

A 5 h osmotic shock experiment released a similar concentration of 26.42 µg/g DW into the aqueous phase. The alkaline fraction was not analyzed due to time constraints.

4.5.8 Discussion: Osmotic shock extraction of *P. palmata*

The osmotic shock experiments demonstrated that vanadium can be efficiently released from algal cells without mechanical disruption. After 3 h, approximately 73 % of the vanadium was detected in the aqueous phase, while the remaining 27 % was solubilized in the alkaline fraction. When both fractions were combined, the total vanadium concentration (38.7 µg/g DW) closely matched the value obtained by complete digestion (36-38 µg/g DW). This indicates that osmotic shock coupled with alkaline extraction is capable of recovering the entire vanadium content present in the algae.

Comparing the results of the 3 h and 5 h osmotic shock aqueous phases, similar concentrations were observed (~28 and 26 µg/g DW), suggesting that a longer incubation does not necessarily increase vanadium release.

These aqueous results resemble those with buffer extractions, where the majority of vanadium was also found in the water-soluble phase. However, osmotic shock combined with alkaline extraction appears even more effective, as it can recover the full vanadium content.

The main limitation of this method is its time demand, 3 h osmotic shock + centrifugation, followed by 1 h alkaline extraction + centrifugation, make it less practical for high-throughput applications.

4.5.9 Results: Combined osmotic shock and Ultra-Turrax® extraction of *P. palmata*

To evaluate whether combining mechanical and non-mechanical disruption methods could improve vanadium recovery, a 3 h osmotic shock (aqueous phase) was followed by alkaline extraction, while the samples were simultaneously processed with an Ultra-Turrax® homogenizer at two different speeds, 13.500 rpm and 24.000 rpm. Results are seen at Table 24.

Table 24: Results of combined extraction methods with two different homogenization speed

Speed	Phase	C_{sample} [µg/g DW]	% of V	Total [µg/g DW]
13.500 rpm	Aqueous	26.26	74.6	
	Alkaline	8.95	25.4	
	Combined		100	35.21
24.000 rpm	Aqueous	27.84	80.5	
	Alkaline	6.74	19.5	
	Combined		100	34.58

At 13.500 rpm, the aqueous phase contained 26.26 µg/g DW vanadium, making it 74.6% of total vanadium content, and the alkaline phase contained 8.95 µg/g DW with 25.4% of total vanadium content, resulting in a total recovery of 35.21 µg/g DW. At 24.000 rpm, the aqueous phase yielded 27.84 µg/g DW with 80.5% of vanadium content and the alkaline phase 6.74 µg/g DW with 19.5% of the total vanadium content, with a total of 34.58 µg/g DW.

4.5.10 Discussion: Combined osmotic shock and Ultra-Turrax® extraction of *P. palmata*

The combination of osmotic shock, alkaline extraction and Ultra-Turrax® homogenization released vanadium concentrations in the range of 34–35 µg/g DW, which is close to the values obtained by osmotic shock alone (38.7 µg/g DW). The distribution between aqueous (~75–80%) and alkaline (~20–25%) phases was comparable to that seen in the non-mechanical osmotic shock method, confirming that most vanadium is solubilized during the aqueous step. Small variations in total vanadium recovery between replicates are expected due to biological sample heterogeneity.

But more importantly, the combination of methods did not lead to a significant improvement in vanadium yield compared to osmotic shock alone. Instead, the additional steps would increase experimental complexity, requiring more instrumentation, and introducing the potential for sample loss during each step.

Additionally, Ultra-Turrax® homogenization carries the risk of shear stress and heating of the sample, which could cause partial denaturation or inactivation of proteins, including vanadium-dependent haloperoxidases. This could limit the suitability of the combined approach for preparing these enzyme extracts.

4.5.11 Results: Direct alkaline extraction of *P. palmata*

As an alternative to osmotic shock followed by alkaline extraction, dried *P. palmata* was extracted directly with the alkaline solution (0.12 M NaOH + 10 mM β-mercaptoethanol). The sample was incubated at room temperature for 1 h under stirring, followed by centrifugation (10.000 × g, 30 min, 4 °C). The supernatant was diluted and analyzed by HR-CS GFAAS. Results are summarized in Table 25.

Table 25: Results after direct alkaline extraction

Method	C_{AAS} [µg/L]	DF	m_{sample} [g]	C_{sample} [µg/g DW]
Direct alkaline extraction	5.304	500	4.0034	39.75

This method yielded a vanadium concentration of 39.75 µg/g DW, which corresponds to approximately the full vanadium content previously determined by complete digestion (36-38 µg/g DW).

4.5.12 Discussion: Direct alkaline extraction of *P. palmata*

Direct alkaline extraction successfully released the entire vanadium content from *P. palmata*, achieving a concentration slightly higher than that obtained by complete digestion. This suggests that the method is highly effective for solubilizing vanadium, without requiring a prior osmotic shock step.

Compared to the aqueous + alkaline osmotic shock approach, the direct method offers several advantages. It primarily reduces the processing time a total of approximately 5 h to less than 2 h. Since there is no pellet resuspension step required, the risk of sample loss has lowered and lastly the results of the measured vanadium content are comparable.

The main potential problem is that the strongly alkaline conditions may pose a risk of partial protein denaturation or loss of enzymatic activity.

4.5.13 Results: Ultra-Turrax® extraction of fresh algae

Fresh algal samples of *P. palmata* and *C. crispus* with Tris-HCl buffer (20 mg/mL biomass) were homogenized with an Ultra-Turrax® for a few minutes at gradually increasing speed. After centrifugation, the supernatants were analyzed by HR-CS GFAAS. Results are summarized in Table 26.

Table 26: Results of Ultra-Turrax® extraction of fresh material from P. palmata and C. crispus

Species	C_{AAS} [µg/L]	DF	m_{sample} [g]	m_{sample} DW [g]	C_{sample} [µg/g DW]
P. palmata	7.084	100	10.0986	1.54	23.02
C. crispus	2.507	100	10.0628	1.90	6.59

For *P. palmata*, a vanadium concentration of 23.02 µg/g DW was measured, while *C. crispus* yielded 6.59 µg/g DW. These results are in line with values obtained from digested fresh samples, suggesting that mechanical homogenization can effectively release vanadium from fresh material.

4.5.14 Discussion: Ultra-Turrax® extraction of fresh algae

When applied to fresh algae, Ultra-Turrax® homogenization produced vanadium concentrations comparable to those obtained by digestion of fresh samples. The method appeared to work better with fresh than with dried and milled material, which is reasonable since in the intact state, shear forces can disrupt the cell walls more efficiently. For dried and powdered samples, the additional homogenization did not provide much benefit, as the cell walls were already fragmented.

Between the two tested species, *P. palmata* yielded higher vanadium concentrations than *C. crispus* which is in line with previous tested samples. Nevertheless, the limitations typically associated with Ultra-Turrax® remain relevant. In particular, long homogenization increases the risk of sample heating, which may lead to denaturation or inactivation of proteins. This issue is more pronounced in fresh algae, where stronger shear forces and longer processing times are required due to tougher cell walls. Both species differ in their cell wall properties. *C. crispus* has

thick, mucilaginous cell walls with strong water-binding capacity, making them harder to disrupt mechanically. In contrast, *P. palmata* cell walls are less resistant, allowing more efficient homogenization.

4.5.15 Results: Alkaline extraction of fresh algae

Fresh samples of *P. palmata* and *C. crispus* were extracted with alkaline buffer (0.12 M NaOH + 10 mM β-mercaptoethanol), in a concentration of 5 mg/mL. After centrifugation, the supernatants were analyzed by HR-CS GFAAS. The results are listed in Table 27.

Table 27: Vanadium content after alakline extraction of fresh algae

Species	C_{AAS} [µg/L]	DF	m_{sample} [g]	m_{sample} DW [g]	C_{sample} [µg/g DW]
P. palmata	2.999	200	10.1095	1.5402	38.94
C. crispus	3.431	50	10.2948	1.9464	8.81

The measured vanadium concentrations were 38.94 µg/g DW for *P. palmata* and 8.81 µg/g DW for *C. crispus*. For *P. palmata*, the concentration exceeded the value obtained from digestion of fresh material (22.6 µg/g DW) and approached the level determined for dried samples (38 µg/g DW). For *C. crispus*, the concentration was similar to values measured in dried material (9 µg/g DW).

4.5.16 Discussion: Alkaline extraction of fresh algae

The results show that alkaline extraction is highly effective for fresh algal material, especially for *P. palmata*, where the measured concentration even exceeded the value obtained by digestion of fresh samples and matched the concentration from dried material. This suggests that alkaline treatment is capable of fully releasing vanadium-containing enzymes regardless of whether the biomass is dried or fresh.

For *C. crispus*, alkaline extraction of fresh samples yielded 8.8 µg/g DW, closely comparable to the dried material 9.2 µg/g DW. This indicates that alkaline conditions are sufficiently harsh to overcome the structural resistance of its mucilaginous cell walls, which otherwise challenge the mechanical disruption.

Despite its high efficiency, the method still holds the limitations of using strong alkaline conditions. The problem with potential denaturation of proteins and a risk of reduced enzyme

activity is still apparent. Additionally, fresh samples are less homogeneous than dried and milled samples, resulting in looser pellets after centrifugation and some processing difficulties. A pre-homogenization step with Ultra-Turrax® could help reduce the presence of large undisintegrated cell fragments and improve handling.

4.6 Results: Precipitation

Following the cell disruption, the supernatants S1 were precipitated with ammonium sulfate. This stepwise precipitation was performed to further separate and purify protein fractions.

4.6.1 Results: *P. palmata* – Ultra-Turrax® extraction (fresh material)

Cell disruption with Ultra-Turrax® in TRIS-HCl buffer released vanadium into the soluble extract S1, with a concentration of 27.29 µg/g DW (100 %). Stepwise ammonium sulfate precipitation was performed to separate protein fractions and evaluate the distribution of vanadium. Results are summarized in Table 28.

Table 28: Results of precipitation after Ultra-Turrax® extraction of fresh P. palmata

Fraction	AS %	C_{AAS} [µg/L]	m_{sample} [g]	m_{sample} DW [g]	DF	C_{sample} [µg/g DW]	% of V
S1	0	8.335	13.028	1.985	100	27.29	100
S2	30	8.179	13.028	1.985	100	24.72	90.58
P3	60	1.247	13.028	1.985	100	6.28	23.02
S3	60	6.538	13.028	1.985	100	19.76	72.41

Precipitation with 30 % ammonium sulfate S2 resulted in only a slight reduction of vanadium, resulting in 24.72 µg/g (90.58 %), the pellet P2 was discarded and not measured. After further precipitation at 60 % saturation, the protein pellet P3 contained only a low vanadium concentration of 6.28 µg/g (23.02 %), while the supernatant S3 retained the majority of vanadium with a concentration of 19.76 µg/g (72.41 %).

4.6.2 Results: *P. palmata* – osmotic shock extraction (dried material)

Cell disruption of *P. palmata* by osmotic shock released measurable amounts of vanadium into the aqueous extract (S1), with a concentration of 28.32 µg/g, defined as 100 % of the extractable vanadium. Stepwise ammonium sulfate precipitation was performed to separate protein fractions and evaluate the distribution of vanadium. Results are summarized in Table 29.

Table 29: Results of precipitation after osmotic shock of dried P. palmata

Fraction	AS %	C_{AAS} [µg/L]	m_{sample} DW [g]	DF	C_{sample} [µg/g DW]	% of V
S1	0	7.085	2.5	200	28.34	100.00
S2	30	7.105	2.5	200	28.42	100.28
S3	60	6.264	2.5	200	25.06	88.41
P3	60	0.4953	2.5	100	1.981	6.99
S4	90	10.19	2.5	100	20.38	71.91

At 30 % ammonium sulfate saturation S2, the supernatant retained most of the vanadium with about 28.42 µg/g (100.35 % relative to S1), while the pellet P2 was discarded as it contained mainly contaminant proteins and cell debris. Further precipitation at 60 % saturation (S3) again resulted in the majority of vanadium remaining in the supernatant with 25.06 µg/g (88.47 %), whereas the protein pellet P3 contained only a very small fraction of vanadium 0.99 µg/g (3.5%). A final precipitation step at 90 % saturation reduced the vanadium concentration in the supernatant to 20.38 µg/g (71.96 %), but still, most of the element remained soluble.

4.6.3 Results: *C. crispus* – Ultra-Turrax® extraction (fresh material)

Cell disruption with Ultra-Turrax® in Tris-HCl buffer released vanadium into the soluble extract S1 with a concentration of 3.48 µg/g dry weight (100 %). Stepwise ammonium sulfate precipitation was performed to separate protein fractions and evaluate the distribution of vanadium. Results are summarized in Table 30.

Table 30: Results of precipitation after Ultra-Turrax® extraction of fresh C. crispus

Fraction	AS %	C_{AAS} [µg/L]	m_{sample} [g]	m_{sample} DW [g]	DF	C_{sample} [µg/g DW]	% of V
S1	0	1.328	10.10	1.91	100	3.48	100.00
S2	30	1.918	10.10	1.91	50	2.51	72.13
S3	60	1.601	10.10	1.91	50	2.10	60.34
P3	60	1.775	10.10	1.91	10	0.46	13.22
S4	90	1.201	10.10	1.91	50	1.57	45.11

At 30 % ammonium sulfate saturation S2, vanadium decreased to 2.51 µg/g which makes about 72.13 % of the total vanadium content, the Pellet P2 was discarded and not measured. During the next precipitation step at 60% S3 was measured at 2.10 µg/g which is about 60.34 % of the vanadium content. The corresponding pellet P3 contained only a small fraction 0.46 µg/g or 13.22 %. Even after 90 % saturation, most vanadium remained in the supernatant S4 which yielded a concentration of 1.57 µg/g.

4.6.4 Results: *P. palmata* – alkaline extraction (fresh material)

Alkaline extraction of fresh *P. palmata* released vanadium into the soluble fraction S1, with a concentration of 38.9 µg/g (100%). Stepwise ammonium sulfate precipitation was performed to separate protein fractions and evaluate the distribution of vanadium. Results are summarized in Table 31.

Table 31: Results of precipitation after alkaline extraction of fresh P. palmata

Fraction	AS %	C_{AAS} [µg/L]	m_{sample} [g]	m_{sample} DW [g]	DF	C_{sample} [µg/g DW]	% of V
S1	0	2.999	10.11	1.54	200	38.94	100.00
S2	30	4.263	10.11	1.54	100	27.68	71.07
S3	60	7.911	10.11	1.54	50	25.68	65.95
P2	30	9.690	10.11	1.54	50	31.46	80.78
P3	60	5.892	10.11	1.54	50	19.13	49.12

After precipitation with 30 % ammonium sulfate, the supernatant retained most of the vanadium with 27.68 µg/g, making it about 71.07 % of the total vanadium content, this time more vanadium got lost during the first precipitation step. The pellet P2 was measured this time and yielded 31.46 µg/g which makes is about 80 % of the initial vanadium content. At 60 % saturation, vanadium in the supernatant S3 yielded 24.6 µg/g, while the pellet P3 this time contained a lot more vanadium with 19.13 µg/g which is nearly 50 % of the total vanadium content. Combining S2 with P2 and S3 with P3 results in much higher vanadium content than initially measured in S1. Together S3+P3 yield 44.81 µg/g which is more the amount than initially believed to be in the sample. Taking only this number into account S3 makes about 57.3 % and P3 42.7 % of their combined vanadium content.

4.6.5 Results: *C. crispus* – alkaline extraction (fresh material)

Alkaline extraction of fresh *C. crispus* released vanadium into the soluble fraction S1, with a concentration of 7.08 µg/g (100 %). Stepwise ammonium sulfate precipitation was performed to separate protein fractions and evaluate the distribution of vanadium. Results are summarized in Table 32.

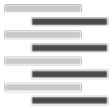

Table 32: Results of precipitation after alkaline extraction of fresh C. crispus

Fraction	AS %	C_{AAS} [µg/L]	m_{sample} [g]	m_{sample} DW [g]	DF	C_{sample} [µg/g DW]	% of V
S1	0	1.367	10.29	1.93	100	7.080	100.00
S2	30	1.341	10.29	1.93	50	3.473	49.05
S3	60	2.148	10.29	1.93	25	2.781	39.28
P2	30	2.087	10.29	1.93	20	2.162	30.53
P3	60	6.578	10.29	1.93	20	6.814	96.24

After the first step of precipitation with 30 % ammonium sulfate, the supernatant retained about half of the vanadium with 3.473 µg/g, making it about 49 % of the total vanadium content, this time more vanadium got lost during the first precipitation step. This is confirmed through the vanadium content detected in P2 which was 2.162 µg/g. At the second precipitation step with 60 % saturation, vanadium was primarily detected in the pellet P3 with a concentration of 6.814 µg/g. The supernatant, S3 yielded 2.781 µg/g. Also, here S3+P3 contained about 9.595 µg/g which is 35.5% more than initially measured in S1. This makes about 29 % of S3 and 71 % of P3.

4.6.6 Results: *P. palmata* – alkaline extraction (dried material)

Alkaline extraction of dried *P. palmata* released vanadium into the soluble fraction S1, with 34.2 µg/g detected (100 %). Stepwise ammonium sulfate precipitation was performed to separate protein fractions and evaluate the distribution of vanadium. Results are summarized in Table 33.

Table 33: Results of precipitation after alkaline extraction of dried P. palmata

Fraction	AS %	C_{AAS} [µg/L]	m_{sample} DW [g]	DF	C_{sample} [µg/g DW]	% of V
S1	0	4.564	4.0034	500	34.20	100.00
S2	30	3.663	4.0034	500	27.45	80.26
P2	30	4.772	4.0034	100	11.92	34.85
S3	60	6.553	4.0034	250	24.55	71.79
P3	60	2.905	4.0034	100	7.26	21.22
S4	90	5.484	4.0034	250	20.55	60.08

After precipitation with 30 % ammonium sulfate, the supernatant retained most of the vanadium with 27.45 µg/g, making it about 80 % of the total vanadium content, this time more vanadium got lost during the first precipitation step. The pellet P2 was measured this time and yielded 11.9 µg/g which makes is about 34.85 % of the initial vanadium content. At 60 % saturation, vanadium was again primarily detected in the supernatant, S3 yielded 24.6 µg/g, while the pellet P3 contained only 7.3 µg/g (21.22 %). At 90% saturation, the supernatant S4 still contained 20.6 µg/g or 60.08 % of vanadium.

4.6.7 Results: Combined results of precipitation

To provide an overview of the precipitation experiments, the percentual distribution and absolute concentrations of vanadium across fractions are summarized in Figure 25 and Table 34.

Only the relevant supernatant S3 and pellet P3 after 60% ammonium sulfate precipitation were taken under consideration. The percentual distribution was taken from Table 34. were S3+P3 make up the total vanadium content.

Table 34: Combined results of precipitation after different extraction methods

Species	Method	Sample	S3 [µg/g]	P3 [µg/g]	total [µg/g]	% of V in S3	% of V in P3
C. crispus	Alkaline	fresh	2.78	6.81	9.60	28.98	71.02
C. crispus	Ultra-Turrax®	fresh	2.10	0.46	2.56	82.03	17.97
P. palmata	Alkaline	fresh	25.68	19.13	44.81	57.31	42.69
P. palmata	Ultra-Turrax®	fresh	19.76	6.28	26.04	75.88	24.12
P. palmata	Alkaline	dried	24.55	7.26	31.81	77.18	22.82
P. palmata	Osmotic shock	dried	25.06	1.98	27.04	92.67	7.33

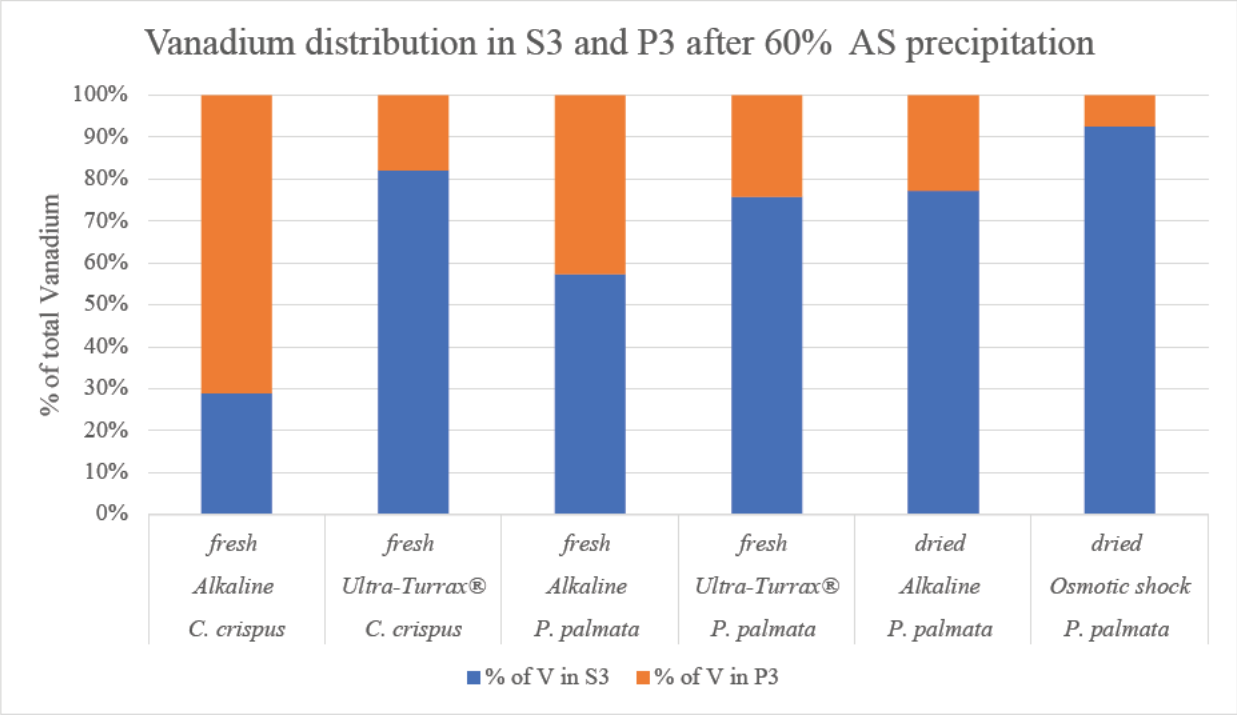

Figure 25: Visualization of vaandium distribution after 60% ammonium sulfate precipitation

Through the visualization of the vanadium distribution after the different cell distribution methods and the precipitation with AS, it is clear that mostly, throughout both algal species, the majority of vanadium remained in the supernatant. The only exception is the alkaline extraction, practically of the fresh material, here the pellet has the most amount of vanadium. In the alkaline extraction of fresh *C. crispus*, the total vanadium content (28.98 µg/g DW) even extends the results from previous tested samples. The pellet here has the highest amount of total vanadium with more than 70 % and only 30 % in the supernatant. It is not clear if this is just an inconsistency of sample material or a result of favorable extraction conditions. In the alkaline extraction of fresh *P. palmata* the total vanadium content extends over 55 % in the pellet and around 45 % in the supernatant. All other methods (Ultra-Turrax®, osmotic shock) in dried and fresh material only show a distribution of total vanadium content in the pellet around 7-24 % while the rest remains in the supernatant. The least amount of vanadium in the pellet was precipitated from the aqueous phase after osmotic shock. Even though the alkaline extraction of the fresh material is most successful around 30-45 % of vanadium still remains supernatant.

4.6.8 Discussion: Precipitation

The stepwise ammonium sulfate precipitation experiments carried out with *P. palmata* and *C. crispus* consistently showed that vanadium was mainly retained in the supernatant, whereas the pellets contained mostly only a smaller fraction of vanadium. This pattern was observed regardless of extraction method (Ultra-Turrax®, osmotic shock, or alkaline extraction) and whether fresh or dried material was used.

This was most pronounced in the osmotic shock extraction of dried *P. palmata*, where less than 10 % of vanadium was recovered in the pellet. In contrast, alkaline extraction of fresh biomass yielded the highest relative pellet recovery (ca. 55-70%), particularly for *P. palmata* and *C. crispus*. These results highlight that ammonium sulfate precipitation of alkaline extracts yielded the most vanadium in P3, suggesting some stabilization of vanadium–protein complexes under these conditions. Even still a majority of vanadium remains soluble (ca. 30-45 %). Which may make precipitation with ammonium sulfate not as effective as a stand-alone method to concentrate vanadium-dependent enzymes as assumed or suggests that vanadium content in these red algae is not only associated with V-HPOs but with other proteins or it remains unbound.

Interestingly, in the alkaline extractions of fresh biomass, the apparent vanadium content calculated for S3+P3 in *P. palmata* and *C. crispus* exceeded the initial concentration in S1 (e.g., 44.8 µg/g *C. crispus* and. 38.9 µg/g for *P. palmata*). This discrepancy likely reflects the calculation basis, as concentrations were normalized to the dry weight of the initial sample, while the actual recovery depends on the yields of supernatant and pellet fractions. Without precise mass balances (fraction volumes and pellet dry weights), the apparent “over-recovery” cannot be corrected, but it highlights that vanadium is partitioned between multiple fractions and that its recovery is highly sensitive to processing steps.

The observed high vanadium levels in supernatants imply that either, vanadium is loosely bound or present in non-protein complexes, or the specific enzymes are diluted among a large background of proteins. The partial enrichment in alkaline extracts of fresh biomass is promising but not selective enough for preparative purposes.

4.7 Results: Protein quantification- different extraction methods

To investigate the relationship between protein yield and vanadium content in *P. palmata*, different extraction methods (osmotic shock+ alkaline extraction, Ultra-Turrax® in aqueous buffer, and alkaline extraction) were applied. The resulting extracts were analyzed for protein concentration using the ROTI® Quant protein assay and for vanadium content using GFAAS.

Protein concentrations determined by ROTI® Quant protein assay are summarized in Figure 26.

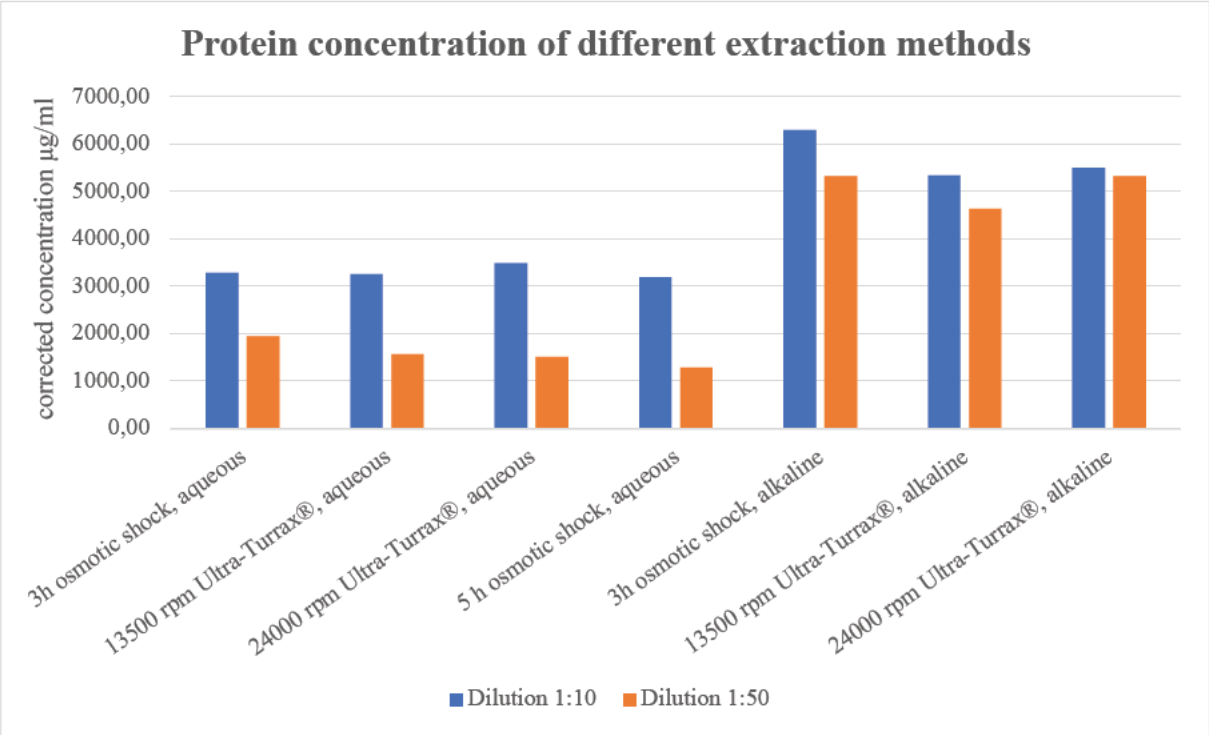

Figure 26: Protein concentration of different methods

Across the aqueous extractions (osmotic shock and Ultra-Turrax®), no major differences in the protein yield were observed, with corrected concentrations ranging between 3200-3500 µg/ml (1:10 dilution). In contrast, the alkaline extracts consistently showed higher protein concentrations, almost twofold compared to the aqueous phase, reaching up to 6300 µg/ml (1:10 dilution). In all cases, protein concentrations obtained from 1:10 dilutions were constantly higher than those from 1:50 dilutions.

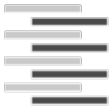

Table 35: Vanadium content of different extraction methods

Phase	Method	C_{AAS} [µg/L]	m_{sample} DW [g]	DF	C_{sample} [µg/g DW]
aqueous	3h osmotic shock	7.085	2.5	200	28.34
aqueous	13.500 rpm Ultra-Turrax®	6.564	2.5	200	26.26
aqueous	24.000 rpm Ultra-Turrax®	6.959	2.5	200	27.84
aqueous	5 h osmotic shock	6.604	2.5	200	26.42
alkaline	3h osmotic shock	1.297	2.5	200	10.38
alkaline	13.500 rpm Ultra-Turrax®	1.119	2.5	200	8.95
alkaline	24.000 rpm Ultra-Turrax®	0.8429	2.5	200	6.74

Vanadium quantification revealed an opposite trend (Table 35). Despite the lower protein content in aqueous extracts, vanadium concentrations were noticeably higher (26-28 µg/g DW) compared to alkaline extracts (6-10 µg/g DW). Normalized to the total vanadium recovered, approximately 73 % of vanadium was present in the aqueous phase, while only 27 % was detected in the alkaline phase (Table 36). The overall vanadium concentrations (33-39 µg/g DW) were in line with values from previous experiments.

Table 36: Division of total vanadium content into aqueous and alkaline phase

Condition	C_{total} µg/g	% of V aqeoues phase	% of V alkaline phase
3h osmotic shock	38.72	73.20	26.80
13.500 rpm Ultra-Turrax®	35.21	74.57	25.43
24.000 rpm Ultra-Turrax®	34.58	80.50	19.50

4.7.1 Discussion: Protein quantification- different extraction methods

The protein assay and vanadium quantification results revealed a clear discrepancy between protein content and vanadium distribution. Alkaline extraction yielded almost double the protein concentration compared to aqueous extracts, indicating that more proteins were solubilized under alkaline conditions. However, these extracts contained considerably less vanadium, suggesting that vanadium-associated proteins were not efficiently recovered or even damaged under alkaline conditions.

In contrast, the aqueous extractions, although yielding lower protein concentrations, consistently contained higher vanadium levels. This indicates that vanadium is associated with a specific subgroup of soluble proteins that are preserved under mild aqueous extraction conditions but either degraded, denatured, or solubilized differently under alkaline treatment.

The distribution of vanadium between phases further emphasizes that the majority (73 %) is retained in the aqueous extracts, while only a smaller fraction (27 %) is recovered in alkaline extracts. This suggests that aqueous conditions are more suitable for maintaining the integrity of vanadium-protein complexes, most likely vanadium haloperoxidases.

The subsequent ammonium sulfate precipitation, as seen in the previous results confirm the tendencies observed in earlier experiments. Vanadium did not co-precipitate efficiently with the higher protein fractions, but instead remained in the soluble phase. This reinforces the conclusion that ammonium sulfate fractionation alone is not suitable for selectively enriching vanadium-dependent proteins.

4.8 Results: Protein quantification- after precipitation

For this protein quantification, the supernatants of fresh *C. crispus* after alkaline extraction and Ultra-Turrax® disruption following stepwise ammonium sulfate precipitation were measured (Table 37, Figure 27).

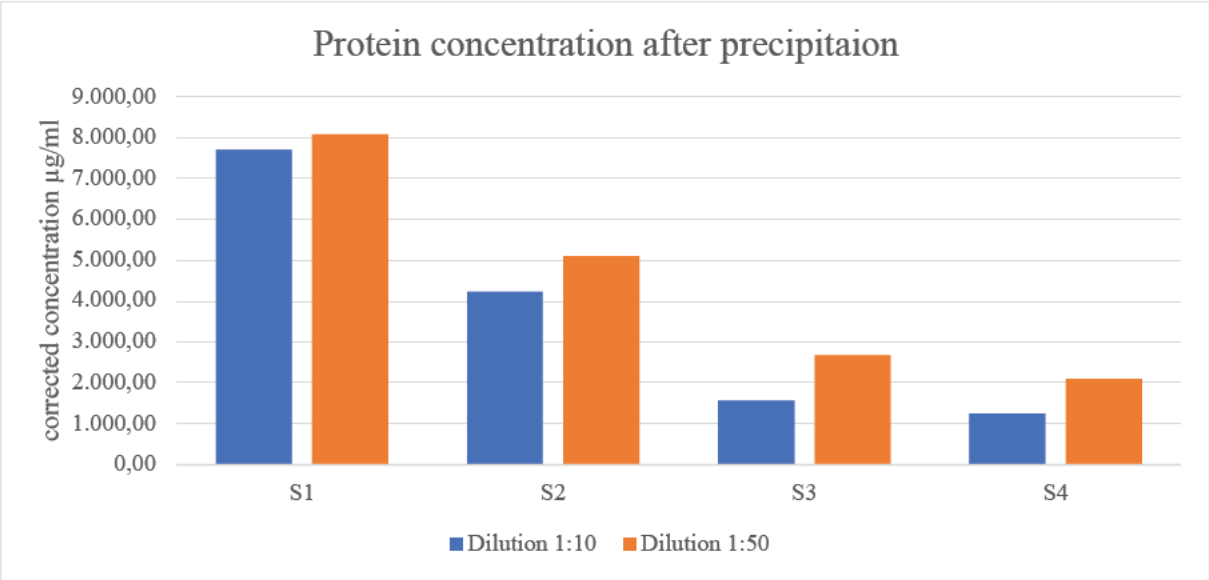

Figure 27: Protein concentration after precipitation of fresh C. crispus

The crude extract S1 contained the highest protein concentration, with corrected values of 7710–8094 µg/ml depending on dilution. After precipitation at 30 % ammonium sulfate saturation, the supernatant S2 showed a reduced protein content of 4230–5114 µg/ml. Further precipitation at 60 % saturation resulted in a prominent decrease of soluble protein S3 with 1557–2680 µg/ml, while a final precipitation step at 90 % saturation left only 1244–2103 µg/ml in the supernatant.

Table 37: Protein concentration after precipitation of fresh C. crispus

Fraction	AS %	DF	C_{AAS} [µg/L]	m_{sample} [g]	m_{sample} DW [g]	C_{sample} [µg/g DW]	% of V
S1	0	100	3.076	20.023	3.786	8.13	100.00
S2	30	100	2.531	20.023	3.786	6.69	82.28
S3	60	100	2.272	20.023	3.786	6.00	73.86
S4	90	100	1.664	20.023	3.786	4.40	54.10

This is also reflected in vanadium concentrations found in the supernatants, which are steadily decreasing through each step. The initial extract S1 contained 8.13 µg/g DW, which decreased after 30 % ammonium sulfate precipitation to about 6.69 µg/g DW in S2 which is about 82.28 % of the initial extract. At 60 % saturation, vanadium decreased to 6.00 µg/g DW (74 %), and at 90 % saturation to 4.40 µg/g DW (54 %). Therefore, both protein and vanadium were gradually reduced in the soluble fractions, but neither were completely removed by precipitation.

4.8.1 Discussion: Protein quantification- after precipitation

The combined analysis of protein and vanadium distribution in *C. crispus* highlights that ammonium sulfate fractionation reduces soluble protein concentrations but does not completely precipitate vanadium-associated proteins or that not all vanadium is bound to such proteins.

Although the overall protein levels dropped by around 70–80 % from the crude extract S1 to the 90 % supernatant S4, more than half of the vanadium remained soluble at the highest salt saturation in S4 (54.10 %). This indicates that vanadium is not tightly co-localized with the bigger protein fractions precipitated by ammonium sulfate. Instead, vanadium likely remains associated with a minor subgroup of soluble proteins or small molecular complexes that are resistant to salt-induced precipitation, or they remain freely as unbound vanadate ions.

Compared to *P. palmata*, the overall vanadium concentrations in *C. crispus* were, as expected lower, nevertheless the precipitation pattern was similar, with vanadium being largely found in the supernatants rather than co-precipitating with proteins. This supports the conclusion that ammonium sulfate precipitation is unsuitable as a strategy to enrich vanadium-binding proteins, such as haloperoxidases, from red algae or that not all vanadium is bound to the V-HPOs remaining unbound in the solution.

4.9 Results: SEC- desalting

After alkaline extraction and stepwise ammonium sulfate precipitation (30% and 60%), the protein pellet (P3) was resuspended in Tris-HCl buffer and subjected to SEC desalting on a 5 mL HiTrap Desalting column, with a flowrate of 1 ml/min. The Figure 28. shows the group separation of salt and proteins of the injected aliquots.

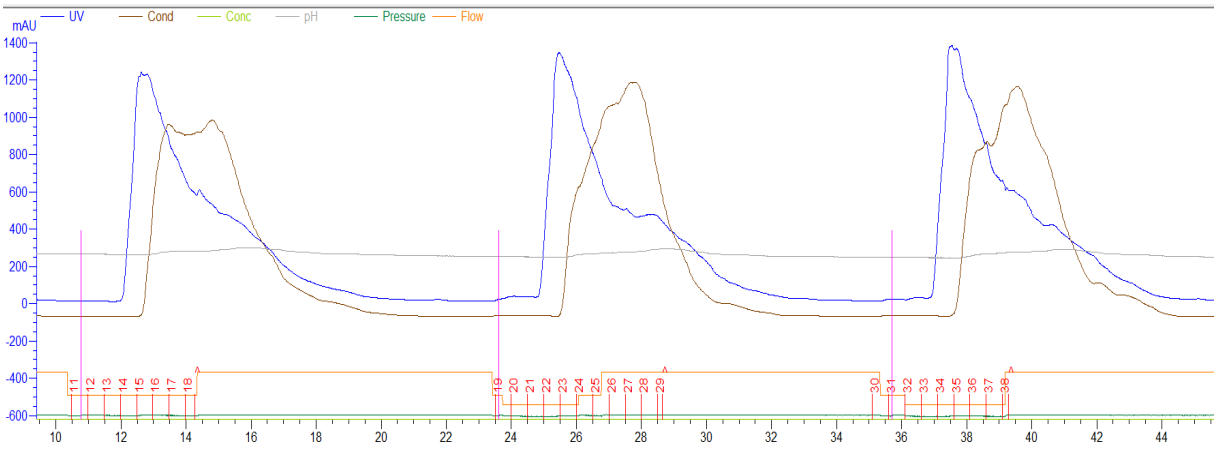

Figure 28: Chromatogram of desalting with SEC

(Source: own image, Laurie Ramadani 2025)

The chromatogram displayed distinct UV peaks corresponding to protein elution (blue curve) and conductivity peaks indicating salt (brown curve). Proteins eluted in the void volume of the column, slightly earlier than the salt peak. However, the separation between protein and salt was not complete. As a result, fractions containing proteins still overlapped with high salt concentrations, and these fractions had to be discarded.

As expected for group separation, all proteins present in the sample eluted together. This prevented distinction between target proteins (e.g., vanadium-dependent enzymes) and other proteins. The SEC step therefore served only as a desalting and buffer exchange method but not as a purification step.

4.9.1 Discussion: SEC- desalting

The desalting step using SEC was an essential requirement for following ion exchange chromatography, since high salt concentrations interfere with binding efficiency and resolution. The method successfully reduced the salt content and exchanged the buffer to Tris-HCl, but the resolution between protein and salt was limited. Therefore, part of the protein-containing fractions overlapped with the salt peak and had to be discarded, resulting in protein loss.

The poor separation between protein and salt may also be linked to the column parameters. In SEC, resolution depends on the ratio of sample volume to column bed volume, this means that smaller sample volumes and larger columns improve the separation between protein and salt. Therefore, using a column with a larger bed volume or applying smaller aliquots per run could reduce protein loss during desalting and improve the efficiency of buffer exchange.

4.10 Results: IEXC- protein purification *P. palmata*

After desalting, the SEC fractions containing the desalted proteins were pooled and loaded onto a 1 mL HiTrap DEAE Sepharose Fast Flow column with 50 mM Tris-HCl buffer (pH 7.4). Proteins were eluted stepwise with 0.2 M and 0.3 M KCl at a flow rate of 1 mL/min.

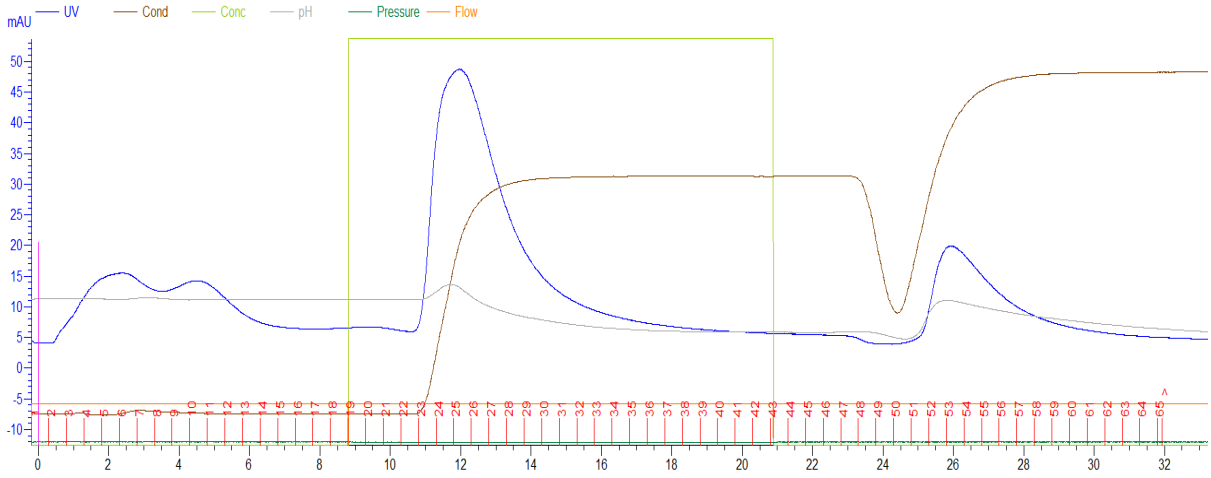

Figure 29: Chromatogram of AIEXC from P. palmata

(Source: own image, Laurie Ramadani 2025)

The chromatogram (Figure 29) showed three groups of peaks, a small flow-through (no KCl), a large peak at 0.2 M KCl, and a smaller peak at 0.3 M KCl. The UV peaks correspond to protein elution (blue curve) and conductivity peaks indicating salt (brown curve).

Vanadium concentrations were measured in pooled fractions by AAS (Table 38).

Table 38: Vanadium content of pooled fraction after AIEXC purification

Peak	KCl (M)	V (µg/mL, AAS)
1	0.0	0.299
2	0.2	4.257
3	0.3	0.293

The flow-through contained 0.299 µg/mL vanadium, the 0.2 M KCl fraction contained 4.257 µg/mL, and the 0.3 M KCl fraction contained 0.293 µg/mL. This means that vanadium was almost only present in the 0.2 M KCl fraction.

4.10.1 Discussion: IEXC- protein purification *P. palmata*

The DEAE chromatography separated the protein mixture into different fractions and showed that vanadium is concentrated in the 0.2 M KCl fraction. This suggests that vanadium-containing proteins bind only moderately to the column and are released when 0.2 M KCl is applied. Proteins that bind more strongly and elute at 0.3 M KCl did not contain vanadium, while proteins that did not bind at all (flow-through) also lacked vanadium.

This result is not comparable to the study by Ohshiro et al. (2002), where haloperoxidases were reported to elute at 0.3 M KCl. Several reasons could explain this difference, such as small changes in the enzyme properties, buffer conditions, or the use of stepwise elution in this study instead of a continuous gradient.

To verify the presence of haloperoxidases, SDS-PAGE analysis was performed using the pooled fractions.

4.11 Results: IEXC- protein purification *C. crispus*

Protein extracts of *C. crispus*, obtained after SEC desalting, were further purified with the anion exchange chromatography (DEAE Sepharose FF, 1 mL HiTrap, 50 mM Tris-HCl pH 7.4). Elution was performed stepwise with 0.2 M and 0.3 M KCl at a flow rate of 1 mL/min.

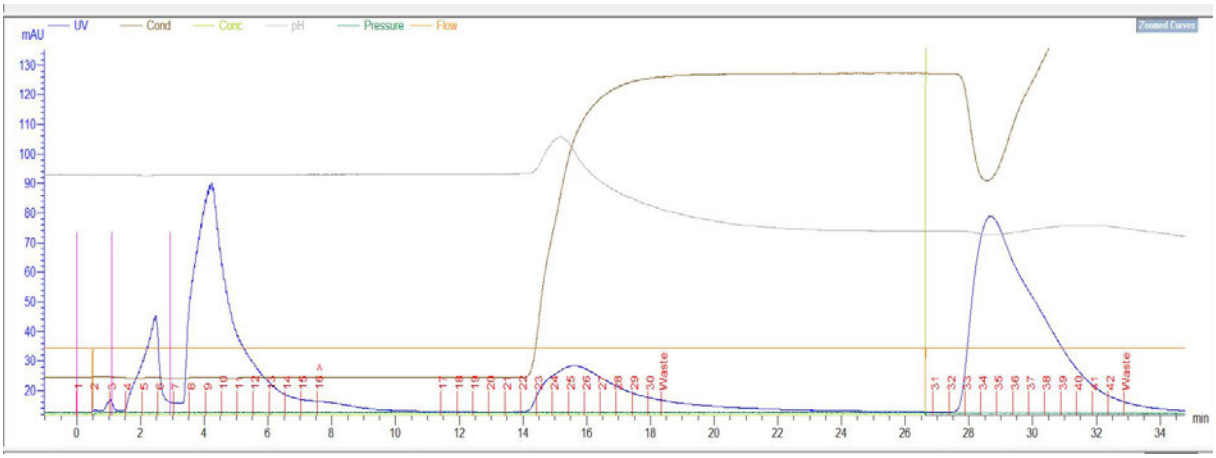

Figure 30: Chromatogram of AIEXC from C. crispus

(Source: own image, Laurie Ramadani 2025)

The chromatogram revealed several peaks, first the flow-through after infection, a second elution peak with 0.2 M KCl, and a later peak with 0.3 M KCl. The smallest peak was observed at 0.2 M KCl and the biggest were after injection and at 0.3 M KCL (Figure 30). The UV peaks correspond to protein elution (blue curve) and conductivity peaks indicating salt (brown curve).

Fractions were pooled according to the observed peaks and analyzed for vanadium content by AAS. But no detectable vanadium was found in any of the fractions, independent of their elution position.

4.11.1 Discussion: IEXC- protein purification *C. crispus*

In contrast to *P. palmata*, where vanadium was clearly found in the 0.2 M KCl fraction, the DEAE chromatography of *C. crispus* did not show any measurable vanadium signal in any of the protein fractions. This indicates that either *C. crispus* does not contain vanadium-dependent haloperoxidases under the tested extraction conditions, or that the concentration was below the detection limit of AAS.

The chromatogram confirmed that proteins were successfully bound and eluted, so the absence of vanadium was not due to a failure of the separation process. Rather, it reflects either biological differences between the species or technical limitations. Previous experiments with *C. crispus* already showed generally lower vanadium contents compared to *P. palmata*. Combined with the fact that size exclusion chromatography (SEC) causes significant sample dilution and protein loss, it is likely that any vanadium present was reduced below the detection level during the preparation process.

This outcome highlights the two points that firstly vanadium haloperoxidases are not universally present at detectable levels across red algal species, and secondly, that losses during sample handling can influence vanadium detectability. Optimizing sample recovery, for example by minimizing SEC dilution or using alternative desalting methods, could improve sensitivity in future experiments.

4.12 Results: SDS-PAGE

To further investigate the presence of V-HPOs, protein fractions from both *P. palmata* and *C. crispus* were analyzed by SDS-PAGE. This method provides an overview of the protein composition from the enzyme extracts, ammonium sulfate fractions, to the DEAE chromatography fractions, and allows the detection of proteins near the expected molecular weight of ~67 kDa. In contrast to AAS, which indirectly detects vanadium as a marker for haloperoxidases, SDS-PAGE enables the direct visualization of protein bands and therefore serves as an additional approach to confirm the presence of the target enzyme. The SDS-PAGE results as well as the lane loading scheme are presented in the figures below. (Figure 31, Figure 32, Figure 33)

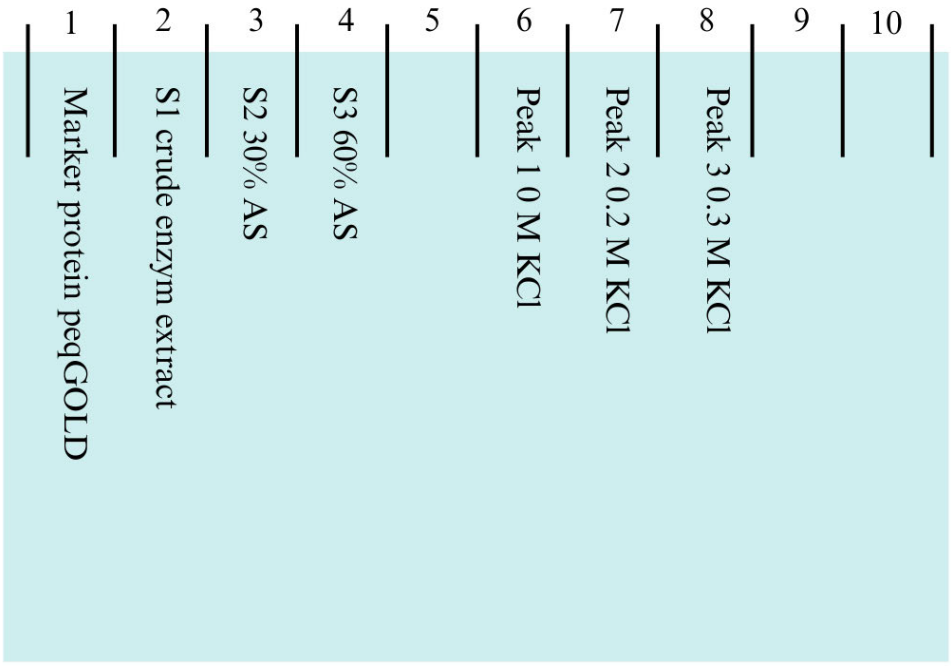

Figure 31: Lane scheme of SDS-PAGE

Overview of the lane assignment in SDS-PAGE gels. Lane 1: molecular weight marker (peqGOLD). Lane 2: crude enzyme extract (S1). Lane 3: supernatant after 30% ammonium sulfate precipitation (S2). Lane 4: supernatant after 60% ammonium sulfate precipitation (S3). Lane 5: empty. Lanes 6–8: DEAE chromatography fractions (0 M, 0.2 M, 0.3 M KCl) *(Created in https://BioRender.com)*.

All samples were mixed with the Laemmle buffer containing SDS and DTT. The samples were than desaturated for 5 min at 95°C before there pipetted into the gel pockets.

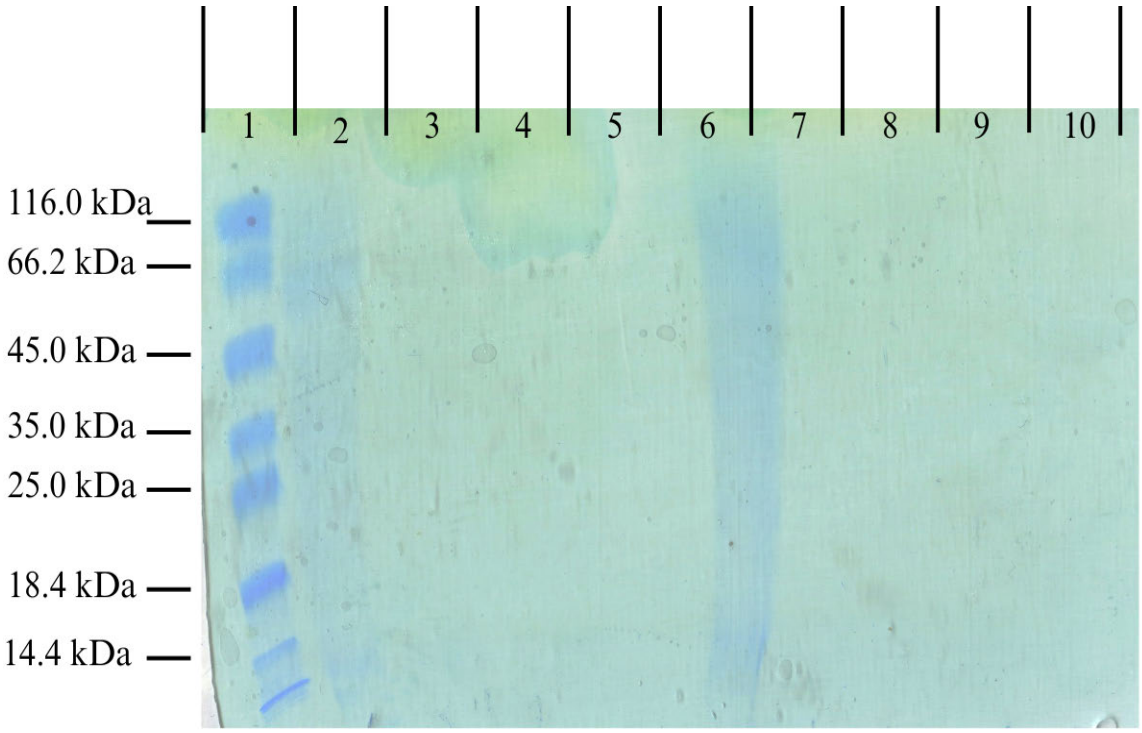

Figure 32: SDS-PAGE analysis of Palmaria palmata

No distinct protein bands were detected, including around the expected ~67 kDa region (Source: own image, Laurie Ramadani 2025).

P. palmata

Figure 32 shows the SDS gel from samples taken from *P. palmata*. No distinct protein bands were visible in any of the *P. palmata* lanes. The gel showed very faint background staining, but no clear bands could be detected across the expected molecular weight range, including the region around 67 kDa where vanadium haloperoxidases would be expected.

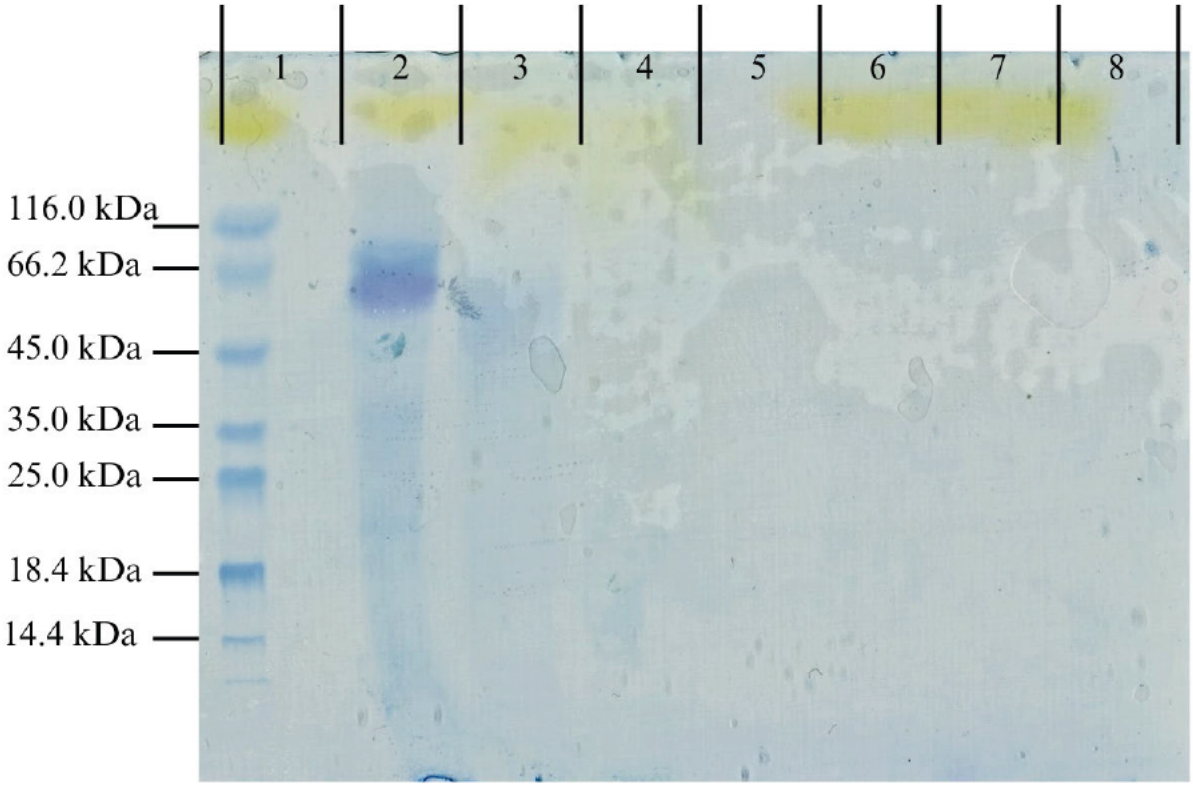

Figure 33: SDS-PAGE analysis of Chondrus crispus

Distinct bands at ~67 kDa were visible in the crude extract and 30% ammonium sulfate fraction, while other lanes showed no bands (Source: own image, Laurie Ramadani 2025).

C. crispus

The gel seen in Figure 33, shows samples taken from *C. crispus* during the downstream process. In *C. crispus*, the crude extract S1 (lane 2) displayed visible protein bands with high intensity and with low intensity in lane 3 30% AS. In both cases the distinct band was detectable at ~67 kDa. Lane 4 in which the supernatant from the 60% AS precipitation was loaded, shows no visible band, as at it was wished in this lane. All other lanes, of DEAE fractions, showed no visible protein bands.

4.12.1 Discussion: SDS-PAGE

The SDS-PAGE analysis revealed very weak or absent protein signals for *P. palmata*, with no detectable bands in the crude extract or in any subsequent fractions. This result is surprising, as *P. palmata* had previously shown measurable protein concentrations in the ROTI® Quant assay and high vanadium concentrations in the enrichment chromatography fractions. One possible explanation is that the vanadium detected in the IEXC fractions does not originate from vanadium-dependent haloperoxidases (V-HPOs) but may instead reflect freely dissolved vanadate anions that remained unbound to proteins. The absence of visible bands could also reflect technical issues such as protein loss during preparation, insufficient protein loading, or interference with staining sensitivity. Consequently, it cannot be concluded from this gel whether haloperoxidases are present in *P. palmata*.

In *C. crispus*, protein bands were visible in the crude extract, including a distinct band around 67 kDa, but not in the fractionated samples. This is consistent with earlier observations of low overall protein yield and relatively low vanadium content in this species. However, the detection of a 67 kDa band despite low vanadium levels suggests that *C. crispus* may accumulate smaller amounts of vanadium overall, but that the vanadium present is more tightly bound to V-HPOs. In contrast, *P. palmata* appears to accumulate larger amounts of vanadium, much of which may remain unbound rather than being bound to haloperoxidases. The absence of visible bands in the IEXC fractions of *C. crispus* could also be explained by protein dilution and losses during SEC and subsequent purification steps, which may have reduced protein concentrations below the detection limit of Coomassie staining.

Taken together, these results highlight the technical challenges of detecting V-HPOs by SDS-PAGE. While *P. palmata* was initially considered the stronger candidate for V-HPO detection based on its high vanadium content, the SDS-PAGE findings suggest that *C. crispus* may in fact be a more promising candidate. The visible bands at ~67 kDa indicate that vanadium in *C. crispus* is more likely bound to haloperoxidases, whereas in *P. palmata* the vanadium may remain largely unbound.

Several technical factors likely contributed to the inconclusive results in both species. First, the protein concentration after SEC and DEAE was likely too low, so that the amount loaded on the gel fell below the sensitivity limit of Coomassie staining. In addition, residual salts (like AS) or buffer (EDTA) components may have interfered with staining efficiency, also

incomplete denaturation or reduction during sample preparation could also have prevented proteins from entering the gel properly. Losses during handling, could have further reduced protein recovery. Lastly, Coomassie staining itself has limited sensitivity, which means that low-abundance proteins such as haloperoxidases might not be visible under these conditions. To improve future experiments, samples could be concentrated before loading, and more sensitive staining methods such as silver stain would help to detect proteins at lower concentrations.

5 Conclusion

This study focused on the role of vanadium and vanadium-dependent haloperoxidases (V-HPOs) in red algae, specifically *Palmaria palmata* and *Chondrus crispus*, and aimed to establish whether a measurable relationship exists between vanadium accumulation and the potential production of halogenated organic compounds (HOCs). By combining validated analytical techniques with protein extraction and purification strategies, this work provides both methodological advances and new biological insights into the trace metal metabolism of marine macroalgae.

The first part of the work successfully established a robust and validated method for vanadium quantification using high-resolution continuum source graphite furnace atomic absorption spectrometry (HR-CS GFAAS). Method validation confirmed the accuracy, precision, and reproducibility of the system. The calibration curve showed excellent linearity ($r = 0.9987$), the method detection limit (LOD = 0.57 µg/L) and quantification limit (LOQ = 1.85 µg/L) were sufficiently low for trace analysis, and recovery experiments demonstrated that no significant vanadium losses occurred during digestion. Comparative analysis with certified reference material and an independent method (TXRF) further confirmed the reliability of the results, with deviations falling within acceptable inter-method variability ranges. Precision testing showed intra- and inter-day relative standard deviations below 2%, highlighting the stability of the method.

Among the different digestion techniques tested, the HACH digestion system proved superior to dry ashing and wet digestion, yielding the highest vanadium recovery (35.5 µg/g DW) and demonstrating better efficiency, shorter processing times, and reduced risk of contamination. Consequently, it was selected as the standard method for following analyses.

The analysis of different pre-dried algal species revealed clear species-specific differences in vanadium accumulation. *P. palmata* contained by far the highest vanadium concentration (36.4 µg/g DW), supporting its classification as an efficient trace metal accumulator and confirming earlier reports of high vanadium levels in this species. In contrast, *C. crispus* showed strong variability between samples, while one variant contained a moderate concentration (9.3 µg/g DW), the other exhibited only trace amounts (0.01 µg/g DW). This discrepancy highlights the

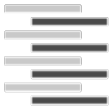

influence of environmental factors such as collection site, seawater chemistry, and possibly anthropogenic inputs on vanadium uptake. Brown algae (*Ascophyllum nodosum*, *Himanthalia elongata*) accumulated only low levels (around 1.3 µg/g DW), and calcified red algae (*Lithothamnium*) contained intermediate concentrations (4.3 µg/g DW). These results confirm that vanadium accumulation is highly species-dependent, with red algae, particularly *P. palmata*, being the most efficient accumulators.

In the second part of the thesis, cell disruption and protein extraction methods were systematically evaluated to release and enrich vanadium-dependent haloperoxidases.

Ultrasonic disruption proved to not be suitable because of the contamination from the probe tip, which uncontrollably releases vanadium into the sample solution. The Ultra-Turrax® homogenizer achieved efficient disruption but carried a higher risk of protein inactivation due to shear stress. Osmotic shock, combined with alkaline extraction, provided a milder, non-mechanical method that preserved soluble proteins but required longer processing times. Alkaline extraction without prior osmotic shock proved to be the most effective extraction method, the only concern here were potential protein denaturation because of alkaline high conditions. However, the consistently high protein content measured in these alkaline extracts suggests that significant denaturation did not occur.

Following extraction, stepwise ammonium sulfate precipitation was performed. At 60 % saturation, only limited amounts of vanadium co-precipitated, with the most successful case observed in fresh material after alkaline extraction, where 55-70 % of vanadium was detected in the pellet. Nevertheless, a large amount of vanadium constantly remained in the soluble phase. Protein quantification confirmed that precipitation reduced the protein content in the supernatant after each step, which was expected, however, this decrease in protein content did not correlate with vanadium distribution, since vanadium levels in the supernatant remained constantly high. This suggests that vanadium is either associated with a subgroup of soluble proteins resistant to salt-induced precipitation or is present in the soluble fraction in an unbound form.

Protein quantification of aqueous and alkaline extracts supported this assumption. Aqueous extracts contained lower total protein but higher relative vanadium levels, whereas alkaline extracts showed the opposite trend, with high protein concentrations but little vanadium. These findings indicate that vanadium is likely bound to a specific subgroup of soluble proteins that

remain stable under mild conditions. Therefore, ammonium sulfate precipitation is seen as not ideal for enriching vanadium-binding proteins like haloperoxidases.

Further purification steps with SEC for desalting effectively reduced salt and enabled ion-exchange, but the proteins eluted nearly simultaneously with the salt peak which led to significant loss since the fraction with salt needed to be discarded. Since SEC also led to dilution, the fractions used for IEXC were significantly low in protein content and vanadium.

In anion-exchange (DEAE) the pooled fraction peaks reveled that only for *P. palmata,* in the 0.2 M KCl fraction, significant concentrations of vanadium were found (4.26 µg/g). In contrast, *C. crispus* DEAE fractions contained no detectable vanadium despite protein elution, plausibly reflecting its lower starting vanadium content, species biology, and high dilution/loss during SEC.

Lastly, the SDS-PAGE outcomes provided an unexpected shift in interpretation. For *P. palmata*, no definitive bands were visible despite measurable protein content and clear vanadium enrichment by DEAE, which suggests that much of the vanadium in this species may remain unbound rather than incorporated into proteins. In *C. crispus*, by contrast, the crude extract displayed a band near ~67 kDa consistent with VBPOs, while lanes from after precipitation and ion exchange were faint or not visible, likely due to protein loss and dilution effects. These findings suggest that although *P. palmata* accumulates more vanadium overall, *C. crispus* may actually bind vanadium more directly to haloperoxidases, making it a stronger candidate for the presence of active V-HPOs. Collectively, the gels emphasize the sensitivity limits and sample-prep fragility of this workflow and could use a more sensitive detection method (e.g., silver staining) and better concentration prior to electrophoresis.

In conclusion, this study provides new insights into the link between vanadium content, V-HPOs, and the possible formation of halogenated organic compounds (HOCs) in Baltic red algae. While *P. palmata* showed the highest vanadium concentrations and enrichment in ion-exchange fractions, the absence of protein bands suggests that vanadium may remain largely unbound in this species. By contrast, *C. crispus* showed lower vanadium levels but detectable protein bands consistent with V-HPOs, making it a stronger candidate for functional haloperoxidase activity. The lower total amount of vanadium in *P. palmata* compared to literature values of ~130 µg/g, as well as the consistently low concentrations in *C. crispus*, can

likely be explained by the fact that all samples originated from the Baltic Sea, which is generally poorer in vanadium than open ocean waters.

The work purposely focused on vanadium as a proxy for haloperoxidase content and activity, and therefore did not include direct measurement of HOCs. Future studies should combine vanadium quantification with halocarbon analysis (e.g., bromoform) and enzyme activity assays. Methodological improvements such as gentler desalting methods, optimized ion-exchange protocols, and alternative enrichment strategies will also be essential to minimize protein loss and enable purification of active enzymes. These modifications would make it possible to establish clear, quantitative links between vanadium content, V-HPO activity, and HOC production in Baltic red algae.

From an ecological perspective, the ability of red algae to accumulate vanadium and produce halogenated metabolites is likely an important adaptation for defense, antifouling, and competition in their environment. From a biotechnological and pharmaceutical point of view, the findings highlight the potential of the algae as a promising source of bioactive halogenated compounds, and they underline the value of V-HPOs as stable and versatile biocatalysts.

In sum, this thesis established a validated and reliable platform for vanadium quantification, demonstrated clear species-specific differences in vanadium accumulation, and developed a methodological framework for the extraction and preliminary enrichment of vanadium-dependent haloperoxidases. While a direct correlation between vanadium and HOC occurrence has not yet been proven, the results provide a solid foundation for future work. Further research should focus on scaling up protein purification, performing activity assays, and directly linking vanadium levels to halogenated compound profiles. Such studies will not only help clarify fundamental ecological processes in the Baltic Sea but may also pave the way for identifying novel halogenated metabolites with pharmaceutical and industrial applications.

References

Andrews, P. 1965. *The Gel-Filtration Behaviour of Proteins Related to their Molecular Weights over a Wide Range*.

Barth, H.G., Boyes, B.E. and Jackson, C. 1994. *Size Exclusion Chromatography*. Available at: https://pubs.acs.org/sharingguidelines.

Bauer, S., Blomqvist, S. and Ingri, J. 2017. Distribution of dissolved and suspended particulate molybdenum, vanadium, and tungsten in the Baltic Sea. *Marine Chemistry* 196, pp. 135–147. doi: 10.1016/j.marchem.2017.08.010.

Bergfeld, F.A.C.P.; et al. [no date]. *Safety Assessment of Red Algae-Derived Ingredients as Used in Cosmetics The Expert Panel for Cosmetic Ingredient Safety members are: Chair, Wilma F*. Available at: https://www.cir-.

Butler, A. and Carter-Franklin, J.N. 2004. The role of vanadium bromoperoxidase in the biosynthesis of halogenated marine natural products. *Natural Product Reports* 21(1), pp. 180–188. doi: 10.1039/b302337k.

Butler, A. and Sandy, M. 2009. Mechanistic considerations of halogenating enzymes. *Nature* 460(7257), pp. 848–854. doi: 10.1038/nature08303.

Cardozo, K.H.M. et al. 2007. Metabolites from algae with economical impact. *Comparative Biochemistry and Physiology - C Toxicology and Pharmacology* 146(1-2 SPEC. ISS.), pp. 60–78. doi: 10.1016/j.cbpc.2006.05.007.

Chopin, T., Bird, C.J., Murphy, C.A., Osborne, J.A., Patwary3, M.U. and Floc, J.-Y. 1996. *A molecular investigation of polymorphism in the North Atlantic red alga Chondrus crispus (GigartinaIes)**.

Čmiková, N. et al. 2024. Seaweed Nutritional Value and Bioactive Properties: Insights from Ascophyllum nodosum, Palmaria palmata, and Chondrus crispus. *Life* 14(11). doi: 10.3390/life14111522.

Collén, J. et al. 2014. Chondrus crispus - A present and historical model organism for red seaweeds. In: *Advances in Botanical Research*. Academic Press Inc., pp. 53–89. doi: 10.1016/B978-0-12-408062-1.00003-2.

Crans, D.C., Smee, J.J., Gaidamauskas, E. and Yang, L. 2004. The Chemistry and Biochemistry of Vanadium and the Biological Activities Exerted by Vanadium Compounds. *Chemical Reviews* 104(2), pp. 849–902. doi: 10.1021/cr020607t.

Dawczynski, C., Schubert, R. and Jahreis, G. 2007. Amino acids, fatty acids, and dietary fibre in edible seaweed products. *Food Chemistry* 103(3), pp. 891–899. doi: 10.1016/j.foodchem.2006.09.041.

D'Hondt, E. et al. 2017. Cell disruption technologies. In: *Microalgae-Based Biofuels and Bioproducts: From Feedstock Cultivation to End-Products*. Elsevier Inc., pp. 133–154. doi: 10.1016/B978-0-08-101023-5.00006-6.

Digesdahl ® Aufschlussapparatur. [no date]. Available at: http://www.hach.com.

Domínguez-González, R., Romarís-Hortas, V., García-Sartal, C., Moreda-Piñeiro, A., Barciela-Alonso, M.D.C. and Bermejo-Barrera, P. 2010. Evaluation of an in vitro method to

estimate trace elements bioavailability in edible seaweeds. *Talanta* 82(5), pp. 1668–1673. doi: 10.1016/j.talanta.2010.07.043.

Duong-Ly, K.C. and Gabelli, S.B. 2014. Salting out of proteins using ammonium sulfate precipitation. In: *Methods in Enzymology*. Academic Press Inc., pp. 85–94. doi: 10.1016/B978-0-12-420119-4.00007-0.

Fredericqi, S., Brodie2, J., Hommersand1, M.H., Frederlcq, S., Brodie, J. and Hommers, M.H. 1992. *Developmental morphology of Chondrus crispus (Gigartinaceae, Rhodophyta)*.

El Gamal, A.A. 2010. Biological importance of marine algae. *Saudi Pharmaceutical Journal* 18(1), pp. 1–25. doi: 10.1016/j.jsps.2009.12.001.

Gomes, T.A., Zanette, C.M. and Spier, M.R. 2020. An overview of cell disruption methods for intracellular biomolecules recovery. *Preparative Biochemistry & Biotechnology* 50(7), pp. 635–654. Available at: https://www.tandfonline.com/doi/full/10.1080/10826068.2020.1728696.

Hall, M. 2018. Size Exclusion Chromatography (SEC). In: *Biopharmaceutical Processing: Development, Design, and Implementation of Manufacturing Processes*. Elsevier, pp. 421–432. doi: 10.1016/B978-0-08-100623-8.00021-9.

Harnedy, P.A. and FitzGerald, R.J. 2013. Extraction of protein from the macroalga Palmaria palmata. *LWT* 51(1), pp. 375–382. doi: 10.1016/j.lwt.2012.09.023.

Hasan, M.M. 2017. ALGAE AS NUTRITION, MEDICINE AND COSMETIC: THE FORGOTTEN HISTORY, PRESENT STATUS AND FUTURE TRENDS. *World Journal of Pharmacy and Pharmaceutical Sciences*, pp. 1934–1959. doi: 10.20959/wjpps20176-9447.

Hofmann, A. and Clokie, S. 2018. *Wilson and Walker's Principles and Techniques of Biochemistry and Molecular Biology*. Hofmann, A. and Clokie, S. eds. Cambridge University Press. Available at: https://www.cambridge.org/highereducation/books/wilson-and-walkers-principles-and-techniques-of-biochemistry-and-molecular-biology/2159004E019DDD87C0A97EE8DB72B79F#contents.

Holthuizen, P. and Çopuroğlu, O. 2024. Quantification of surface grinding during the sample preparation of cementitious materials by optical profilometry. *Journal of Microscopy* 294(2), pp. 128–136. doi: 10.1111/jmi.13256.

Jimenez-Escrig SC, A.B. and Sanchez-Muniz Ph D Prf, F.J. 2000. *DIETARY FIBRE FROM EDIBLE SEAWEEDS: CHEMICAL STRUCTURE, PHYSICOCHEMICAL PROPERTIES AND EFFECTS ON CHOLESTEROL METABOLISM*.

Jungbauer, A. and Hahn, R. 2009. Chapter 22 Ion-Exchange Chromatography. In: *Methods in Enzymology*. Academic Press Inc., pp. 349–371. doi: 10.1016/S0076-6879(09)63022-6.

Kakko, N., Ivanova, N. and Rantasalo, A. [no date]. *CHEM-E3140 Bioprocess Technology II Cell disruption methods Group 1*.

Kamenarska, Z., Taniguchi, T., Ohsawa, N., Hiraoka, M. and Itoh, N. 2007. A vanadium-dependent bromoperoxidase in the marine red alga Kappaphycus alvarezii (Doty) Doty displays clear substrate specificity. *Phytochemistry* 68(10), pp. 1358–1366. doi: 10.1016/j.phytochem.2007.03.003.

Kielkopf, C.L., Bauer, W. and Urbatsch, I.L. 2021. Sodium Dodecyl Sulfate–Polyacrylamide Gel Electrophoresis of Proteins. *Cold Spring Harbor Protocols* 2021(12), p. pdb.prot102228. doi: 10.1101/pdb.prot102228.

Korpinen, S., Laamanen, M., Andersen, J.H. and Asplund, L. 2010. *Hazardous substances in the Baltic Sea An integrated thematic assessment of hazardous substances in the Baltic Sea*

Baltic Sea Environment Proceedings No. 120 B Helsinki Commission Baltic Marine Environment Protection Commission. Helsinki, Finland. Available at: http://www.helcom.fi/stc/files/Publications/Proceedings/bsep120B.pdf [Accessed: 3 September 2025].

Kruse, J., Wörner, J., Schneider, J., Dörksen, H. and Pein-Hackelbusch, M. 2024. Methods for Estimating the Detection and Quantification Limits of Key Substances in Beer Maturation with Electronic Noses. *Sensors* 24(11). doi: 10.3390/s24113520.

Leblanc, C. et al. 2015. Vanadium haloperoxidases: From the discovery 30 years ago to X-ray crystallographic and V K-edge absorption spectroscopic studies. *Coordination Chemistry Reviews* 301–302, pp. 134–146. doi: 10.1016/j.ccr.2015.02.013.

Liu, Y., Wei, S.Z. and Jiang, T. 2024. Design of chromium-vanadium steel based on design loop combining property-oriented design criteria and machine learning prediction model. *Journal of Materials Research and Technology* 32, pp. 86–96. doi: 10.1016/j.jmrt.2024.07.159.

Maa, Y.-F. and Hsu, C. 1996. *Liquid-liquid emulsification by rotor/stator homogenization*.

Maa, Y.F. and Hsu, C.C. 1997. Protein denaturation by combined effect of shear and air-liquid interface. *Biotechnology and Bioengineering* 54(6), pp. 503–512. doi: 10.1002/(SICI)1097-0290(19970620)54:6<503::AID-BIT1>3.0.CO;2-N.

Magpusao, J., Oey, I. and Kebede, B. 2021. Opportunities and Challenges of Algal Protein Extraction and Production. In: *Innovative Food Processing Technologies*. Elsevier, pp. 216–233. doi: 10.1016/B978-0-08-100596-5.23026-6.

Marinho-Soriano, E., Fonseca, P.C., Carneiro, M.A.A. and Moreira, W.S.C. 2006. Seasonal variation in the chemical composition of two tropical seaweeds. *Bioresource Technology* 97(18), pp. 2402–2406. doi: 10.1016/j.biortech.2005.10.014.

Marshall, M.R. 2010. Ash Analysis. pp. 105–115. doi: 10.1007/978-1-4419-1478-1_7.

Martin, D.F. 2013. *Column Chromatography*. Martin, D. ed. InTech. doi: 10.5772/47823.

Millan-Linares, M.C. et al. 2019. Nutraceutical extract from dulse (Palmaria palmata L.) inhibits primary human neutrophil activation. *Marine Drugs* 17(11). doi: 10.3390/md17110610.

Mišurcová, L. 2011. Chemical Composition of Seaweeds. In: *Handbook of Marine Macroalgae: Biotechnology and Applied Phycology*. John Wiley and Sons, pp. 171–192. doi: 10.1002/9781119977087.ch7.

Ohshiro, T. 2002. Expression of the vanadium-dependent bromoperoxidase gene from a marine macro-alga Corallina pilulifera in Saccharomyces cerevisiae and characterization of the recombinant enzyme. *Phytochemistry* 60(6), pp. 595–601. Available at: https://linkinghub.elsevier.com/retrieve/pii/S0031942202001607.

Park, S.J., Sharma, A. and Lee, H.J. 2024. An Update on the Chemical Constituents and Biological Properties of Selected Species of an Underpinned Genus of Red Algae: Chondrus. *Marine Drugs* 22(1). doi: 10.3390/md22010047.

Prabhasankar, P., Ganesan, P. and Bhaskar, N. 2009. Influence of Indian Brown Seaweed (Sargassum marginatum) as an Ingredient on Quality, Biofunctional, and Microstructure Characteristics of Pasta. *Food Science and Technology International* 15(5), pp. 471–479. doi: 10.1177/1082013209350267.

Punitha, T., Phang, S.M., Juan, J.C. and Beardall, J. 2018. Environmental Control of Vanadium Haloperoxidases and Halocarbon Emissions in Macroalgae. *Marine Biotechnology* 20(3), pp. 282–303. doi: 10.1007/s10126-018-9820-x.

Rehder, D. 2012. The potentiality of vanadium in medicinal applications. *Future Medicinal Chemistry* 4(14), pp. 1823–1827. doi: 10.4155/fmc.12.103.

Romera, E., González, F., Ballester, A., Blázquez, M.L. and Muñoz, J.A. 2007. Comparative study of biosorption of heavy metals using different types of algae. *Bioresource Technology* 98(17), pp. 3344–3353. doi: 10.1016/j.biortech.2006.09.026.

ROTI ® Quant universal. [no date]

Sheath, R.G. 2003. RED ALGAE. In: *Freshwater Algae of North America*. Elsevier, pp. 197–224. Available at: https://linkinghub.elsevier.com/retrieve/pii/B9780127415505500064.

Show, K.Y., Lee, D.J., Tay, J.H., Lee, T.M. and Chang, J.S. 2015. Microalgal drying and cell disruption - Recent advances. *Bioresource Technology* 184, pp. 258–266. doi: 10.1016/j.biortech.2014.10.139.

Stévant, P., Schmedes, P.S., Le Gall, L., Wegeberg, S., Dumay, J. and Rebours, C. 2023. Concise review of the red macroalga dulse, Palmaria palmata (L.) Weber & Mohr. *Journal of Applied Phycology* 35(2), pp. 523–550. doi: 10.1007/s10811-022-02899-5.

Tack, F.M.G., Singh, S.P. and Verloo, M.G. 1997. *Comparison of ashing procedures for the determination of trace elements in plant leaves*.

The fitness for purpose of analytical methods : a laboratory guide to method validation and related topics. 2014. Eurachem.

Tonkur, H., Can, M.F. and Sabah, E. 2022. Rheological behavior of sepiolite suspensions homogenized by ultra-turrax high-speed homogenizer. *Physicochemical Problems of Mineral Processing* 58(5). doi: 10.37190/ppmp/153415.

VWR International GmbH, 2018. *peqGOLD Protein Marker I (Cat. No. 27-1010)* data sheet v01.2018. Darmstadt: VWR International GmbH.

Wada, O.Z., Rashid, N., Wijten, P., Thornalley, P., Mckay, G. and Mackey, H.R. 2024. Evaluation of cell disruption methods for protein and coenzyme Q10 quantification in purple non-sulfur bacteria. *Frontiers in Microbiology* 15. doi: 10.3389/fmicb.2024.1324099.

Walch, N. and Jungbauer, A. 2017. Continuous desalting of refolded protein solution improves capturing in ion exchange chromatography: A seamless process. *Biotechnology Journal* 12(6). doi: 10.1002/biot.201700082.

Welz, B. 2005. High-resolution continuum source AAS: The better way to perform atomic absorption spectrometry. *Analytical and Bioanalytical Chemistry* 381(1), pp. 69–71. doi: 10.1007/s00216-004-2891-8.

Wever, R. and Van Der Horst, M.A. 2013. The role of vanadium haloperoxidases in the formation of volatile brominated compounds and their impact on the environment. *Dalton Transactions* 42(33), pp. 11778–11786. doi: 10.1039/c3dt50525a.

Wever, R., Krenn, B.E. and Renirie, R. 2018. Marine Vanadium-Dependent Haloperoxidases, Their Isolation, Characterization, and Application. In: *Methods in Enzymology*. Academic Press Inc., pp. 141–201. doi: 10.1016/bs.mie.2018.02.026.

Wingfield, P. 1998. Protein Precipitation Using Ammonium Sulfate. *Current Protocols in Protein Science* 13(1). doi: 10.1002/0471140864.psa03fs13.

Winter, J.M. and Moore, B.S. 2009. Exploring the chemistry and biology of vanadium-dependent haloperoxidases. *Journal of Biological Chemistry* 284(28), pp. 18577–18581. doi: 10.1074/jbc.R109.001602.

Xu, M. et al. 2024. A critical review of the edible seaweed Palmaria palmata (L.) Weber & Mohr and its bioactive compounds in the “omics” era. *Algal Research* 82. doi: 10.1016/j.algal.2024.103606.

Yasumitsu, T., Liu, G., Leveque, J.M., Aonuma, S., Duclaux, L., Kimura, T. and Komatsu, N. 2013. A rosette cooling cell: More effective container for solubilization of single-walled carbon nanotubes under probe-type ultrasonic irradiation. *Ultrasonics Sonochemistry* 20(1), pp. 37–39. doi: 10.1016/j.ultsonch.2012.06.009.

Zhang, Y. et al. 2024. Total Reflection X-ray Fluorescence Spectrometry: A Comprehensive Review of Critical Components, Analytical Benefits and Practical Applications. *Critical Reviews in Analytical Chemistry*, pp. 1–20. doi: 10.1080/10408347.2024.2411245.

Zvěřina, O., Vychytilová, M., Rieger, J. and Goessler, W. 2023. Fast and simultaneous determination of zinc and iron using HR-CS GF-AAS in vegetables and plant material. *Spectrochimica Acta - Part B Atomic Spectroscopy* 201. doi: 10.1016/j.sab.2023.106616.

Addendum

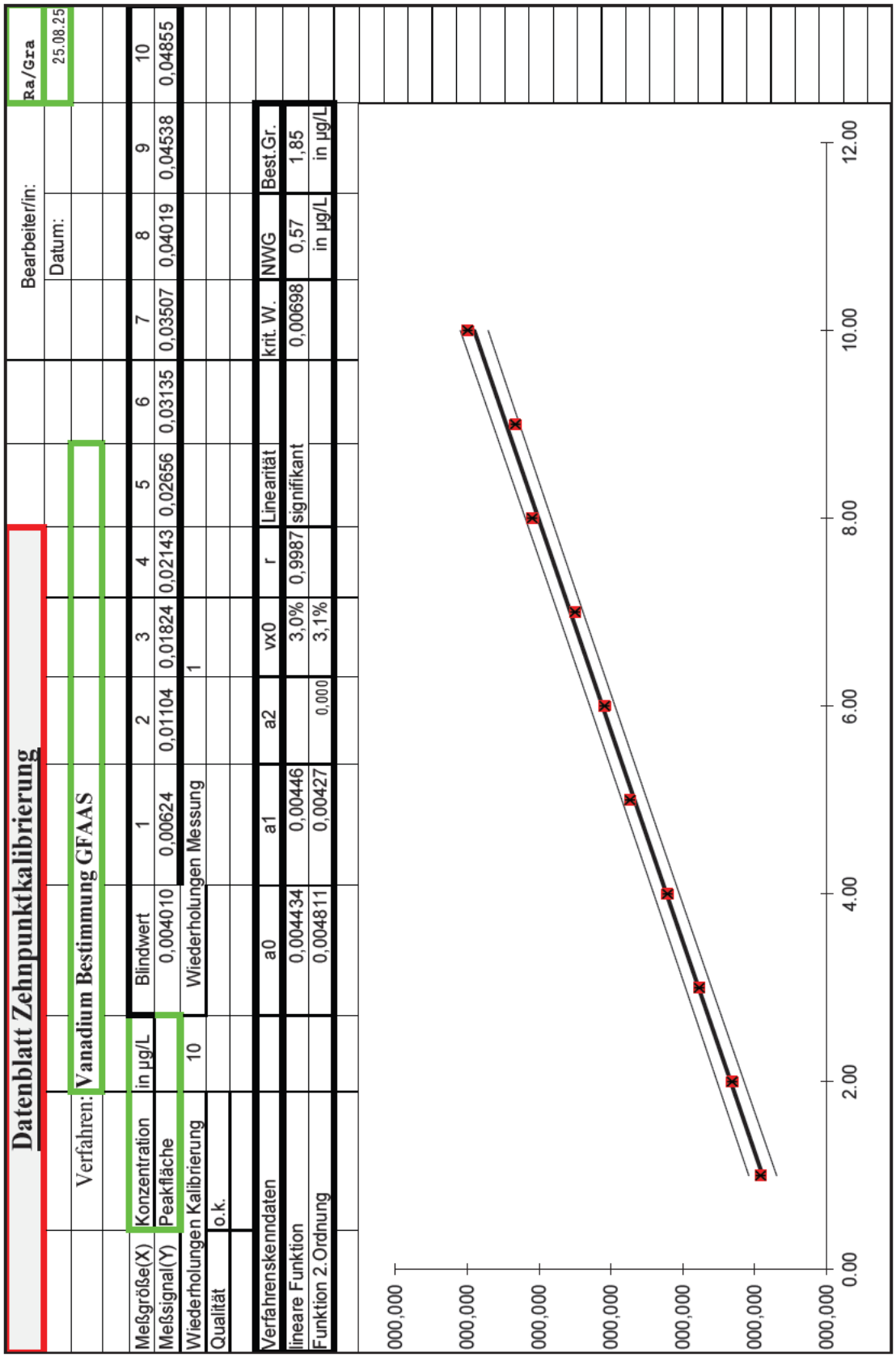

Seite 1